



NUCLEAR WASTE SOCIÉTÉ DE GESTION
MANAGEMENT DES DÉCHETS
ORGANIZATION NUCLÉAIRES

Phase 2 Geoscientific Preliminary Assessment
Acquisition, Processing and Interpretation of
High-Resolution Airborne Geophysical Data

TOWNSHIP OF HORNEPAYNE AND AREA, ONTARIO



APM-REP- 1332-0205

NOVEMBER 2017

This report has been prepared under contract to the NWMO. The report has been reviewed by the NWMO, but the views and conclusions are those of the authors and do not necessarily represent those of the NWMO.

All copyright and intellectual property rights belong to the NWMO.

For more information, please contact:

Nuclear Waste Management Organization

22 St. Clair Avenue East, Sixth Floor


Toronto, Ontario M4T 2S3 Canada

Tel 416.934.9814

Toll Free 1.866.249.6966

Email contactus@nwmo.ca

www.nwmo.ca

 Sander Geophysics	Airborne Geophysics Acquisition and Interpretation	Issue Date:	December 2017
------------------------------------------------------------------------------------------------------------	----------------------------------------------------	-------------	---------------

PHASE 2 GEOSCIENTIFIC PRELIMINARY ASSESSMENT

ACQUISITION, PROCESSING AND INTERPRETATION OF HIGH-RESOLUTION AIRBORNE GEOPHYSICAL DATA

TOWNSHIP OF HORNEPAYNE AND AREA, ONTARIO

Prepared for:

Nuclear Waste Management Organization (NWMO)

by:

Sander Geophysics Limited (SGL)

NWMO REPORT NUMBER:

APM-REP-01332-0205

Signatures



Martin Bates, Ph.D.



Martin Mushayandevu, Ph.D.

Peter Tschirhart
Dec 8, 2016

Peter Tschirhart, M.Sc.

Executive Summary

This technical report documents the results of the acquisition, processing and interpretation of high-resolution airborne geophysical data conducted as part of the Phase 2 Geoscientific Preliminary Assessment, to further assess the suitability of the Hornepayne area to safely host a deep geological repository (Geofirma, 2017). This study followed the successful completion of a Phase 1 Geoscientific Desktop Preliminary Assessment (Geofirma, 2013). The desktop Phase 1 study identified potentially suitable areas warranting further studies such as high-resolution surveys and geological mapping. High-resolution surveying was completed over two potentially suitable areas; one located in the Black-Pic batholith south of the Township of Hornepayne and one located in the metasedimentary rocks of the Quetico Subprovince north of the Township.

The purpose of the Phase 2 acquisition, processing and interpretation of geophysical data was to provide an updated interpretation of the geological characteristics of the potentially suitable bedrock unit identified in Phase 1 and to provide additional information to further assess the geology of the Hornepayne area. Both magnetic and gravimetric data were acquired during the surveys in order to provide data to interpret the geometry and thickness of the potentially suitable bedrock units; the nature of geological contacts; bedrock lithologies; the degree of geological heterogeneities and the nature of intrusive phases within the pluton in the area; as well as the nature of structural features such as faults, shears zones, and alteration zones. The grids of the acquired magnetic and gravimetric data and associated processed grids (first, second and horizontal derivatives, total gradient amplitude, trend analysis solutions and tilt angle) were analyzed and interpreted together with the mapped bedrock geology and other available geological information (e.g. magnetic susceptibility and rock density). The survey allowed for a characterization of the gravity and magnetic signatures of the Black-Pic batholith and internal plutons and greenstone belt units, as well as the metasedimentary rocks of the Quetico Subprovince and the dominant signature of the Quetico-Wawa subprovince boundary.

The Black-Pic batholith corresponds to a fairly gentle gravity gradient decreasing to the south away from the subprovince boundary. Although previously mapped as homogeneous gneissic tonalite, the Black-Pic batholith has internal variations in magnetic character. The magnetic data along the subprovince boundary shear zone in the northern portion of the Black-Pic batholith is interpreted as a complex and heterogeneous mixture of lithologies which has undergone deformation and metamorphism, and may also include slivers of mafic to ultramafic metavolcanic rocks. In the central portion of the Black-Pic batholith is a narrow band of a strong magnetic fabric trending east-northeast that may contain some amount of mafic metavolcanic bedrock. The weakly magnetized southern portion of the Black-Pic batholith that is lacking in fabric is interpreted to represent the core of a large-scale fold through the Black-Pic batholith where gneissic layering is suggested to be either shallowly dipping or non-existent.

Intense deformation and metamorphism apparent in the magnetic and gravity data in the Quetico Subprovince is limited within a 14 km wide zone north of the mapped subprovince boundary with tight folding apparent farther north. The Quetico Subprovince becomes generally non-magnetic farther away from the deformation zone. The Black-Pic batholith and the Quetico metasedimentary rocks are intruded by numerous dyke swarms (Matachewan, Abitibi, Biscotasing, Sudbury and unclassified dykes).

Preliminary forward modelling was completed on two profile lines covering the principle features of the Black-Pic batholith and Quetico metasedimentary rocks and surrounding intrusions and greenstone belts within the study area. The Black-Pic batholith has been modelled with depths ranging from 4 km to 7 km with density and magnetic susceptibility variability and intensity increasing towards the subprovince boundary. Rocks of the Quetico Subprovince have been modelled locally as extending to depths typically greater than 6 km.

1	INTRODUCTION.....	7
1.1	Study Objective.....	7
1.2	Geophysical Survey Area.....	7
2	SUMMARY OF GEOLOGY	9
2.1	Geological Setting	9
2.2	Bedrock Geology	9
2.2.1	Metasedimentary Rocks of the Quetico Subprovince	10
2.2.2	Intrusive Rocks of the Quetico Subprovince	10
2.2.3	Intrusive Rocks of the Wawa Subprovince	10
2.2.4	Mafic Dykes.....	11
2.3	Structural History.....	12
2.3.1	Mapped Structures and Named Faults.....	14
2.3.2	Metamorphism	14
2.4	Quaternary Geology	15
3	DATA SOURCE ACQUISITION AND QUALITY.....	17
3.1	Magnetic Data.....	18
3.2	Gravity Data	18
3.3	Digital Elevation Data.....	19
3.4	Additional Data Sources.....	20
3.4.1	OGS Mapped Bedrock Geology.....	20
3.4.2	Geological Base Maps.....	20
3.4.3	OGS PETROCH Lithogeochemical Database	20
3.4.4	Densities and Magnetic Susceptibilities.....	21
3.4.5	Ontario Precambrian Bedrock Magnetic Susceptibility Geodatabase.....	21
3.4.6	Other Magnetic Susceptibility Measurements.....	21
4	GEOPHYSICAL DATA PROCESSING METHODS.....	22
4.1	Gravity Data Processing.....	22
4.1.1	Bouguer Correction	23
4.1.2	Static and Level Corrections.....	23
4.1.3	Gridding and Filtering.....	23
4.2	Magnetic Data Processing	24
4.2.1	Levelling.....	24

4.2.2	Micro-Levelling.....	25
4.2.3	Gridding.....	25
4.3	Gravity and Magnetic Derivative Products.....	25
4.3.1	Total Magnetic Intensity Reduced to Pole.....	25
4.3.2	Vertical Derivatives of Total Magnetic Intensity and Bouguer Gravity	26
4.3.3	Total Horizontal Gradient of Total Magnetic Intensity and Bouguer Gravity	26
4.3.4	Total Gradient Amplitude of Total Magnetic Intensity	27
4.3.5	Tilt Angle	27
4.3.6	Trend Analysis Method	27
5	GEOPHYSICAL INTERPRETATION.....	29
5.1	Results of Qualitative Analysis	29
5.1.1	Metasedimentary Rocks of the Quetico Subprovince	29
5.1.2	Black-Pic Batholith	31
5.2	Preliminary 2.5D Modelling	33
5.2.1	Model Descriptions.....	34
5.2.2	Model Results	36
6	SUMMARY OF RESULTS	43
7	REFERENCES	45
8	FIGURES.....	51

1 Introduction

This technical report documents the results of the acquisition and interpretation of high-resolution airborne geophysical data (gravity and magnetic) conducted as part of the Phase 2 Geoscientific Preliminary Assessment, to further assess the suitability of the Hornepayne area to safely host a deep geological repository (Geofirma, 2017). This study followed the successful completion of a Phase 1 Geoscientific Desktop Preliminary Assessment (Geofirma, 2013). The desktop Phase 1 study identified potentially suitable areas warranting further studies such as high-resolution surveys and geological mapping. High-resolution surveying was completed over two potentially suitable areas; one located in the Black-Pic batholith south of the Township of Hornepayne and one located in the metasedimentary rocks of the Quetico Subprovince north of the Township.

1.1 Study Objective

The main purposes of the acquisition and interpretation of high-resolution magnetic and gravity data are as follows:

- Acquire high-resolution airborne magnetic and gravimetric data within a geophysical survey area that encompasses the general potentially suitable areas in the Black-Pic batholith and metasedimentary rocks of the Quetico Subprovince identified in the Phase 1 Geoscientific Desktop Preliminary Assessment (Geofirma, 2013).
- Characterize the geophysical response of the bedrock units (e.g. bedrock contacts, intrusive phases, potential natural resources, etc.)
- Characterize the extent of bedrock heterogeneity (e.g. ductile fabric, complexity, etc.).
- Interpret the geophysical character of potential structures (faults, dykes, joints, etc.).
- Develop initial models of bedrock units at depth (2.5D forward modeling).

1.2 Geophysical Survey Area

The Township of Hornepayne is located in north-central Ontario approximately 400 km north of Sault Ste. Marie, 340 km east of Thunder Bay and 260 km west of Timmins. The settlement area of Hornepayne is situated on Highway 631, approximately 100 km north of Highway 17. The geophysical survey in the Hornepayne area consists of two survey blocks of high-resolution coverage, north and south of the settlement area, which are connected by north-south oriented control lines. The two survey blocks encompass an area of over 1,000 km². The location of the geophysical survey area is shown in Figure 1.1 overlying the bedrock geology, and the full set of survey lines are shown in Figure 1.2. The geophysical survey area is bounded by the coordinates presented in Table 1.1 (NAD-83 datum, UTM zone 16N).

Table 1.1: Coordinates of the survey area (NAD-83, UTM 16N)

Easting (m)	Northing (m)
Hornepayne South Block	
665062	5425000
641523	5425000
641523	5450500
665062	5450500
Hornepayne North Block	
662500	5474000
681000	5474000
681000	5459000
654000	5459000
654000	5467000
662500	5467000

2 Summary of Geology

The detailed geology of the Hornepayne area was described in the Phase 1 Geoscientific Desktop Preliminary Assessment (Geofirma, 2013). The following subsections provide a brief description of the geologic setting, bedrock geology, structural history and mapped structures, metamorphism and Quaternary geology of the Hornepayne area. The focus of the following section is the bedrock units and important structural features in the areas identified during Phase 1 as being potentially suitable to host a deep geological repository.

2.1 Geological Setting

The Hornepayne area is located within the Superior Province of northern Ontario. The Superior Province is a stable craton created from a collage of ancient plates and accreted juvenile arc terranes that were progressively amalgamated over a period of more than 2 billion years (e.g., Percival et al., 2006). The Superior Province covers an area of approximately 1,500,000 km² and is divided into subprovinces, including the Wawa and Quetico subprovinces. The Hornepayne south survey block is located entirely within the Wawa Subprovince, whereas north survey block is located entirely within the Quetico Subprovince (Figure 1.1).

The Wawa Subprovince is comprised of multiple units of volcanic and associated metasedimentary rocks (greenstone belts) separated by extensive granitic plutons and batholiths. These volcanic and metasedimentary units typically occur in elongate narrow geometries and represent volumetrically a relatively minor percentage of the rocks. The surrounding granitic bodies are composed primarily of tonalite to granodiorite, and represent the vast majority of the rock present throughout the area.

The Quetico Subprovince is an expansive geological domain comprised predominantly of metasedimentary rocks (Zaleski et al., 1995). Numerous granitic intrusions, and rare mafic to ultramafic intrusions are also located throughout the Quetico Subprovince (Williams, 1989; Sutcliffe, 1991).

Several generations of Paleoproterozoic diabase dyke swarms, ranging in age from ca. 2.473 to 2.101 Ga intrude all bedrock units in the Hornepayne area (Hamilton et al., 2002; Buchan and Ernst, 2004; Halls et al., 2006).

2.2 Bedrock Geology

The main bedrock geology units present within the two Hornepayne survey blocks include the Black-Pic batholith of the Wawa Subprovince and the metasedimentary rocks of the Quetico Subprovince. Additionally, a sliver of the Strickland pluton occurs in the southeastern portion of the southern survey block, and the southern boundary of a granite-granodiorite intrusion is located along the northern boundary of the northern survey block (Figure 1.1). All bedrock units in the Hornepayne area are transected by three generations of diabase dykes. The bedrock in the Hornepayne area has experienced several generations of ductile and brittle deformation, and the individual rock units have been subjected to varying amounts of metamorphism.

A detailed description of these bedrock units, and structural and metamorphic events, can be found in the Phase 1 Geoscientific Desktop Preliminary Assessment (Geofirma, 2013), and are summarized in the following subsections. A description of the bedrock geology units surrounding, but not included within the individual Phase 2 Hornepayne interpretation areas, can also be found in the aforementioned reference, and are not repeated here.

2.2.1 Metasedimentary Rocks of the Quetico Subprovince

Metasedimentary rocks of the Quetico Subprovince occur in the northern portion of the Hornepayne assessment area and underlie the entire northern survey block, with the exception of the northernmost boundary, which is located along the contact of a granite-granodiorite intrusion (Figure 1.1).

Metasedimentary rocks of the Quetico Subprovince include wacke-pelite-arenite rocks of the Quetico belt, as well as varying amounts of ironstone, conglomerate, and siltstone (Williams and Breaks, 1996; Zaleski et al., 1999). Rocks within the Quetico Subprovince have experienced varying degrees of metamorphism and deformation, and commonly exhibit gneissic and migmatitic textures (Percival, 1989; Zaleski et al., 1999). Extensive deformation can be observed in numerous small-scale folds, shear zones, and boudinaged units (Williams and Breaks, 1996). Evidence of extensive metamorphism includes significant volumes of leucosome, resulting from partial melting and segregation during high-grade metamorphism (Williams and Breaks, 1996).

The Quetico Subprovince has been interpreted to be an accretionary prism of an Archean volcanic island-arc system, which developed where the Wawa and Wabigoon belts formed converging arcs (Percival and Williams, 1989). The timing of the Quetico-Wawa belt accretion has been constrained between ca. 2.689 Ga and 2.684 Ga (Percival, 1989), and the metasedimentary rocks have been dated at 2.700 to 2.688 Ga (Percival, 1989; Zaleski et al., 1999).

2.2.2 Intrusive Rocks of the Quetico Subprovince

The southern boundary of a mapped granite-granodiorite intrusion straddles the northern boundary of the Hornepayne northern survey block (Figure 1.1). Similar intrusions have been mapped in the region, and described as quartzo-feldspathic gneisses (Coates, 1970) and biotite leucogranite (Percival, 1989). In general, granitic rocks in the Quetico Subprovince are typically medium- to coarse-grained and massive (Percival, 1989). Information on the depth or age of these intrusions in the Hornepayne area is not available.

2.2.3 Intrusive Rocks of the Wawa Subprovince

Black-Pic Batholith

The Black-Pic batholith is a regionally-extensive intrusion located within the Wawa Subprovince, encompassing an area of approximately 3,000 km². With the exception of several relatively small granitic intrusions (e.g., Strickland pluton), the bedrock underlying the southern survey block is entirely contained within this batholith (Figure 1.1).

The Black-Pic batholith comprises a multi-phase suite of hornblende-biotite monzodiorite, foliated tonalite, and pegmatitic granite, with subordinate foliated diorite, granodiorite, granite and crosscutting aplitic to pegmatitic dykes (Williams and Breaks, 1989; Zaleski and Peterson, 1993). Local lithological variations occur throughout the batholith, including upper levels of the tonalite, which are frequently cut by granitic sheets of pegmatite and aplite, and are generally more massive (Williams and Breaks, 1989). Also present throughout the batholith are zones of migmatized sedimentary rocks and massive granodiorite to granite. The contact between these rocks and the tonalitic rocks is gradational and associated with extensive sheeting of the tonalitic unit (Williams and Breaks, 1989; Williams et al., 1991).

The Black-Pic batholith is interpreted to be a domal structure with shallow dipping foliation radiating outward from its centre (Williams et al., 1991). Structurally deeper levels of the tonalite suite contain a strong sub-horizontal foliation and a weak north-trending mineral elongation lineation (Williams and

Breaks, 1989).

The age of emplacement of the Black-Pic batholith has been constrained by U-Pb (zircon) dating of the oldest recognized phase of the tonalite at ca. 2.720 Ga (Jackson et al., 1998). A younger monzodioritic phase has also been dated at ca. 2.689 Ga (Zaleski et al., 1999). The thickness of the batholith in the Hornepayne area is not known but regional geologic models of the area (e.g., Lin and Beakhouse, 2013) suggest it may extend to a considerable depth.

Strickland Pluton

Part of the Strickland pluton occurs in the southeast portion of the Hornepayne area bordering the Black-Pic batholith. The pluton occupies an area of approximately 600 km² and has maximum dimensions in the area of 34 km north-south and 55 km east-west (Figure 1.1). Stott (1999) described the Strickland pluton as a relatively homogeneous, quartz-porphyritic granodiorite. Although near the outer margin of the pluton, adjacent to greenstone belt rocks, granodiorite to tonalite and diorite are present. In the area west of the Kabinakagami greenstone belt, Siragusa (1977) noted that massive quartz monzonite (i.e., monzogranite in modern terminology) intrudes the granodioritic and trondhjemitic rocks in the form of medium-grained to pegmatitic dykes and small sills and irregular bodies.

Some degree of post-emplacement deformation and metamorphism of the Strickland pluton is indicated by the observed presence of fine- to medium-grained titanite and the widespread presence of hematite-filled fractures and weak alteration of silicate minerals (Stott, 1999). Stott (1999) noted that the pluton is petrographically similar to the ca. 2.697 Ga Dotted Lake batholith, located southwest of the Hornepayne area, and suggested that these plutons are members of an intrusive suite commonly found along the margins of greenstone belts in this part of the Wawa Subprovince.

No readily available information regarding the thickness of the Strickland pluton was found, although it may extend to a significant depth.

2.2.4 Mafic Dykes

Multiple diabase dyke swarms crosscut the Hornepayne area (Figure 1.1), including:

- Northwest-trending Matachewan dykes (ca. 2.473 Ga; Buchan and Ernst, 2004). This dyke swarm is one of the largest in the Canadian Shield. Individual dykes are generally up to 10 metres wide, and have vertical to subvertical dips. Matachewan dykes are mainly quartz-diabase dominated by plagioclase, augite, and quartz (Osmani, 1991).
- North-northeast-trending Marathon dykes (ca. 2.121 Ga; Buchan et al., 1996; Hamilton et al., 2002). These dykes form a fan-shaped distribution pattern around the northern, eastern, and western flanks of Lake Superior. The dykes vary in orientation from northwest to northeast, and occur as steep to subvertical sheets, typically a few metres to tens of metres thick, but occasionally up to 75 metres thick (Hamilton et al., 2002). The Marathon dykes are quartz-diabase dominated by equigranular to subophitic clinopyroxene and plagioclase (Osmani, 1991).
- Northeast-trending Biscotasing dykes (ca. 2.167 Ga; Hamilton et al., 2002). Locally, Marathon dykes also trend northeast and cannot be separated with confidence from the Biscotasing Suite dykes.

- Northeast-trending Abitibi dykes (ca. 1.14 Ga; Ernst and Buchan, 1993). These dykes occur locally in the Hornepayne area crosscutting older dykes.

The four dyke swarms in the Hornepayne area are generally distinguishable by their unique strike directions, crosscutting relationships and, to a lesser extent, by magnetic amplitude.

2.3 Structural History

Information on the structural history of the Hornepayne area is based predominantly on structural investigations of the Hornepayne and Dayohessarah greenstone belts (Polat, 1998; Peterson and Zaleski, 1999) and the Hemlo gold deposit and surrounding region (Muir, 2003). Additional studies by Lin (2001), Percival et al. (2006), and Williams and Breaks (1996) have also contributed to the structural understanding of the area. The aforementioned studies were performed at various scales and from various perspectives. Consequently, the following summary of the structural history of the Hornepayne area should be considered as a best-fit model that incorporates relevant findings from all studies. The structural history of the Hornepayne area is described below and summarized in Table 2.1.

The Hornepayne area straddles a structurally complex boundary between the metasedimentary-migmatitic Quetico Subprovince and the volcano-plutonic Wawa Subprovince within the Archean Superior Province.

The structural history of the Hornepayne and nearby Schreiber-Hemlo greenstone belts is generally well characterized and includes multiple phases of deformation (Polat et al., 1998; Peterson and Zaleski, 1999; Lin, 2001; and Muir, 2003). Polat et al. (1998) interpreted that the Schreiber-Hemlo and surrounding greenstone belts represent collages of oceanic plateaus, oceanic arcs, and subduction-accretion complexes amalgamated through subsequent episodes of compressional and transpressional collision.

On the basis of overprinting relationships between different structures, Polat et al. (1998) suggested that the Schreiber-Hemlo greenstone belt underwent at least two main episodes of deformation that also affected rocks of the Wawa Subprovince, including the Hornepayne area. These deformation events can be correlated with observations from Peterson and Zaleski (1999) and Muir (2003), who reported at least five and six generations of structural elements, respectively. Two of these generations of structures account for most of the ductile strain, and although others can be distinguished on the basis of crosscutting relationships, they are likely the products of progressive strain events. Integration of the structural histories detailed in Williams and Breaks (1996), Polat et al. (1998), Peterson and Zaleski (1999), Lin (2001), and Muir (2003) suggests that six deformation events occurred within the Hornepayne area. The first four deformation events (D_1 - D_4) are associated with brittle-ductile deformation of the greenstone belts. D_5 and D_6 were associated with a combination of brittle deformation and fault propagation through all rock units in the Hornepayne area. The main characteristics of each deformation event are summarized in Table 2.1.

Table 2.1: Summary of the Geological and Structural History of the Hornepayne Area (adapted from AECOM, 2014)

Approximate Time Period (years before present)	Geological Event
2.89 to 2.77 Ga	Progressive growth and early evolution of the Wawa-Abitibi terrane by collision, and ultimately accretion, of distinct geologic terranes
2.770 – 2.673 Ga	<ul style="list-style-type: none"> - ca. 2.720 Ga: Volcanism and subordinate sedimentation associated with the formation of the Manitouwadge-Hornepayne greenstone belt - ca. <2.693: Deposition of sedimentary rocks in the Hornepayne greenstone belt and the Quetico Subprovince - ca. 2.720-2.678 Ga: Inferred emplacement of granitoid intrusions in the Hornepayne area. Emplacement of the Pukaskwa and Black-Pic gneissic complexes at ca. 2.72 Ga Emplacement of Loken Lake pluton (ca. 2.687 Ga), Nama Creek pluton (2.680 Ga), and Fourbay Lake pluton (ca. 2.678 Ga) - ca. 2.719 to 2.673 Ga: Four generations of ductile-brittle deformation (D₁-D₄) D₁: ca. 2.719 – 2.691 Ga D₂: ca. 2.691 – 2.683 Ga D₃: ca. 2.682 – 2.679 Ga D₄: ca. 2.679 – 2.673 Ga
2.675 to 2.669 Ga	Peak metamorphism of the Hornepayne greenstone belt
2.666 to 2.650 Ga	Peak metamorphism of the Quetico Subprovince
2.5 to 2.100 Ga	<ul style="list-style-type: none"> - ca. 2.5 Ga: Supercontinent fragmentation and rifting in Lake Superior area; development of the Southern Province - ca. 2.473 Ga: Emplacement of the Matachewan dyke swarm - ca. 2.167 Ga: Emplacement of Biscotasing dyke swarm - ca. 2.121 Ga: Emplacement of the Marathon dyke swarm
1.9 to 1.7 Ga	Penokean Orogeny in Lake Superior and Lake Huron areas; possible deposition and subsequent erosion in the Hornepayne area
1.150 to 1.090 Ga	Rifting and formation of the Midcontinent Rift structure - ca. 1.1 Ga
540 to 355 Ma	Possible coverage of the area by marine seas and deposition of carbonate and clastic rocks subsequently removed by erosion
145 to 66 Ma	Possible deposition of marine and terrestrial sediments of Cretaceous age, subsequently removed by erosion
2.6 to 0.01 Ma	Periods of glaciation and deposition of glacial sediments

The earliest recognizable deformation phase (D₁) is associated with rarely preserved small-scale isoclinal (F₁) folds, ductile shear zones that truncate, and a general lack of penetrative foliation development. Peterson and Zaleski (1999) reported that an S₁ foliation is only preserved locally in outcrop and in thin section. D₁ deformation is poorly constrained between ca. 2.719 and ca. 2.691 Ga (Muir, 2003).

D₂ structural elements include prevalent open to isoclinal F₂ folds, an axial planar S₂ foliation, and L₂ mineral elongation lineations (Peterson and Zaleski, 1999). Muir (2003) interpreted D₂ to have resulted from progressive north-northeast to northeast directed compression that was coincident with the intrusion of various plutons. The S₂ foliation is the dominant meso- to macro-scale regional fabric evident across the study area. Ductile flow of volcano-sedimentary rocks between more competent batholiths may also have occurred during D₂ deformation. This generation of deformation is constrained to between ca. 2.691 and ca. 2.683 Ga (Muir, 2003).

D₃ deformation was the result of northwest-southeast shortening during regional dextral transpression. D₃ structural elements include macroscale F₃ folds, including the regional scale isoclinal fold developed within the Hornepayne greenstone belt (Figure 1.1), and local shear fabrics that exhibit a dextral sense of motion and overprint D₂ structures (Peterson and Zaleski, 1999; Muir, 2003). D₃ deformation did not develop an extensive penetrative axial planar and (or) crenulation cleavage. D₃ deformation is constrained to between ca. 2.682 and ca. 2.679 Ga (Muir, 2003).

D₄ structural elements include isolated northeast-plunging F₄ kink folds with a Z-asymmetry, and associated small-scale fractures and faults overprinting D₃ structures. D₃-D₄ interference relationships are best developed in the Hornepayne greenstone belt and in rocks of the Quetico Subprovince (Muir, 2003). D₄ deformation is roughly constrained to between ca. 2.679 and ca. 2.673 Ga (Muir, 2003).

Details of structural features associated with the D₅ and D₆ deformation events are limited in the literature to brittle faults of various scales and orientations (Lin, 2001; Muir, 2003). Within the Hemlo greenstone belt, Muir (2003) suggested that local D₅ and D₆ faults offset the Marathon and Biscotasing dyke swarms (all ca. 2.2 Ga), and as such, suggested that in the Hemlo region D₅ and D₆ faults propagated after ca. 2.2 Ga. However, since there are no absolute age constraints on specific events, the entire D₅-D₆ interval of brittle deformation can only be constrained to a post-2.673 Ga timeframe that may include many periods of re-activation attributable to any of several post-Archean tectonic events.

2.3.1 Mapped Structures and Named Faults

In the Hornepayne area, in both the Quetico and Wawa subprovinces, only three unnamed faults are indicated on public domain geological maps (Figure 1.1) within the northern and southern survey blocks. These faults display two dominant orientations: northeast and northwest.

Outside of the Hornepayne survey blocks, the east-northeast-trending Shekak River fault, which is mapped immediately east of the Hornepayne southern block affects granitic rocks of the Black-Pic batholith.

2.3.2 Metamorphism

Studies on metamorphism in Precambrian rocks across the Canadian Shield have been summarized in multiple publications (e.g., Fraser and Heywood, 1978; Kraus and Menard, 1997; Menard and Gordon, 1997; Berman et al., 2000; Easton, 2000a, 2000b; and Berman et al., 2005) and the thermochronological record for large parts of the Canadian Shield is documented in a number of studies (Berman et al., 2005; Bleeker and Hall, 2007; Corrigan et al., 2007; and Pease et al., 2008).

The Superior Province of the Canadian Shield largely preserves low pressure, high temperature Neoproterozoic (ca. 2.710-2.640 Ga) metamorphic rocks. The relative timing and grade of regional metamorphism in the Superior Province corresponds to the lithological composition of the subprovinces (Easton, 2000a; Percival et al., 2006). Subprovinces comprising volcano-sedimentary assemblages and synvolcanic to syntectonic plutons (i.e., granite-greenstone terranes) are affected by relatively early lower greenschist to amphibolite facies metamorphism. Subprovinces comprising both metasedimentary- and migmatite-dominated lithologies, such as the English River and Quetico, and dominantly plutonic and orthogneissic domains, such as the Winnipeg River, are affected by relatively late middle amphibolite to granulite facies metamorphism (Breaks and Bond, 1993; Corfu et al., 1995). Subgreenschist facies metamorphism in the Superior Province is restricted to limited areas, notably within the central Abitibi greenstone belt (e.g., Jolly, 1978; Powell et al., 1993).

In general, most of the Canadian Shield preserves a complex episodic history of Neoproterozoic metamorphism overprinted by Paleoproterozoic tectonothermal events culminating at the end of the Grenville orogeny ca. 950 Ma. The distribution of contrasting metamorphic domains in the Canadian Shield is a consequence of relative uplift, block rotation, and erosion resulting from Neoproterozoic orogenesis, subsequent local Proterozoic orogenic events and broader epeirogeny during later Proterozoic and Phanerozoic eons.

In the Hornepayne area, metasedimentary rocks of the Quetico Subprovince exhibit granulite facies metamorphic conditions close to the boundary between the Wawa and Quetico subprovinces (Williams and Breaks, 1989, 1996; Zaleski and Peterson 1995; Pan et al., 1994).

Geothermobarometric and geochronological calculations by Pan et al. (1994) indicate that low pressure-high temperature, amphibolite facies metamorphism in metasedimentary rocks of the Quetico Subprovince had been in place before ca. 2.666 Ga, in agreement with the period ca. 2.671-2.665 Ga estimated by Percival and Sullivan (1988). This prograde amphibolite facies regional metamorphism would have been initiated ca. 2.675 Ga, increased after ca. 2.666 Ga and reached granulite facies under a thermal peak of 680-700 degrees Celsius (°C) and 4-6 Kbar perhaps ca. 2.658 Ga. Granulite facies metamorphism would have lasted until ca. 2.650 Ga, after which a retrograde event would have occurred at 550-660°C, 3-4 Kbar. After the retrogression, hydrothermal alteration occurred at 200-400°C, 1-2 Kbar.

Within the Black-Pic batholith and other smaller plutons typically display greenschist facies metamorphism (Geofirma, 2013). Locally, higher metamorphic grades up to upper amphibolite facies are recorded in rocks along the margins of plutons. No records exist that suggest that rocks in the Hornepayne area may have been affected by thermotectonic overprints related to post-Archean events.

2.4 Quaternary Geology

The Quaternary geology of the Hornepayne area is described in detail in the remote sensing and terrain evaluation completed as part of the Phase 1 Geoscientific Desktop Preliminary assessment (JDMA, 2013). An overview of the relevant Quaternary features is summarized below.

The Quaternary sediments in the Hornepayne area comprise glacial and post-glacial materials that overlie the bedrock. All glacial landforms and related materials are associated with the Wisconsinan glaciation, which began approximately 115,000 years ago (Barnett, 1992). Throughout the majority of the Hornepayne area, bedrock outcrops are common and the terrain is dominantly classified, for surficial purposes, as a bedrock-drift complex, i.e., thin drift cover that only locally achieves thicknesses that mask or subdue the bedrock topography. When present, drifts overlying the bedrock are typically limited in thickness and the ground surface reflects the bedrock topography. Beyond bedrock-drift complexes, valleys and lowland areas present, which typically exhibit extensive and thick surficial deposits, frequently have a linear geometry.

The main direction of the most recent glacial advance in the Hornepayne area was from the north-northeast (Gartner and McQuay, 1980a; 1980b). In the Hornepayne area, a common glacial deposit is stony, sandy till (ground moraine) which forms a veneer in rocky upland areas. The till composition is variable and two types are regionally recognizable (Geddes et al. 1985; Geddes and Kristjansson, 1986). A moderately loose, locally derived, very stony variety with a sandy texture dominates in areas of thin till cover in the western part of the area. A calcareous, silty till, rich in "exotic" carbonate lithologies derived from the James Bay Lowland (Geddes and Kristjansson, 1986) occurs in two

facies, one of which is stone poor, massive, silty, and quite dense. The other more dominant facies is less compact and slightly sandier, and has a variable stone content. In some areas, the calcareous till is capped by coarser, locally derived till or till-like material. Geddes and Kristjansson (1986) noted that in areas where there is little relief on the land surface, the calcareous till is usually prominent, especially in areas on the leeward side of significant topographic features. It is typical of the stony till to have a more hummocky or moranic surface expression.

The most significant Quaternary landforms occurring in the southern survey block of the Hornepayne area are two large northeast-trending esker complexes in the Bayfield Lake and West Larkin Lake-Shekak River areas. These esker complexes consist of sands and gravels and can exceed 15 metres in depth (Gartner and McQuay, 1980a; 1980b). The most significant Quaternary landforms occurring in the northern survey block are moraine in the southeastern part, and glaciolacustrine plains in the northwestern part.

Glaciolacustrine sediments cover the west-central portion and form a narrow northeastern belt that transects the southern survey block, and partly cover the northwest corner of the northern block. These sediments comprise stratified to laminated sand, silt, and clay that were deposited during the incursion of glacial lakes (Prest, 1970; Gartner and McQuay, 1980a; 1980b; Kettles and Way Nee, 1998). The thickness of glaciolacustrine deposits is variable, ranging from several tens of metres to a relative thin drape over bedrock (Kettles and Way Nee, 1998).

Minor organic-rich alluvial deposits and eolian deposits are also locally present throughout the Hornepayne area, and have limited extents. Alluvial deposits are organic-rich, consist of sand, silt and clay, and are typically present along water courses. Eolian deposits consist of sand and are present as dunes developed on certain glacial deposits (Gartner and McQuay, 1980a; 1980b; Geddes and Kristjansson, 1986; Kettles and Way Nee, 1998).

3 Data Source Acquisition and Quality

Sander Geophysics Limited (SGL) completed a fixed-wing high-resolution airborne magnetic and gravity survey in the Hornepayne area between July 26 and October 7, 2015. The survey area comprised two survey blocks north and south of the settlement area of Hornepayne. The survey blocks were designed to cover the potentially suitable areas in the Black-Pic batholith and metasedimentary rocks in the Quetico Subprovince identified in the Phase 1 preliminary assessment and capture relevant geological features.

The survey included a total of 12,694 km flight lines covering a surface area of over 1,000 km². Flight operations were conducted out of the Manitouwadge Municipal Airport, in Manitouwadge, Ontario using a Cessna 208B Grand Caravan. Data were acquired along traverse lines flown in an east-west direction spaced at 100 m, and control lines flown north-south spaced at 500 m. Control lines were continued between the Hornepayne North and Hornepayne South blocks allowing for lower resolution data coverage in the area in-between (Figure 1.2). The survey was flown at an approximate altitude of 80 m above ground level, with an average ground speed of 100 knots (approximately 185 km/h or 50 m/s). Airborne magnetic and gravity data were acquired using equipment with very high sensitivity and accuracy. The airborne magnetic data was recorded using a magnetometer sensor mounted in a fiberglass stinger extending from the tail of the aircraft. The airborne gravity data was recorded using a gravimeter, which includes three orthogonal accelerometers that are mounted on a stabilized platform inside the cabin of the aircraft. Table 3.1 gives a quick reference of the details of the survey.

Table 3.1: Survey Details

Survey Particulars	
Survey Start Date:	July 26, 2015
Survey End Date:	October 7, 2015
Field Office Location:	Manitouwadge
Airport Used:	Manitouwadge Municipal Airport (CYMG)
Aircraft Type:	Cessna 208B Grand Caravan
Total line kilometers:	12,693.5
Traverse Line numbers:	1001 – 1490
Traverse Line direction:	east –west
Traverse Line spacing:	100 m
Control Line numbers:	166 – 242, 806- 815, 817, 819
Control Line direction:	north – south
Control Line spacing:	500 m
Survey Altitude:	Smoothed drape with target height of 80 m above ground
Digital Terrain Source:	SRTM
Number of Flights (numbers):	22 (2004 – 2007, 2009 – 2011, 2013, 2015, 2017 – 2023, 2025 – 2027, 2030, 2033, 2064)
Aircraft Target Ground Speed:	100 knots
Magnetic Field Reference location	(NAD83 UTM 16N): 545,105 m E, 5,427,638 m N
Magnetic Field Inclination (+ve down):	74.3388°
Magnetic Field Declination (+ve east):	-6.9914°
Approximate total field value:	56,669.4 nT

Magnetic Reference Field Model:	World Magnetic Model (2015) interpolated to date and location of acquisition
Fundamental Gravity Network Ties:	Referenced to the local gravity value established by Sander Geophysics at the Ottawa Airport
Survey Base Gravity Value:	980854.00 mGal
Survey Base Parking Location (NAD83):	583,674.60 m E 5,437,649.6 m N Height: 331.306 m (above WGS-84 ellipsoid)
Base Station Locations (NAD83):	REF1: 587,100.5 m E, 5,442,586.9 m N Height: 290.93 m (above WGS-84 ellipsoid) REF2: 587,097.4 m E, 5,442,600.3 m N Height: 292.54 m (above WGS-84 ellipsoid) REF3: 584,501.4 m E, 5,441,099.0 m N Height: 307.26 m (above WGS-84 ellipsoid)
Field Acquisition Datum:	WGS-84
UTM Projection:	UTM 16N

3.1 Magnetic Data

Total magnetic field measurements were recorded with a single cesium magnetometer mounted in a fibreglass stinger extending from the tail of the survey aircraft. SGL's hardware and software system, AIRComp, was used to remove the effects of the aircraft and its manoeuvres from the recorded magnetic data. Coefficients to be used for compensation were derived by processing the calibration flight data, based on principles presented by Leliak (1961). The compensation coefficients were applied to data recorded during normal survey operations to produce compensated magnetic data.

Low-pass filtered reference station diurnal was subtracted from the airborne data on a reading by reading basis. As more than one reference station was used, the reference station value could be interpolated, based on the relative distance of the reading from each reference station.

Both the ground and airborne systems used the Geometrics G-822A cesium magnetic sensor. Total magnetic field measurements were recorded at 160 Hz in the aircraft, and then later down sampled to 10 Hz in the processing. A second order Butterworth 0.9 Hz low pass filter is utilised in the process for compensation and anti-aliasing. The ground systems recorded magnetic data at 11 Hz.

A pre-planned drape surface was prepared for the survey to guide the aircraft over the topography in a consistent manner, as close to the minimum clearance as possible. The drape surface was prepared with digital elevation model (DEM) data obtained from the Shuttle Radar Topography Mission (SRTM) (<http://srtm.usgs.gov/>) for the area. The DEM included an extension beyond the survey boundary to allow the aircraft to achieve the drape clearance before coming on line.

Details of the processing of the magnetic data are provided in Section 4.2 of this report.

3.2 Gravity Data

Gravity data were acquired with SGL's propriety AIRGrav (*Airborne Inertially Referenced Gravimeter*) system, which uses a Schuler tuned inertial platform supporting three orthogonal accelerometers, which remain fixed in inertial space, independent of the manoeuvres of the aircraft, allowing precise isolation from the effects of the movement of the aircraft. The gravity sensor used in AIRGrav is a very

accurate accelerometer with a wide dynamic range. The system is not affected by the strong vertical motions of the aircraft, allowing the final gravity data to be almost completely unaffected by in-flight conditions classified as “moderate turbulence” or better. The instrument is also considered to be an inertial navigator and as such, the platform levelling was essentially unaffected by horizontal accelerations.

In typical survey flying, accelerations in an aircraft can reach 0.1 G, equivalent to 100,000 milligal. Data processing must extract gravity data from this very noisy environment. This was achieved by modelling the gravity due to movements of the aircraft in flight as measured by extremely accurate Global Positioning System (GPS) measurement. These measurements are affected by noisy conditions in the ionosphere, and by the variable conditions (e.g. temperature, pressure and humidity) within the troposphere. SGL has developed a full suite of programs to carry out all the necessary corrections.

The GPS data are extracted from the airborne and reference station acquisition system and reformatted. Differential corrections to correct the airborne ranges for variations calculated from the base station GPS data were performed. Each recorded position was recalculated based on these ranges. The original reference system for all GPS data was the WGS-84 datum. Positions were then converted to the local datum, reference system and desired projection. Each line was then checked for data continuity and quality.

An extremely accurate location of the base station GPS receiver is determined using an IGS permanent GPS Reference Station to apply differential corrections (<http://igs.org/network>). This technique provides a final base station receiver location with an accuracy of better than a few decimetres. The entire airborne data set is then reprocessed differentially using the recalculated base station location.

Gravity data were recorded at 128 Hz. Accelerations were filtered and resampled to 10 Hz to match the GPS, using specially designed filters to avoid biasing the data. Gravity was calculated by subtracting the GPS derived accelerations from the inertial accelerations. The calculated gravity was corrected for the Eötvös effect and latitude corrected (i.e. normal gravity), and the sample interval was then reduced to 2 Hz. These operations were all performed by SGL’s proprietary GravGPS software. A detailed description of gravity processing is provided in Section 4.1 of this report.

3.3 Digital Elevation Data

Digital elevation data were collected during the survey using a laser altimeter (Riegl LD90-31K-HiP) mounted to the base of the aircraft. The elevation data were sampled at a rate of 3.3 Hz, which is consistent with a sample roughly every 16 m along the profile line. Even though the laser altimeter can record returns from more than 700 m above the ground with a high degree of certainty, some laser data dropouts occurred while flying over the areas of poor reflectivity. The laser data shows the effects of the dense tree cover; variable penetration of the canopy results in a high-frequency variation of recorded altitude. The raw laser data were processed with an iterative de-spiking routine designed to remove many of the early laser returns from trees.

Digital elevation data were also collected using a King radar altimeter mounted to the base of the aircraft. Elevation data were sampled at a rate of 10 Hz, which is consistent with a sample roughly every 6 m. The radar data penetrates the canopy less as it records the first return within the footprint of its signal. The radar altimeter data were filtered to remove high-frequency noise using a 67-point low pass filter.

A digital elevation model (DEM) was derived by subtracting the laser altimeter data from the differentially corrected DGPS altitude with respect to the Canadian Geodetic Vertical Datum 2013 (CGVD2013). Short sections of poor laser data due to locally weak reflectivity were replaced using King radar data. The DEM reflects the presence of vegetation (for example trees) and buildings and thus is not considered to be a digital terrain model (DTM).

The digital elevation data were gridded to form a DEM grid using a cell size of 25 m over the Hornepayne survey area. The 25 m gridding cell was applied to present the highest resolution of the digital elevation model within the boundaries of the survey block comprising the principal survey area (Figure 3.1).

3.4 Additional Data Sources

In addition to the acquired data, a number of other publically available data sources were used. These are detailed below.

3.4.1 OGS Mapped Bedrock Geology

The Precambrian Geoscience Section of the Ontario Geology Survey has compiled a 1:250,000 scale map of the bedrock geology of Ontario (OGS, 2011). This map was recently revised and issued as 'Miscellaneous Release – Data 126 – Revision 1'. The data is publically available as a seamless GIS data set and includes such details as bedrock units, major faults, dyke swarms, iron formations and kimberlites. The Ontario Geology Survey bedrock geology map has been further updated based on information from the Precambrian geology compilation map series (M2668; Johns and McIlraith, 2003). This resource was of fundamental importance in assisting with the geophysical interpretation of the acquired potential field data. The mapped bedrock geology was used for both qualitative and quantitative aspects of the interpretation. In the case of the qualitative interpretation, the mapped bedrock geology gave the overall context for the magnetic and gravity data. For the 2.5D modelling, the mapped bedrock geology provided initial surface constraints.

3.4.2 Geological Base Maps

Several additional geological maps are available (P0288, M2129, OFM0142, P0476, M2355) in and around the Hornepayne survey area (Fenwick, 1965; 1967; Williams and Breaks, 1990; Giblin, 1968; Siragusa, 1976). The bedrock geologic information was assessed and incorporated as needed into the project geodatabase. Structural measurements including foliations, gneissic layering and bedding planes, folds and faults provided structural constraints and were incorporated into the qualitative and quantitative interpretations.

3.4.3 OGS PETROCH Lithochemical Database

The Ontario Geological Survey has a publicly available PETROCH Lithochemical Database (Haus and Pauk, 2010). The database contains detailed rock chemical data collected by OGS geoscientists, which includes information about rock type, chemical composition, age, stratigraphy, major oxide values, sample location and specific gravity. Twenty-three data points are located immediately southeast of the Hornepayne survey area in the Strickland pluton and 8 are located west of the survey area, west of the Dayohessarah greenstone belt. This information was used in the interpretation to: 1) obtain further information on the composition of major mapped rock units where samples have been taken; and 2) constrain the density of rock units used in the 2.5D modelling.

3.4.4 Densities and Magnetic Susceptibilities

Bedrock densities and magnetic susceptibilities in the Hornepayne area were gathered from a database maintained by the Geological Survey of Canada (GSC, 2015). The database includes classification of rock type, and measured densities and magnetic susceptibilities. Three data points occur directly within the survey area – in the Black-Pic batholith and the metasedimentary rocks of the Quetico Subprovince, and 21 occur in the rock units immediately surrounding the survey area. No magnetic susceptibility values were given for these rock units and only the density information was used in the modelling.

3.4.5 Ontario Precambrian Bedrock Magnetic Susceptibility Geodatabase

The Ontario Geological Survey has a publicly available Ontario Precambrian Bedrock Magnetic Susceptibility Geodatabase for 2001 to 2012 (Muir, 2013), which is known as Miscellaneous Release – Data 273 (MRD 273-Rev). This GIS database contains measurements of magnetic susceptibilities and rock classifications for points across Ontario. No data points occur directly within the Hornepayne area, but 61 occur 55 km west of the Hornepayne area.

3.4.6 Other Magnetic Susceptibility Measurements

Additional magnetic susceptibility data was obtained from Miles (1998) for several lithologies in the region of the Manitouwadge greenstone belt west of the Hornepayne area. Statistics (minimum, maximum, mean, standard deviation) were presented. The lithologies and unit numbers/name were simplified from Zaleski and Peterson (1995). These values are based on samples collected in the vicinity of the Manitouwadge Synform, 55 km west of the Hornepayne survey area.

4 Geophysical Data Processing Methods

4.1 Gravity Data Processing

Advanced gravity processing allows for the generation of high-resolution gravity data. These processes involve the use of GPS phase angle corrections, the integration of GPS processing with inertial data from the gravimeter and the advanced analysis of system states and uncertainties. This processing helps reduce system noise and allows for the generation of high quality, low noise raw gravity data through a wider range of survey conditions than was previously possible. The following standard corrections were applied to the gravity data (Telford et al 1990; Blakely, 1996):

- a. Eötvös correction,

$$\delta g_{Eötvös} = -2 W_s v_x \cos \Phi - \frac{v_x^2}{\frac{r}{(1 - e^2 \sin^2 \Phi)^{1/2}} + h} - \frac{v_y^2}{\frac{r(1 - e_2)}{(1 - e^2 \sin^2 \Phi)^{3/2}} + h}$$

where Φ is the latitude of the aircraft, v_x and v_y are the velocities of the aircraft in the x (east) and y (north) direction, r is the Earth's radius at the equator (6,378,137 m), e is a correction for Earth's flattening towards the poles (0.0818191908426), W_s is the angular velocity of Earth's rotation ($7.2921158553 \times 10^{-5}$ rad/s), and h is the altitude of the plane above the ellipsoid;

- b. Normal gravity,

$$g_{Normal} = \frac{9.7803267715 (1 + 0.0019318513353 \sin^2 \Phi)}{\sqrt{1 - 0.0066943800229 \sin^2 \Phi}}$$

where Φ is the latitude of the aircraft;

- c. Free air correction,

$$g_{fa} = - (0.3087691 - 0.0004398 \sin^2 \Phi) h + 7.2125 \times 10^{-8} h^2$$

where h is the height of the aircraft in metres above the ellipsoid;

- d. Full 3D Bouguer correction, g_b . See below for a description of the Bouguer correction technique;
 e. Static correction, g_{sc} , based on static ground recordings and repeat lines;
 f. Level correction, g_{lc} , based on line intersections.

Thus, the Bouguer anomaly in mGal is determined:

$$BouguerAnomaly = G - g_{fa} - g_b - g_{sc} - g_{lc}$$

where G is the calculated gravity in mGal adjusted for Eötvös effect and normal gravity.

4.1.1 Bouguer Correction

Shuttle Radar Topography Mission (SRTM) digital elevation model data were used to calculate the Bouguer corrections for gravity processing. The SRTM data contains information in a grid with a 3 arcsecond spacing, approximately equal to 100 m cell spacing, which has a higher density than the line spacing for this survey, and therefore provides terrain data at a better resolution between the survey lines than the SRTM data. Coverage up to 160 km from the survey block was kept for accurate regional corrections.

Terrain corrections were computed using software developed by SGL. The algorithm calculates the topographic attraction of the terrain using a mass prism model with a constant density. The difference between the topographic attraction and the simple Bouguer correction is the terrain correction. The terrain and Bouguer corrections were calculated for the bedrock at the height of the aircraft using a density of 2.67 g/cm³.

Terrain corrections were filtered to match the degree of filtering applied to the gravity data as described below.

4.1.2 Static and Level Corrections

The gravimetric data were levelled to compensate for instrument variations in two steps. A single constant shift determined from ground static recordings was applied on a flight-by-flight basis. The pre- and post-flight readings were averaged for each flight and the difference between the average value and the local gravity value was removed. This acts as a simple but effective coarse levelling of the data.

Intersection statistics were then used to adjust individual survey lines. Unlike magnetic levelling, individual intersections were not used to make corrections. Instead, intersection differences from whole lines were averaged and a single adjustment was applied to each survey line and each control line. Minor adjustments were calculated for sections of each line based on statistics from groups of intersections. The adjustments were smoothed and applied to line data that was filtered as described below. Grids of adjusted data were inspected to determine that the adjustments were appropriate.

4.1.3 Gridding and Filtering

Statistical noise in the data was reduced by applying a cosine tapered low-pass filter to the time series line data. For this survey, a 20 second (1000 m) half-wavelength filter was employed. The data were gridded using a minimum curvature algorithm that averages all values within any given grid cell and interpolates the data between survey lines to produce a smooth grid. The algorithm produces a smooth grid by iteratively solving a set of difference equations by minimizing the total second horizontal derivative while attempting to honour the input data (Briggs, 1974). Grids were generated using a 25 m grid cell size.

Low-pass spatial filtering is applied to the grid for noise reduction. Essentially, the survey area is over-sampled as the line spacing is smaller than the grid filter used. A range of grid filters were used and evaluated for noise levels and signal content. Final data for this survey was filtered with a 1.0 km half-wavelength grid filter.

The gravity data were gridded using a cell size of 25 m and 250 m over the Hornepayne area. The 25 m gridding cell was applied to present the highest resolution of data within the boundary of the survey block, comprising the principal survey area. The 250 m gridding cell was applied to include the

extensions of the flight lines beyond the survey block, comprising the extended survey area. The Bouguer gravity with a terrain correction of 2.67 g/cm³ is displayed in Figures 4.1 (principal survey area, grid cell size of 25 m) and Figure 4.2 (extended survey area, grid cell size of 250 m). The Free Air gravity is displayed in Figures 4.3 (principal survey area, grid cell size of 25 m) and Figure 4.4 (extended survey area, grid cell size of 250 m).

4.2 Magnetic Data Processing

The airborne magnetometer data were recorded at 160 Hz, and down sampled to 10 Hz for processing. A second order Butterworth 0.9 Hz low pass filter is utilized in the process for compensation and anti-aliasing. All magnetic data were plotted and checked for any spikes or noise. A 0.244 second static lag correction due to signal processing, plus a dynamic lag correction which varies between 0.04 s and 0.06 s, depending on the instantaneous velocity of the aircraft, was determined on a line-by-line basis using SGL's Dynlag software.

Ground magnetometer data were inspected for cultural interference and edited where necessary. All reference station magnetometer data were filtered using a 121-point low-pass filter to remove any high-frequency noise, but retain the low-frequency diurnal variations.

A correction for the International Geomagnetic Reference Field (IGRF) year 2015 model was applied to all ground magnetometer data using the fixed ground station location and the recorded date for each flight. The mean residual value of the reference station was calculated (173.141 nT) and subtracted to remove any bias when correcting the local anomalous field on the survey grid. Diurnal variations in the airborne magnetometer data were removed by subtracting the reference station data after subtraction of the mean residual.

The airborne magnetometer data were also corrected for the IGRF using the location, altitude, and date of each point. IGRF values were calculated using the year 2015 IGRF model. The altitude data used for the IGRF corrections are DGPS heights above the WGS84 datum.

4.2.1 Levelling

Intersections between control and traverse lines were determined by a program which extracts the magnetic, altitude, and x and y values of the traverse and control lines at each intersection point. Each control line was adjusted by a constant value to minimize the intersection differences, calculated as follows:

$\sum|i - a|$ summed over all traverse lines, where:

i = (individual intersection difference)

a = (average intersection difference for that traverse line)

Adjusted control lines were further corrected locally to minimize any residual differences. Traverse line levelling was carried out by a program called CLEVEL that interpolates and extrapolates levelling values for each point based on the two closest differences at intersections. After traverse lines were levelled, the control lines are matched to them. This ensured that all intersections tie very closely and permitted the use of all data in the final products.

CLEVEL provides a curved correction using a function similar to spline interpolation. A third degree polynomial was used to interpolate between two intersections. CLEVEL allows intersection points to be preserved with no mismatch and interpolation is smooth with the first derivative continuously approaching the same value from both sides of the intersection points.

The levelling procedure was verified through inspection of the magnetic anomaly and vertical derivative grids, by plotting profiles of corrections along lines, and by examination of levelling statistics to check for steep correction gradients.

4.2.2 Micro-Levelling

Micro-levelling is occasionally applied to magnetic data to remove any residual diurnal effects by using directional filters to identify and remove artifacts that are long wavelengths parallel to survey lines and short wavelengths perpendicular to survey lines. No micro-levelling was applied to the Hornepayne magnetic data.

4.2.3 Gridding

The grid of the total magnetic intensity was made using a minimum curvature algorithm to create a two-dimensional grid equally sampled in the x and y directions following Briggs (1974). The final grids of the magnetic data were created with 25 m grid cell size appropriate for survey lines spaced at 100 m. Grids were also made that included the 1000 m spaced lines that extend out from the main block area. These were gridded with a cell size of 250 m. The magnetic data were gridded using a cell size of 25 m and 250 m over the Hornepayne area. The 25 m gridding cell was applied to present the highest resolution of data within the boundary of the survey block, comprising the principal survey area. The 250 m gridding cell was applied to include the extensions of the flight lines beyond the survey block, comprising the extended survey area. The total magnetic intensity (or more correctly, the magnetic anomaly) is displayed in Figures 4.5 (principal survey area, grid cell size of 25 m) and Figure 4.6 (extended survey area, grid cell size of 250 m).

4.3 Gravity and Magnetic Derivative Products

Filters may be applied to the data to enhance different wavelength information that arises from different sources. In many cases, filtering is best achieved by transforming the data from the space domain to the frequency domain by Fourier transform since frequency characteristics of the filter to be applied are more precisely defined in the frequency domain. The filtered derivatives created to assist with interpretation are described below.

4.3.1 Total Magnetic Intensity Reduced to Pole

Reduction to the pole (RTP) transforms anomalies as if they were at the north magnetic pole. The basic assumption is that magnetic anomalies arise from induced magnetization. This assumption may not always be true where significant magnetic remanence occurs. The method allows direct comparison of anomaly shapes from different magnetic latitudes, and if the assumptions hold true, the anomaly will be symmetrically disposed about the causative body. Reduction to pole is essentially a phase shift filter applied in the frequency domain, and is described by Baranov and Naudy (1964):

$$F(k_x, k_y) = \frac{1}{[\sin I + i \cos I \cos(D - \theta)]^2}$$

where

- θ is the angle in the k_x k_y plane
- I is the local magnetic inclination
- D is the local magnetic declination

For ease of calculation, this transformation was performed through filtering in the frequency domain using a constant (average/central) inclination and declination which was considered valid throughout the entire grid. The inclination used was 74.394°, and the corresponding declination used was -7.953° representing a station approximately at the centre of the survey. The total magnetic intensity reduced to the pole is shown in Figure 4.7 (principal survey area, grid cell size of 25 m) and Figure 4.8 (extended survey area, grid cell size of 250 m).

4.3.2 Vertical Derivatives of Total Magnetic Intensity and Bouguer Gravity

If k_x and k_y are the wave numbers of the potential field in the two-dimensional frequency domain, the n^{th} vertical derivative of a potential field is easily derived in the Fourier domain by applying the following filter:

$$F(k_x, k_y) = (-k)^n \quad \text{where } k = \sqrt{(k_x^2 + k_y^2)}$$

Vertical derivatives act as high-pass filters that enhance high-frequency data and suppress low-frequency data. The first vertical derivative ($n=1$) enhances the rapid changes in gravity or magnetic field at the edges of anomalies and is therefore useful for delimiting the extents of causative bodies. The second vertical derivative ($n=2$) enhances high-frequency signal variations even more, such that textural variations in the character or the potential field (especially for magnetic data) can be used to delimit domains of a specific geophysical response.

The first vertical derivative of the reduced to pole total magnetic intensity is shown in Figure 4.9 (principal survey area, grid cell size of 25 m) and Figure 4.10 (extended survey area, grid cell size of 250 m). The first vertical derivative of the Bouguer gravity with a terrain correction using a density of 2.67 g/cm³ is shown in Figure 4.11 (principal survey area, grid cell size of 25 m) and Figure 4.12 (extended survey area, grid cell size of 250 m). The first vertical derivative of the free air gravity is shown in Figure 4.13 (principal survey area, grid cell size of 25 m) and Figure 4.14 (extended survey area, grid cell size of 250 m). The second vertical derivative of the pole reduced total magnetic intensity is shown in Figure 4.15 (principal survey area, grid cell size of 25 m) and Figure 4.16 (extended survey area, grid cell size of 250 m). The gravity data do not contain high-frequency information to render its second vertical derivative useful for interpretation.

4.3.3 Total Horizontal Gradient of Total Magnetic Intensity and Bouguer Gravity

Horizontal gradients are most conveniently calculated in the space domain. Total horizontal gradient of a potential field (T) is from the gradients in the horizontal x and y planes as follows (Nabighian, 1972):

$$\text{Total horizontal derivative} = \sqrt{(\partial T / \partial x)^2 + (\partial T / \partial y)^2}$$

Horizontal gradient grids are used primarily for edge detection of causative bodies (contacts, faults with large vertical displacement), and the data may also be employed for trend analysis and depth to source calculations.

Total horizontal derivatives of the pole reduced total magnetic intensity, Bouguer gravity (2.67g/cm³ terrain corrections) and free air gravity are shown in Figures 4.17, 4.19, 4.21 (principal survey area, grid cell size of 25 m) and Figures 4.18, 4.20, 4.22 (extended survey area, grid cell size of 250 m).

4.3.4 Total Gradient Amplitude of Total Magnetic Intensity

The total gradient amplitude, otherwise known as the 3D analytic signal amplitude, of a potential field (T) is defined as:

$$|A(x, y)| = \sqrt{(\partial T / \partial x)^2 + (\partial T / \partial y)^2 + (\partial T / \partial z)^2}$$

$|A(x, y)|$ is the amplitude of the analytic signal and T is the magnetic intensity at a point (x, y) . The horizontal derivatives are easily calculated in the space domain, whilst the vertical derivative is calculated in the frequency domain. The analytic signal is mostly independent of field direction and direction of magnetization, and is independent of the type of magnetization (induced or remanent). This means that all similar bodies have a similar analytic signal response, and that peaks in the analytic signal are symmetric and centred over the middle of narrow bodies and the edges of wide bodies. The amplitude however is affected by the strike of a body such that north-south oriented bodies at low latitudes are relatively weak for magnetic data. The analytic signal highlights areas where the field varies quickly in any direction, such as for contacts. The total gradient amplitude of the total magnetic intensity is shown in Figure 4.23 principal survey area, grid cell size of 25 m) and Figure 4.24 (extended survey area, grid cell size of 250 m).

4.3.5 Tilt Angle

The tilt angle can be applied to the pole reduced total magnetic intensity to preferentially enhance the weaker magnetic signals. This is particularly useful for mapping texture, structure, and edge contacts of weakly magnetic sources. The arctan operator restricts the tilt angle to within the range of -90° to $+90^\circ$, irrespective of the amplitude and wavelength of the field and enhances weak anomalies compared to the stronger anomalies. The tilt angle (Miller and Singh, 1994; Verduzco et al., 2004; Salem et al., 2007) is defined as:

$$\theta = \tan^{-1} \frac{\text{vertical component of gradient}}{\text{horizontal component of gradient}} = \tan^{-1} \left[\frac{\frac{\partial T}{\partial z}}{\frac{\partial T}{\partial h}} \right]$$

The vertical and horizontal gradients of the reduced to pole total magnetic intensity calculations are described above in subsections 4.3.2 and 4.3.3. The tilt angle grid for the reduced to pole total magnetic intensity is displayed in Figure 4.25 (principal survey area, grid cell size of 25 m) and Figure 4.26 (extended survey area, grid cell size of 250 m).

4.3.6 Trend Analysis Method

Depth trend as implemented by Phillips (1997) can be utilized for the depth estimation using the horizontal gradient grid (HG). It uses the horizontal gradient of the reduced to pole total magnetic intensity and gravity grids to estimate strikes of and depths to thick and thin edges, respectively (Phillips, 2000). The method relies on the general principle that shallow sources produce anomalies with steep gradients, whereas deep sources produce anomalies with broad gradients. Depth estimates from the RTP magnetic and gravity data estimate the minimum and maximum depths to the top edge of the layer, respectively (Phillips, 2000).

The program uses a 5 by 5 window to both locate the crests of maxima and determine their strike direction. Once a crest is located and the strike direction is known, data within the window and within a belt perpendicular to the strike can be used to determine the depth of the contact by performing a least squares fit to the theoretical shape of the HG over a contact. If " h " is the horizontal distance to the contact, " d " is the depth to the top of the contact and " K " is a constant, then the theoretical curve is

given by (Roest and Pilkington, 1993):

$$HG(h) = K/(h^2 + d^2)$$

The least-squares fit gives an estimate of both the depth and its standard error, which can be expressed as a percentage of the depth. Only depth estimates with standard errors of 20% or better are retained in the final interpretation.

Due to the assumption of thick sources, the depth estimates obtained using the above procedure represent minimum depths. It is also possible to assume very thin sources and use a standard "pseudogravity" transformation instead of reduction to the pole (Roest and Pilkington, 1993). In this case the same analysis is done on the HG of the pseudogravity field, and the depth estimates represent maximum depths. Figures 4.27 and 4.28 show the depth results from the trend analysis solutions for the Bouguer gravity and the reduced to pole total magnetic intensity, respectively. Solutions depths from Bouguer gravity data represent depth below the topographic surface while solution depths from magnetic data represent depths from the sensor

5 Geophysical Interpretation

The geophysical interpretation of the acquired gravity and magnetic data in the Hornepayne area involved qualitative analysis of the various products derived from the magnetic and gravity grids (described in Section 4), and 2.5D forward modelling of the gravitational and magnetic data along two profile lines covering the principle features of the Black-Pic batholith and metasedimentary rocks of the Quetico Subprovince and adjacent plutons and greenstone belts within the Hornepayne area.

5.1 Results of Qualitative Analysis

Qualitative analysis of the gravity derivative products was used to provide general indications about the location and general geometry of the Black-Pic batholith, the subprovince boundary and metasedimentary rocks of the Quetico Subprovince; the variation in depth to bottom across the batholith and within the metasediments; density variations within the rock units; and the presence of major or deep seated structures. Qualitative analysis of the magnetic derivative products was used to: identify the presence of potential features within the batholith and metasedimentary rocks, such as faults and dykes (documented in SRK, 2017); and evaluate variation in the magnetic character of the batholith and metasedimentary rocks that may indicate changing composition of the rock or other potential heterogeneities.

For the qualitative geophysical interpretation, the Bouguer gravity (Figure 5.1), its first vertical derivative (Figure 5.2) and its total horizontal derivative (Figure 5.3), as well as the total magnetic intensity reduced to the pole (Figure 5.4), its first vertical derivative (Figure 5.5), and its total horizontal derivative (Figure 5.6), were primarily utilized. In addition, the total gradient amplitude was used for interpretation of the magnetic data (Figure 4.23 and 4.24) because: (a) it has a maxima over vertical magnetic contacts regardless of the direction of magnetization; and (b) the magnetic intensity reduced to pole requires the assumption of only induced magnetization with the result that anomalies from remanently and anisotropically magnetized bodies can be severely distorted. Unlike the RTP, the total gradient amplitude will produce maxima over the edges of vertical magnetic contacts regardless of the presence of remanent magnetism (MacLeod, 1993).

The following subsections describe the qualitative interpretation made about portions of the metasedimentary rocks of the Quetico Subprovince in the Hornepayne North survey block and the Black-Pic batholith of the Wawa Subprovince in the Hornepayne South block.

5.1.1 *Metasedimentary Rocks of the Quetico Subprovince*

- North of the Quetico-Wawa subprovince boundary the Bouguer gravity data shows a broad regional high that trends east to west, parallel to the mapped Quetico-Wawa subprovince boundary (labelled G-D1 in Figure 5.1). The anomaly reaches a maximum magnitude at approximately 8 km to 11 km north of the subprovince boundary and decreases gradually northwards. The southern edge of the gravity high corresponds roughly to the mapped location of the Quetico-Wawa subprovince boundary. Superimposed on the broad high are a number of subtle short wavelength southeast and northeast trending anomalies following similarly oriented dyke trends.
- The magnetic data shows a number of strong, roughly east to east-northeast trending magnetic anomalies which are consistent with the trend of the Quetico-Wawa subprovince boundary (Figures 5.4 – 5.6). North of the subprovince boundary, both the magnetic and

gravity anomalies are thought to correspond with variations in rock mineralogy and rock density associated with variations in metamorphic grade. It is interpreted that the highest gravity response may correspond to a granulite facies metamorphic overprint, and additional variations may result from slivers of supracrustal rocks distributed along the subprovince boundary (Williams and Breaks, 1996).

- Discrete linear magnetic highs that transect the entire Quetico metasedimentary rocks correspond to the northwest trending Matachewan dykes (Buchan and Ernst, 2004), northeast trending Biscotasing dykes (Hamilton et al., 2002), and several north-northeast trending dykes of unknown origin (possibly Marathon dykes). These linear magnetic highs are coincident with mapped dyke orientations from the Ontario Geological Survey (OGS, 2011).

Specific features identified in the Quetico Subprovince during the qualitative interpretation are discussed below.

- The broad gravity high that makes up most of the northern Hornepayne survey block has been identified (labelled G-D1 in Figures 5.1 – 5.3), although regionally the Quetico Subprovince is typically dominated by low gravity response (Percival, 1989). This gravity high anomaly was defined using the first vertical derivative of the Bouguer gravity in conjunction with the total horizontal derivative of the Bouguer gravity, both of which show a change in the texture of the data outside this boundary. The southern edge of this anomaly matches fairly well with the mapped southern edge of the Quetico Subprovince, and the northern and eastern limits of G-D1 correlate with a large east-west trending anomalous gravity high located immediately north of the subprovince boundary that extends west towards the Township of Manitouwadge (SGL, 2017a). The broad gravity anomaly is thought to correspond with higher density rocks associated with granulite grade metamorphism, as well as potential influence of supracrustal rock slivers near the subprovince boundary (Williams and Breaks, 1996).
- A number of short wavelength southeast trending ridge-like gravity highs are observable within G-D1. These gravity highs do not correlate to any mapped lithologies, but show some correlation with clusters of northwest trending Matachewan dykes visible in the magnetic data. Areas with clusters of denser diabase dykes would have the effect of locally raising the bulk density of the metasedimentary rock, and produce subtle gravity anomalies.
- Magnetic data immediately north of the Quetico subprovince boundary shows a number of short wavelength, east-west trending strong magnetic anomalies which define the edges labeled M-D1 to M-D3 in Figures 5.4 – 5.6. Within these anomalies exist alternating zones of high and low magnetic intensity reflecting the variable magnetic nature and complexity of this region. This area may be highly deformed and metamorphosed along the subprovince boundary shear zone, and may also include slivers of mafic and ultramafic metavolcanic units (Williams and Breaks, 1996). North of the magnetic feature M-D3, the background magnetic intensity decreases to a generally non-magnetic nature typical of the metasedimentary rocks of the Quetico Subprovince.
- North of M-D3 a number of subtle lens shaped magnetic anomalies have been identified (labelled M-A1 to M-A6 in Figures 5.4 to 5.6). These anomalies have a similar character to the magnetic units defined south of M-D3, but are less intense and are only semi-continuous. Although it is not obvious to assign causation, these areas could represent rafts or imbricated material similar to that south of M-D3 within areas of primarily non-magnetic metasediments

and may be regions of high grade metamorphic rocks up to granulite facies (Williams and Breaks, 1996).

- In the northwestern corner of the northern survey block two tight folds separated by a possible fault have been identified from the first vertical derivative of the total magnetic intensity reduced to the pole (folds labelled M-F1 and fault labelled M-L1 in Figures 5.4-5.6). These features illustrate the presence of structural complexities within the metasedimentary rocks of the Quetico Subprovince.

5.1.2 Black-Pic Batholith

- The Bouguer gravity data within the Black-Pic batholith shows a broad low response along the southern portion of the survey area that gradually increases towards the Quetico-Wawa subprovince boundary (Figure 5.1). Locally, within the Bouguer gravity data are subtle northeast and northwest trending short-wavelength features that correspond well to rivers and broad valleys in the digital elevation data (Figure 3.1).
- In general, the reduced to pole total magnetic intensity over the Black-Pic batholith shows a strong east-west trending magnetic fabric at the Quetico-Wawa subprovince boundary with the magnetic intensity decreasing towards the south. The central portion of the Black-Pic batholith tends to show a weaker magnitude and is surrounded by an apparent curved fabric representing a large-scale fold structure within the gneissic tonalite. Interpreted northeast- and northwest-trending dykes are evident within the batholith and surrounding area as linear features with high magnetic responses.

Specific features identified in the Black-Pic batholith of the Wawa Subprovince during the qualitative interpretation are discussed below.

- The northernmost portion of the Black-Pic batholith, adjacent to the subprovince boundary, corresponds to a zone of elevated magnetic intensity observed in the reduced to pole total magnetic intensity and its derivative products. This zone, located between features M-D1 and M-D4 (Figures 5.4 – 5.6), previously mapped as homogeneous gneissic tonalite, shows high magnetic variability and intensity which is consistent with an area highly deformed and metamorphosed along the subprovince boundary shear zone, and may also contain slivers of mafic and ultramafic metavolcanic units in this area as evidence by historic mapping (Williams and Breaks, 1996). Recent mapping within this zone has identified significant lithological variability, including tonalite to granitic units, inclusions of amphibolite slivers and metasedimentary rocks, and migmatites, all of which are highly metamorphosed (Geofirma and Fladgate, 2017). This zone also shows a similar magnetic character to a region mapped as highly foliated tonalite west of the survey area, within the Manitouwadge area, which has been noted to have a high biotite and magnetite content (SGL, 2017a; Zaleski and Peterson, 1995).
- South of M-D4, the east-west trending magnetic fabric is less pervasive and is represented as alternating bands of high and low magnetization (Figure 5.4). The alternating bands observed in the magnetic data are likely to reflect strong and near-vertical to steeply north dipping gneissic layering that has been mapped near the subprovince boundary (Geofirma and Fladgate, 2017). Within the region between M-D6 and M-D7 the east-west magnetic fabric becomes weaker and the western side curves towards the southwest. Within this transitional zone several curvilinear structures are also identified in the magnetic fabric (see M-F2 in Figure 5.4) potentially associated with small-scale folding of the gneissic layering.

- In the central portion of the Black-Pic batholith a narrow zone of east-northeast trending magnetic fabric (approximately 1.5 km wide) shows a pronounced change in the magnetic intensity (labelled M-D7 through M-D10 in Figure 5.4). Based on the bedrock geological map the eastern and western parts of this magnetic zone are along strike with mapped mafic metavolcanic bedrock units associated with thin slivers of greenstone belt. Within the magnetic data it is apparent that the zone between these two separate mapped mafic metavolcanic units may also contain some amount of mafic bedrock. Based on a few local field observations in this area outcrops with up to 15% mafic inclusions have been identified (Geofirma and Fladgate, 2017). South of this zone the Black-Pic batholith becomes moderate to weakly magnetized and the representation of the gneissic layering in the data is limited. This area may reflect the core of a large scale fold with M-D9 and M-D10 defining the northern limb, M-D12 defining the southern limb and M-D11 representing a portion of the interpreted fold hinge zone (Figures 5.4 – 5.6).
- In the southeastern corner of the Hornepayne South survey block a linear band of reduced magnetic intensity has been identified extending northeast from the Dayohessarah greenstone belt (labelled M-D12 in Figure 5.5). The band has a smooth magnetic fabric with a northeast trending magnetic high apparent in the magnetic derivative grids. The similarity in character between this band and those visible farther north near the subprovince boundary deformation zone suggests it may represent a shear zone. This zone is intruded by numerous cross-cutting dykes, none of which shows any clear offset, but several show an overall reduction in their magnetic intensity through this zone. The magnetic intensity reduction of the dykes can be used to infer that fluids have previously moved through this linear zone resulting in breakdown of magnetic mineral.
- A number of small circular magnetic anomalies can be identified throughout the Hornepayne South block (labelled M-A7 in Figures 5.4 – 5.6). These anomalies are generally several hundred meters wide, produce magnetic anomalies greater than 100nT and occur as both positive and negative polarities. These anomalies sometimes occur as clusters. The origin of these anomalies is not understood and they show no correlation to geological, surficial or man-made features. Further west of the survey area a number of similar anomalies are coincident with mapped intrusions of amphibolitic metagabbro (OGS, 1967). Alternatively, these anomalies may represent potential kimberlite pipes of economic interest, and would need to be investigated in the field.
- Though the Bouguer gravity is fairly smooth through the Black-Pic batholith, one area has been identified from the first vertical derivative and total horizontal derivative of the Bouguer gravity (labelled G-D2 in Figures 5.2 and 5.3, respectively) which has a more variable gravity pattern. This area has been mapped entirely as uniform gneissic tonalite associated with the Black-Pic batholith, and is coincident with a number of tight folds interpreted in the magnetic data (labelled M-F2 in Figures 5.4 – 5.6) illustrating some degree of structural complexity. It is possible that the cause of the Bouguer gravity anomaly may also be associated with the inclusion of small unmapped slivers of greenstone or mafics bedrock units with higher rock densities, or alternatively thickness variations of the Black-Pic batholith.

- Two areas of mapped mafic metavolcanics are shown to have subtle but distinguishable anomalies on the Bouguer gravity and its derivatives. The first, labelled G-A1, is a sliver of greenstone within gneissic tonalites of the Black-Pic batholith. The mafic unit produces a subtle gravity anomaly broader than the mapped surficial expression and has no associated magnetic anomaly. The location of the sliver is adjacent to the magnetic shear zone M-D12 described above and may represent a northeastward continuation of the rock units of the Dayohessarah greenstone belt. The second greenstone sliver, bounded by G-A2 is only partially surveyed along the eastern side of the survey block in the area of coarse survey coverage. This sliver only produces a subtle gravity anomaly most obvious in the derivative grids where it has been mapped, however it does not have a coincident magnetic anomaly. Based on the regional bedrock geology map, this greenstone sliver follows a regional trend of mafic metavolcanic fragments that arc around the northern side of the Strickland pluton (see bedrock geology on Figure 5.3).

5.2 Preliminary 2.5D Modelling

The purpose of the 2.5D modelling is to develop an idea of the relatively deep and relatively shallow parts of the Black-Pic batholith and metasedimentary rocks and obtain a rough approximation of the depth to the bottom of these rock units. The preliminary 2.5D modelling used the gravity, magnetic and digital elevation data sets, accompanied with constraints from the qualitative interpretation of the geophysical data and the mapped bedrock geology to provide a preliminary image of the subsurface along two profile lines. The location of the two profile lines is shown in Figures 5.7 and 5.8, and the results of the 2.5D modelling in Figures 5.9 and 5.10.

For the purpose of this initial modelling attempt, density and magnetic susceptibility values were assigned to the bedrock units mapped on the surface and to the bedrock units at depth based on readily available information. In the Hornepayne area, several surface bedrock density and magnetic susceptibility values have been compiled from available literature (data sources discussed in Section 3) and incorporated as constraints into the models. These assumed density and magnetic susceptibility values should be considered as approximate values.

In order to assess the sensitivity of the assigned density and magnetic susceptibilities on the modelled geometry and thickness of the bedrock units, sensitivity tests were performed on both profile lines. The initial approach assumed a fairly simplistic geological model of steeply north dipping contacts with limited internal density variations and a fairly gentle relief at the base of the model at the contact with undifferentiated basement. Alternate density values were then assigned to quantify the change in model depth and geometry with density. Alternate geological structures were also tested to determine density values which were then compared with density measurements taken from field samples. Each alternative model produced a good fit to the data, and taken together they give an idea of the upper and lower bounds on the depth of the model bodies.

It is important to emphasize that the accuracy of these preliminary models is limited at this early stage of the assessment due to limited availability of bedrock densities and magnetic susceptibilities that are key for constraining the model. It is anticipated that the preliminary 2.5D models would be revised and refined if more field data is collected in the future.

5.2.1 Model Descriptions

The preliminary 2.5D forward modelling of gravity and magnetic data was carried out using GMSYS Software (copyright Northwest Geophysical Associates Inc. 2006) running under Geosoft Oasis Montaj (Geosoft, 2015). The modelling considered two profile lines. The locations of the profile lines are shown in Figure 5.7 superimposed on the Bouguer gravity, and in Figure 5.8 superimposed on the total magnetic intensity reduced to the pole. The start and end coordinates of the profiles are listed in Table 5.1.

Table 5.1: Coordinates of 2.5D Model Profiles (UTM 16N, NAD83)

Profile Line	Start		End	
	UTM X	UTM Y	UTM X	UTM Y
1	642460	5406855	642460	5468654
2	663460	5421550	663460	5482055

The process for constructing the models was as follows:

- The location and extent of profile models was taken into consideration during survey planning. Groups of control lines were extended past the northern and southern edges of the Hornepayne survey blocks to capture relevant regional features outside the area of high-resolution coverage. Lines were also continued between the north and south blocks to allow for a continuous regional profile across both survey blocks in the Hornepayne area.
- The profiles were modelled from Bouguer gravity and the total magnetic intensity data. It is possible to model either Free-Air or Bouguer gravity. Both approaches are valid, the difference is that topographic effects have been corrected in the Bouguer gravity, assuming a single density within the range of relief (2.67 g/cm^3 in this instance). Some terrain effects will still occur in the Bouguer gravity where density varies from the assumed value within the range of relief. The best choice depends on the degree to which the single density terrain corrections are applied and correctly handled. The model results should be essentially the same with either approach.
- Large bodies were modelled as extending to infinity perpendicular to the profile line, while small bodies were modelled as extending to a finite distance perpendicular to the profile line.
- Generally speaking, the gravity was modelled first to determine the broad large scale features and the magnetic data were used to refine the model and to help model the overall shape of smaller geological units. Long wavelength magnetic trends associated with large rock units were modelled as opposed to individual discrete anomalies and, as such, only the most prominent dykes and faults were included to fit the observed data.
- Densities for individual greenstone belts or plutons were assumed to be uniform throughout unless there were additional data that suggested the contrary (e.g. well logs, density measurements, etc.). This assumption was only violated if it was impossible to model the gravity using uniform densities. Thus the gravity anomalies were generally accounted for by varying the shapes of the rock units after initial density assumptions were made, rather than by varying the densities within the rock units.

- Depth trend, tilt angle and extended Euler solutions of the Bouguer gravity and magnetic data were used for determining locations and dip estimates of faults and lithological contacts.
- Available geologic mapping (OGS, 2011) and qualitative interpretation of the geophysical data were used to determine the location of the points at which geological boundaries occurred along the surface of the models.
- Density information has been obtained and incorporated into the models from the OGS PETROCH database (Haus and Pauk, 2010) and the GSC rock property database (GSC, 2015); as discussed in Section 3. The density ranges used in the models are listed in Table 5.2.
- In determining the magnetic susceptibilities, measured values from the OGS Precambrian Bedrock Magnetic Susceptibility Geodatabase (Muir, 2013 and Miles, 1998) were used as initial values for modelling, but were adjusted so as to (a) best match the amplitude of the magnetic variations that were obviously associated with terrain, (b) best reproduce the overall long wavelength trend associated with the larger rock units. This approach was employed due to the variability of the measured susceptibilities, in some cases over several orders of magnitude.
- In seeking to model magnetic variations within individual rock units, steeply dipping to vertical boundaries were generally used in the absence of other indications. Where possible these boundaries were set to be coincident with the gravity defined boundaries. Trend analysis solutions for the magnetic field reduced to the pole were used to model the dip of magnetic contacts. Trend analysis solutions are shown in the 2.5D model figures which occur no more than 0.5 km away from the model line.
- The overburden has not been included in the modelling. It is deemed to be sufficiently thin that its effect on the gravity and magnetic anomalies is negligibly small for modelling purposes.
- Where the 2.5D model lines intersect, the geological boundaries, densities, and magnetic susceptibilities have been made to coincide at the model intersection points.

Table 5.2: Densities and magnetic susceptibilities used in the 2.5D models

Layer	Density (g/cm³)	Magnetic Susceptibility (S. I.)
<i>Mafic metavolcanics (2)</i>	2.66 – 2.95	0 – 0.062
<i>Metasediments (5)</i>	2.70 – 2.76	0 – 0.075
<i>Gneissic tonalite (9)</i>	2.65 – 2.74	0 – 0.063
<i>Granite-granodiorite (11)</i>	2.66	0
<i>Granite-granodiorite (13)</i>	2.64	0.008 – 0.014
<i>Dyke</i>	2.66 – 2.72	0.005 – 0.065
<i>Undifferentiated basement</i>	2.69	0

5.2.2 Model Results

This section discusses the results of the 2.5D modelling for the two profile lines considered. It is assumed in these models that the Black-Pic batholith and metasedimentary rocks are underlain by a uniformly dense unit (density of 2.69 g/cm^3) defined as an undifferentiated basement. Distances along the profiles are listed relative to the profiles southern origin.

The 2.5D modeling results for the Hornepayne area are shown in Figure 5.9 to 5.12. The figures show a plan view along the profile line (e.g. top panel Figure 5.9) in order to show the distribution of bedrock units that are included in the model calculations perpendicular to the strike of the profile line. The gravity view (e.g. second panel Figure 5.9) shows the observed gravity data along the profile line, as well as the calculated gravity data, the misfit and the RMS error (i.e. root mean square error). The RMS error is used as a measure of the difference between the observed gravity data and the modelled gravity results. The next gravity view (e.g. third panel Figure 5.9) shows the assignment of the rock density values to each of the bedrock units in the model. The magnetic view (e.g. fourth panel Figure 5.9) shows the observed and calculated magnetic data, as well as the misfit and RMS error between the two data sets. The next magnetic view (e.g. fifth panel Figure 5.9) shows the assignment of the magnetic susceptibility values to each of the bedrock units in the model. The structural view provides the overall interpretation of the modelled results, which are coloured based on geological unit (e.g. sixth panel on Figure 5.9). Each of these model views shows the depth on the y-axis in kilometers relative to mean sea level (MSL).

5.2.2.1 Initial Model Line 1 (Figure 5.9)

As shown in Figures 5.7 and 5.8, Line 1 runs from south to north starting within the Wawa Subprovince at the Dayohessarah greenstone belt, and continuing north through the Black-Pic batholith, across the Quetico-Wawa subprovince boundary and ending in metasedimentary rocks of the Quetico Subprovince (Figure 5.9).

- At the southern end of the profile the Dayohessarah greenstone belt is modelled as a dense bedrock unit extending to approximately 2 km below mean sea level (MSL) surrounded by the Black-Pic batholith. The model is consistent with the observations of Stott (1999) who describes the Dayohessarah greenstone belt as a tight syncline that plunges and opens southwards. The modelled geologic contact on the north side of the greenstone belt is located approximately 1 km north of the mapped contact to better fit the gravity data and is consistent with the edge of the source body as defined by the gravity data in the qualitative analysis. No density measurements were available on mafic metavolcanic rocks within the Dayohessarah greenstone belt; a density of 2.95 g/cm^3 was required to fit the model to the data that is denser than other greenstone belt units modelled elsewhere in the Wawa Subprovince, but well within the range of densities of mafic metavolcanic samples 10 km to the west of the Dayohessarah greenstone belt and in the Kabinakagami greenstone belt 30 km to the east (Haus and Pauk, 2010). The density value assigned to the Dayohessarah greenstone belt is consistent with the understanding that the Dayohessarah belt likely extends to depths between 2 and 3 km below ground surface (AECOM, 2014). Lowering the assigned density value of the Dayohessarah greenstone belt to 2.85 g/cm^3 would increase the depth to the base to approximately 5.5 km below MSL.

- The Dayohessarah greenstone belt has highly variable magnetic properties ranging from strongly magnetic to weakly magnetic units. The strongly magnetic units have been modelled as relatively thin bodies (~500 m wide) and near to the surface so as to produce the high amplitude short wavelength anomalies.
- Immediately north of the Dayohessarah greenstone belt, from 9 km to 11.5 km, a denser section of the Black-Pic batholith was required to fit the Bouguer gravity (density of 2.70 g/cm³ and density contrast of +0.04 g/cc relative to flanking Black-Pic batholith rocks). The southern edge of this denser section, which is in contact with the Dayohessarah greenstone belt, extends vertically while the northern edge dips steeply northwards. The associated gravity anomaly could also be produced by a northward dipping extension of the Dayohessarah greenstone belt into the Black-Pic batholith below surface, but there is no geological evidence to support this. Material with a density higher than that of the undifferentiated basement is required to model the gravity data through this area. Modelling the undifferentiated basement (density of 2.69 g/cm³) at surface does not in this area produce a gravity anomaly large enough to fit the gravity data. Therefore, the model incorporates a locally higher density in the Black-Pic batholith immediately north of the Dayohessarah greenstone belt.
- A broad gravity low occurs in the center of the profile from approximately 12 km to 32 km from the southern end. This gravity low has been modelled as the thickest section of Black-Pic batholith along the profile with a maximum depth of about 7 km, assuming a rock density of 2.66 g/cm³ that is lower than that of the adjacent modelled units (2.70 g/cm³). In general, the geometry of this unit is influenced by the assumed rock density which controls the depth to the base of the units. Densities of local granitoids range from 2.60 – 2.74 g/cm³ (Haus and Pauk, 2010; GSC, 2015). A reduction in the density to 2.57 g/cm³ results in a thinning of the Black-Pic batholith raising its base to about 1 km below MSL in this area. An increase in density to 2.67 g/cm³ has the opposite effect, and increases the thickness of the Black-Pic batholith, lowering its base to about 14 km below MSL.
- Two strong magnetic peaks have been modelled in the central portion of the Black-Pic batholith as vertical dykes hosted within an otherwise weakly magnetic batholith. Strike orientation of these two dykes suggests they are part of the Matachewan dyke swarm. Other high-frequency magnetic anomalies in this area can be correlated to less magnetic dykes of both the Matachewan and Abitibi swarms, and to the curved magnetic lineaments discussed in the qualitative interpretation, however, these have not been modelled.
- Between approximately 32 km and 37 km from the south end of the profile, two subtle gravity high anomalies are superimposed on the overall northwards increasing trend in the Black-Pic batholith. The anomalies are located within the area of chaotic gravimetric texture (labelled G-D2 in Figures 5.1 to 5.3). It is possible that these two subtle gravity high anomalies may represent the inclusion of bedrock units with higher rock densities (~2.70 g/cm³) or a thinning of the Black-Pic batholith or a combination of both. Presented in the model, this area is represented as units with laterally varying density in order for the model to fit the observed Bouguer gravity anomaly, as well as a thinner section of Black-Pic batholith with a depth to base of approximately 3.8 km below MSL. If the batholith units were considered to have a uniform density of 2.66 g/cm³ from 32 km to 37 km, the resultant model would have undifferentiated basement at surface while still not producing an amplitude large enough to fit the more northern of the two Bouguer gravity anomalies. Therefore the northern anomaly

requires the introduction of a bedrock unit whose density is greater than the undifferentiated basement.

- At approximately 36 km from the south end of the profile, the magnetic data begins to show more variability leading up to the deformation zone at the Quetico-Wawa subprovince boundary. At this point the profile begins to transect the more prominent magnetic anomalies observed in the magnetic data, and discussed during the qualitative interpretation (Section 5.1.2). There are also a number of strongly magnetic northwest and northeast trending dykes transected by the profile. Rather than modelling individual dykes and magnetic anomalies in this interval, a broader zone of increased magnetic susceptibility was used to approximate the observed magnetic anomalies. The short wavelength, low amplitude of these anomalies would result in an interpreted shallow depth to source.
- North of approximately 41 km from the south end of the profile, the Bouguer gravity gradually increases up to and past the mapped Quetico-Wawa subprovince boundary. The model incorporates a series of steeply north dipping blocks with gradually higher densities leading up to this boundary with a maximum density of 2.74 g/cm^3 and depth to base of around 5 km below MSL. The increasing density at this boundary reflects the increased metamorphic grade (granulite facies) recognized in the bedrock near the subprovince boundary (Williams and Breaks, 1996). The base of the units is modelled as asymptotic at depth though the geophysical data does not require this structure.
- Magnetic data in the Black-Pic batholith immediately south of the mapped Quetico-Wawa subprovince boundary reflects the highly variable physical properties within the region. Thinner subdivisions of magnetic units from weakly and non-magnetic to highly magnetic were required to fit the observed magnetic data from approximately 43 km to 48.5 km.
- At the Quetico-Wawa subprovince boundary two thin linear zones of mafic metavolcanic rocks have been mapped. Both have been modelled as thin wedges extending to around 1 km below MSL though neither show large associated gravity anomalies typical of mafic volcanic units. The more northern mafic metavolcanic body has been modelled with a density of 2.66 g/cm^3 while the southern wedge a density of 2.85 g/cm^3 . Only a thin portion on the south side of the more northern mafic metavolcanic body is associated with a magnetic anomaly.
- Immediately north of the mapped subprovince boundary a block of metasediments with a density of 2.72 g/cm^3 was required to fit a dip in the observed gravity data. This area also corresponds to a magnetic low. North of this block the Bouguer gravity increases until about 57 km into the profile at which point it tapers off to the north. The density of the metasediments peaks at 2.76 g/cm^3 .
- Metasedimentary rocks of the Quetico Subprovince have been modelled as steeply north dipping sheets becoming asymptotic at depth with varying densities and magnetic susceptibilities. The depth to the base of the metasedimentary rocks gradually increases to the north from just over 5 km below MSL at the subprovince boundary to just over 6 km at the northern end of the profile line.

5.2.2.2 *Alternative Model Line 1 (Figure 5.10)*

- The initial Line 1 model incorporates significant relief on the top of the undifferentiated basement which has a constant density of 2.69 g/cm^3 to produce the observed regional gravity anomaly. A thickening of the Black-Pic batholith which has a nominal density of 2.66 g/cm^3 produces the gravity low at the southern side of the line. A density increase combined with a thickening of both the Black-Pic batholith and the Quetico metasedimentary rocks near the Quetico-Wawa subprovince boundary is used to produce the regional high at the northern side of the line. While essentially maintaining the shape of the smaller geological features in the initial model, the alternative model evaluates the impact of flattening the top of the undifferentiated basement. The alternative model maintains the densities and susceptibilities of the different units as defined in the initial model but incorporates changes in shape of the units above the basement mainly at their base.
- An acceptable fit is obtained by setting the top of the undifferentiated basement to be around 6.2 km below MSL resulting in a marginally higher RMS error compared to the initial model for both gravity and magnetic data. This illustrates that the model is relatively insensitive to the location of top of the undifferentiated basement primarily because of the small density contrast between the Black-Pic batholith and the undifferentiated basement.

5.2.2.3 *Initial Model Line 2 (Figure 5.11)*

As shown in Figures 5.7 and 5.8, Line 2 is a north trending profile line that begins at the northern edge of the Strickland pluton, extends through the Black-Pic batholith and crosses the Quetico-Wawa subprovince boundary, and continues into the Quetico metasedimentary rocks (Figure 5.11). This profile line is a continuation of the north trending profile line through the Strickland and Anahareo plutons south of the Hornepayne area (SGL, 2017b)

- The southern end of Line 2 starts in the Strickland pluton which is modelled with a depth to its base of approximately 1.65 km below MSL with a density of 2.64 g/cm^3 . The pluton is underlain by gneissic tonalites of the Black-Pic batholith modelled with a depth to its base of approximately 7 km below MSL with a density of 2.66 g/cm^3 . The density value used to model the Strickland pluton is on the lower end of the measured density range ($2.64 - 2.71 \text{ g/cm}^3$) of trondhjemite samples measured proximal to the profile line (Haus and Pauk, 2010). The pluton has been modelled locally as slightly magnetic though no magnetic susceptibility values are locally available. A few strongly magnetic northwest trending Matachewan and northeast trending Biscotasing dykes have been included to match high amplitude, short wavelength magnetic anomalies.
- The Strickland pluton has been modelled as thinning northwards to where gneissic tonalites of the Black-Pic batholith are mapped at the surface (OGS, 2011). The contact between the Strickland pluton and the Black-Pic batholith is not well defined by either gravity or magnetic data and is essentially unconstrained by the geophysical data. A density of 2.68 g/cm^3 was assigned to the Black-Pic batholith to fit the model to the Bouguer gravity data on the northern side of the Strickland pluton. The geometry of the Strickland pluton is discussed in greater detail in the White River Phase 2 Geoscientific Preliminary Assessment Report (SGL, 2017b).
- A small raft of mafic metavolcanic rock is incorporated into the model 6.3 km from the southern end of the profile line. This mafic metavolcanic unit produces a very subtle magnetic

anomaly, however the anomaly is obscured by a dyke located immediately to the south. This unit also correlates with a very subtle, approximately +1 mGal gravity anomaly that is broader than the mapped extent of the mafic metavolcanic unit. The mafic metavolcanic unit was modelled to be moderately southward dipping, relatively thin (<300m maximum depth below the surface) and with a density of 2.85 g/cm³, however the mafic volcanic units by themselves do not fit the much broader Bouguer gravity anomaly. The mafic metavolcanic unit is located immediately south of a band of northeast-trending, weakly magnetized fabric extending off the northern end of the Dayohessarah greenstone belt (M-D12 in Figure 5.4-5.6) discussed in the qualitative interpretation.

- The Black-Pic batholith from 5.5 km to 8.5 km from the south end of the profile is associated with a broad +1 mGal Bouguer gravity anomaly. In this part of the model, the Black-Pic batholith was assigned a higher density of 2.70 g/cm³ in order to fit the Bouguer gravity data. Within this zone, from 7.3 km to 8.5 km, the model line transects an area that is interpreted as a northeast-trending, weakly magnetized fabric extending off the northern end of the Dayohessarah greenstone belt (M-D12 in Figure 5.4-5.6). The higher density suggests the presence of small fragments of denser mafic metavolcanics that may exist within this northeast trending band. Modelling also required that this part of the Black-Pic batholith has a reduced magnetic susceptibility compared to the adjacent parts.
- North of approximately 8.5 km, a 1.5 km wide section of the Black-Pic batholith was modelled with a density of 2.66 g/cm³ to fit a local low on the otherwise northerly increasing regional gravity trend. The area of lower gravity was modelled by a body with a vertical north side and steeply south dipping south side extending to the base of the batholith at approximately 7 km depth.
- An additional small portion of the Strickland pluton is transected again by the model line based on the geology map (see Figure 1.1) centered at 11.6 km from the south end of the profile. This unit does not cause any obvious gravity or magnetic anomaly, so for consistency it has been modelled using a density of 2.64 g/cm³, the same as at the southern end of this section of the profile. The magnetic susceptibility of this pluton is modelled to be the same as the surrounding Black-Pic batholith. Along the profile, the pluton is also cut by one strongly magnetic mafic dyke. This small portion of the pluton has been modelled to a depth of approximately 0.15 km below MSL (approximately 400 m thick), though the structure is poorly constrained due to absence of measured rock property values.
- North of approximately 13 km, the profile transects a wide interval of undifferentiated Black-Pic batholith up to the Quetico-Wawa subprovince boundary at 32 km. Several magnetic Biscotasing and Matachewan dykes have been included in the model through this region, though many more were transected and have been averaged together for simplicity. The area of highly variable magnetic fabric discussed in the qualitative interpretation is also transected close to the Wawa subprovince boundary. To model the averaged group of dykes and the magnetic fabric, steeply dipping blocks with variable magnetic susceptibility were employed. The magnetic susceptibility of these blocks generally increases up to the deformation zone at the Quetico-Wawa subprovince boundary. The blocks also become thinner and their magnetic susceptibility more variable. The gravity anomaly generally increases northwards in the Black-Pic batholith from the Strickland pluton towards the Quetico-Wawa subprovince boundary. This anomaly was modelled by increasing the density of the Black-Pic batholith to a maximum of

2.74 g/cm³ at the mapped subprovince boundary. The Black-Pic batholith is also modelled as thickening slightly northwards, attaining a maximum thickness of approximately 7.5 km. Through this region, low-amplitude (1 mGal) short wavelength anomalies are fairly common but have not been incorporated in the model. The frequency of these anomalies suggests that the causative bodies are in the near surface, and may be associated with Quaternary features (e.g. thick overburden, river valleys).

- Immediately north of the mapped Quetico-Wawa subprovince boundary there is a coincident decrease in the magnetic and gravity anomaly over a 1.5 km wide zone, similar to that observed on Line 1 at this boundary. North of the Quetico-Wawa subprovince boundary in the Quetico Subprovince, the magnetic data shows considerable variation modelled by a series of steeply north-dipping blocks with variable magnetic susceptibilities, similar to the southern side of the subprovince boundary. The magnetic susceptibility of the metasedimentary rocks of the Quetico Subprovince decreases northwards eventually becoming non-magnetic. Several Matachewan dykes are transected by the profile in the Quetico Subprovince and are modelled as thin vertical sheets with high magnetic susceptibility reflecting either a single dyke or a series of tightly clustered dykes in plan-view.
- The gravity anomaly north of the Quetico-Wawa subprovince boundary continues to increase northwards and peaks approximately 11 km north of the mapped subprovince boundary. The modelled density increases to a maximum of 2.75 g/cm³ with a depth to undifferentiated basement of approximately 7 km below MSL. The gravity anomaly decreases farther northwards and is modelled by a thinning of the metasediments to minimum thickness of approximately 6 km in the Quetico Subprovince and decrease in density to a minimum of 2.72 g/cm³. This assumed minimum density is the same as the northern most metasedimentary rocks modelled in Line 1 (Figure 5.9). Alternatively, the depth to the base of the Quetico metasedimentary rocks can be maintained at approximately 7.5 km (i.e. no thinning northwards) when a density of 2.715 g/cm³ is used instead of 2.72 g/cm³. There is also a mapped granite-granodiorite intrusion at the northern end of the profile which contributes to the decreased gravity. The intrusion was modelled with a maximum depth to its base of 1.0 km below MSL and a density of 2.66 g/cm³, which is consistent with values measured for other granite-granodiorite intrusions in the region (Haus and Pauk, 2010; GSC 2015).
- This model has primarily used density variations combined with a slight thickening of the batholith and metasediments to match the observed gravity data. The depth to the undifferentiated basement is thinnest at the north end of the profile where the rocks have been modelled assuming a density of 2.72 g/cm³. Near the subprovince boundary zone both the depth to the undifferentiated basement and the assumed densities increase. Varying either the density or the depth the basement alone in the model can generate a suitable fit to the Bouguer gravity data. Where the density is greater than 2.69g/cm³, notably at the northern side of the Quetico-Wawa subprovince boundary, a density increase is required as raising the undifferentiated basement even right up to surface alone cannot model the gravity. At the south end of the profile, more extreme depths to the basement could be used to explain the gravity low because a smaller volume of lower density material is required to produce the same gravity decrease.

5.2.2.4 *Alternative Model Line 2 (Figure 5.12)*

- The dominant gravity high at the Quetico-Wawa subprovince boundary was modelled in the initial model as predominantly due to density increase in both the Black-Pic batholith and the Quetico metasedimentary rocks near the Quetico-Wawa subprovince boundary. Some marginal thickening of about 500 m in the Black-Pic batholith and 1.5 km in the Quetico metasedimentary rocks was incorporated. Small units of the much less dense Strickland lake pluton are incorporated at the southern end of the line. The top of the undifferentiated basement can be flattened more with marginal increase to the misfit. The alternative model looked into feasible more extreme relief on the top of the undifferentiated basement.
- The alternative model has substantial thickening of the Black-Pic batholith and Quetico metasedimentary rocks near the Quetico-Wawa subprovince boundary. The Black-Pic batholith thickens from 3 km to 8 km while the Quetico metasedimentary rocks thicken from 6 km to 8 km. The thinning of units of the Black-Pic batholith at the southern side of the line called for a reduction in the associated densities of the units.
- Though the RMS error associated with the alternative model is slightly lower than the initial model, the extreme relief might be geologically less plausible. The model illustrates the minimal constraint to the relief in the model due to the small density contrast between the Black-Pic batholith and undifferentiated basement.

6 SUMMARY OF RESULTS

The following provides a summary of the qualitative observations and the preliminary 2.5D modelling of the geophysical data, focusing on the area identified during Phase 1 as being potentially suitable within the Black-Pic batholith and metasedimentary rocks of the Quetico Subprovince. The survey allowed for a characterization of the gravity and magnetic signatures of the Black-Pic batholith and internal plutons and greenstone belt units, as well as the metasedimentary rocks of the Quetico Subprovince and the dominant signature of the Quetico-Wawa subprovince boundary.

Black-Pic Batholith

- Although previously mapped as homogeneous gneissic tonalite, magnetic data along the subprovince boundary shear zone in the northern portion of the Black-Pic batholith is interpreted as a complex and heterogeneous mixture of lithologies which has undergone deformation and metamorphism, and may also include slivers of mafic to ultramafic metavolcanic rocks. Alternating bands observed in the magnetic data are likely to reflect near-vertical to steeply north dipping gneissic layering mapped near the subprovince boundary.
- Magnetic data shows a narrow band (~1.5 km) in the central portion of the Black-Pic batholith and is evidence of a strong magnetic fabric trending east-northeast that may contain some amount of mafic metavolcanic bedrock. This interpretation is consistent with the extension of mafic metavolcanic bedrock units located along the eastern and western parts of this magnetic fabric, and is consistent with localized field observations within the fabric with up to 15% mafic inclusions identified.
- The southern portion of the Black-Pic batholith is moderate to weakly magnetized with limited evidence of a magnetic fabric shown in the data. This lack of fabric is interpreted to represent the core of a large-scale fold through the Black-Pic batholith where the gneissic layering is suggested to be either shallowly dipping or non-existent. Bounding this area the interpreted limbs and hinge zone of the fold are coincident with various geophysical anomalies previously discussed.
- In the southeastern corner of the Hornepayne area a linear northeast trending, weakly magnetized fabric is observable in the derivative grids and is interpreted to represent a small localized shear zone. This zone is also broadly coincident with the location of a mapped sliver of mafic metavolcanic rock which may be an extension or fragment of the Dayohessarah greenstone belt to the southwest.
- In general, units within the Black-Pic batholith have been modelled as a series of vertical to steeply north dipping blocks of varying density and magnetic susceptibility. The variability and intensity of these properties increases towards the subprovince boundary. The Black-Pic batholith shows a fairly gentle gravity gradient decreasing to the south away from the subprovince boundary. The presented profile lines modelled depth to undifferentiated basement to a maximum and minimum of approximately 7 km and 4 km, respectively along profile line 1, and 7.5 km and 7 km respectively on profile line 2.
- A number of small circular magnetic anomalies are visible in the Black-Pic batholith though their cause is unknown. The anomalies are several hundreds of meters wide, have amplitudes close to 100 nT, and both positive and negative polarities are observed.

- The Black-Pic batholith is intruded by numerous dyke swarms (Matachewan, Abitibi, Biscotasing, Sudbury and unclassified dykes). Northwest trending Matachewan dykes tend to occur in clusters of several bifurcating dykes. It is clear that several more dykes are apparent in the higher resolution magnetic data compared to what has been previously mapped.

Quetico Metasedimentary Rocks

- In the Quetico Subprovince, a zone of intense deformation and metamorphism is apparent in the magnetic and gravity data and tends to be limited to within a 14 km wide zone north of the mapped subprovince boundary. Tight folding is apparent further north within the metasedimentary rocks. The northern portion of the metasedimentary rocks of the Quetico Subprovince is generally non-magnetic farther away from the deformation zone.
- The discrete east to east-northeast trending magnetic fabric and broad east-trending gravity high is consistent with the strike of the Quetico-Wawa subprovince boundary. In particular, both the magnetic and gravity anomalies are thought to correspond to some sort of variations in rock mineralogy and rock density associated with granulite grade metamorphism, as well as potential slivers of supracrustal rocks incorporated into the rocks near the subprovince boundary (Williams and Breaks, 1996).
- The gravity anomaly within the metasedimentary rocks in the Quetico Subprovince reaches its peak at approximately 8 to 11 km north of the mapped subprovince boundary. The depth to undifferentiated basement in the Quetico Subprovince has been modelled to a maximum of approximately 6 km on profile line 1 and approximately 7.5 km on profile line 2. At the northern end of the profile line 2 the thickness of metasediments thins to approximately 6 km. Note that line extends approximately 13 km farther north than line 1.
- The Quetico metasedimentary rocks are intruded by numerous dyke swarms (Matachewan, Abitibi, Biscotasing, Sudbury and unclassified dykes). Northwest trending Matachewan dykes tend to occur in clusters of several bifurcating dykes. It is clear that several more dykes are apparent in the higher resolution magnetic data compared to what has been previously mapped

The 2.5D models are viewed as preliminary primarily due to the limited availability of bedrock densities and magnetic susceptibilities that are key for constraining the model. More field data would allow for revision and refinement of the models.

7 REFERENCES

- AECOM. 2014. Phase 1 Geoscientific Desktop Preliminary Assessment, Lineament Interpretation, Township of White River, Ontario. Prepared for Nuclear Waste Management Organization (NWMO). NWMO Report Number: APM-REP-06144-0086
- Baranov, V., and Naudy, H. 1964. Numerical Calculation of the Formula of Reduction to the Magnetic Pole. *Geophysics*, **29**: 67-79.
- Barnett, P.J. 1992. Quaternary Geology of Ontario; In: *Geology of Ontario*, Ontario Geological Survey, Special Volume 4, Part 2, 1010-1088.
- Berman, R.G., Easton, R.M. and Nadeau, L. 2000. A New Tectonometamorphic Map of the Canadian Shield: Introduction; *The Canadian Mineralogist*, **38**: 277-285.
- Berman, R.G., Sanborn-Barrie, M., Stern, R.A. and Carson, C.J. 2005. Tectonometamorphism at ca. 2.35 and 1.85 Ga: In: *the Rae Domain, western Churchill Province, Nunavut, Canada: Insights from structural, metamorphic and in situ geochronological analysis of the southwestern Committee Bay Belt*; *The Canadian Mineralogist*, **43**: 409-442.
- Blakely, R.J. 1996. *Potential Theory in Gravity and Magnetic Applications*. Cambridge University Press.
- Bleeker, W. and Hall, B. 2007. The Slave Craton: Geology and metallogenic evolution; In Goodfellow, W.D., ed., *Mineral Deposits of Canada: A Synthesis of Major Deposit-Types, District Metallogeny, the Evolution of Geological Provinces, and Exploration Methods: Geological Association of Canada, Mineral Deposits Division, Special Publication No. 5*, 849-879.
- Breaks, F.W. and Bond, W.D. 1993. The English River Subprovince – An Archean Gneiss Belt: Geology, geochemistry and associated mineralization; Ontario Geological Survey, Open File Report 5846, **1**
- Briggs, I.C. 1974. Machine contouring using minimum curvature, *Geophysics*, **39**: no. 1, 39-48.
- Buchan, K.L. and Ernst, R.E. 2004. Diabase dyke swarms and related units in Canada and adjacent regions. Geological Survey of Canada, Map 2022A, scale 1:5,000,000.
- Buchan, K.L., Halls, H.C. and Mortensen, J.K. 1996. Paleomagnetism, U-Pb geochronology, and geochemistry of Marathon dykes, Superior Province, and comparison with the Fort Frances swarm. *Canadian Journal of Earth Sciences*, **33**: 1583-1595.
- Corfu, F., Stott, G.M. and Breaks, F.W. 1995. U-Pb geochronology and evolution of the English River subprovince, an Archean low P – high T metasedimentary belt in the Superior Province. *Tectonics*, **14**: 1220-1233.
- Corrigan, D., Galley, A.G. and Pehrsson, S. 2007. Tectonic evolution and metallogeny of the southwestern Trans-Hudson Orogen, in Goodfellow, W.D., ed., *Mineral Deposits of Canada: A Synthesis of Major Deposit-Types, District Metallogeny, the Evolution of Geological Provinces, and Exploration Methods: Geological Association of Canada, Mineral Deposits Division, Special Publication No. 5*, 881-902.
- Easton, R.M. 2000a. Metamorphism of the Canadian Shield, Ontario, Canada. I. The Superior

- Province; *The Canadian Mineralogist*, **38**: 287-317.
- Easton, R.M. 2000b. Metamorphism of the Canadian Shield, Ontario, Canada. II. Proterozoic metamorphic history; *The Canadian Mineralogist*, **38**: 319-344.
- Fenwick, K.G. 1967. Geology of the Dayohessarah Lake Area, Ontario Department of Mines, Geological Report 49. Accompanied by Map 2129, Dayohessarah Lake area, District of Algoma, scale 1 inch to 2 miles.
- Fenwick, K.G. 1965. Dayohessarah Lake area, District of Algoma, Ontario; Ontario Geological Survey, Preliminary Map P0288, scale 1:63660.
- Fraser, J.A. and Heywood, W.W. (editors) 1978. Metamorphism in the Canadian Shield; Geological Survey of Canada, Paper 78-10, G. Stott, Pers. Comm, 2013
- Gartner, J.F. and McQuay. D.F. 1980a. Obakamiga Lake Area (NTS 42F/SW). Districts of Algoma and Thunder Bay; Ontario Geological Survey, Northern Ontario Engineering Geology Terrain Study 45, Accompanied by Map 5084, scale 1:100,000.
- Gartner, J.F., and D.F. McQuay. 1980b. Hornepayne Area (NTS 42F/SE), Districts of Algoma and Cochrane. Ontario Geological Survey, Northern Ontario Engineering Geology Terrain Study 46.
- Geddes, R.S. and Kristjansson. F.J. 1986. Quaternary geology of the Hornepayne area, Districts of Thunder Bay and Algoma; Ontario Geological Survey, Map P.2988, Geological Series- Preliminary Map, scale 1:50,000.
- Geddes, R.S., Bajc, A.F. and Kristjansson, F.J. 1985. Quaternary Geology of the Hemlo Region, District of Thunder Bay; In: Summary of Field Work, 1985, Ontario Geological Survey, Ontario Geological Survey, Miscellaneous Paper 126, 151-154.
- Geofirma (Geofirma Engineering Ltd.). 2013. Phase 1 Geoscientific Desktop Preliminary Assessment of Potential Suitability for Siting a Deep Geological Repository for Canada's Used Nuclear Fuel, Township of Hornepayne, Ontario. Prepared for Nuclear Waste Management Organization (NWMO). NWMO Report Number: APM-REP-06144-0003.
- Geofirma and Fladgate. 2017. Phase 2 Geoscientific Preliminary Assessment, Geological Mapping, Township of Hornepayne and Area, Ontario. Prepared for Nuclear Waste Management Organization (NWMO). NWMO Report Number: APM-REP-01332-0207.
- Geosoft. 2015. Oasis montaj geophysical processing system, v 8.5.1, Geosoft Inc.
- Giblin, P.E. 1968. Hornepayne sheet, districts of Algoma and Cochrane, Sault Ste. Marie and Sudbury mining divisions, geological compilation series; Ontario Geological Survey, Map P0476, scale 1:126720.
- GSC (Geological Survey of Canada). 2015. Bedrock densities and magnetic susceptibilities. Geoscience Data Repository for Geophysical and Geochemical Data, gdr.nrcan.gc.ca. (data accessed August 2014).
- Halls, H.C., Stott, G.M., Ernst, R.E. and Davis, D.W., 2006. A Paleoproterozoic mantle plume beneath the Lake Superior region; p.23-24 In: Institute on Lake Superior Geology, 52nd Annual Meeting Sault Ste Marie, Ontario, Part 1, Program and Abstracts.
- Hamilton M.A., David, D.W., Buchan, K.L., and Halls, H.C. 2002. Precise U-Pb dating of reversely

- magnetized Marathon diabase dykes and implications for emplacement of giant dyke swarms along the southern margin of the Superior Province, Ontario. Geological Survey of Canada, Current Research 2002-F6.
- Haus, M., and Pauk, T. 2010. Data from the PETROCH Lithogeochemical database, Ontario Geological Survey, Miscellaneous Release – Data 250, ISBN 978-1-4435-3732-2 [CD] ISBN 978-1-4435-3731-5 [zip file].
- Jackson, S.L. 1998. Stratigraphy, structure and metamorphism; Part 1, p.1--58, in S.L. Jackson, G.P. Beakhouse and D.W. Davis, Geological Setting of the Hemlo Gold Deposit; an Interim Progress Report, Ontario Geological Survey, Open File Report 5977.
- JDMA (J.D. Mollard and Associates [2010] Ltd.), 2013. Phase 1 Geoscientific Desktop Preliminary Assessment, Terrain and Remote Sensing Study, Township of Hornepayne, Ontario. Report prepared for Geofirma Engineering Ltd. and Nuclear Waste Management Organization (NWMO). NWMO Report Number: APM-REP-06144-0004).
- Johns, G.W., and McIlraith, S. 2003. Precambrian geology compilation series-Hornepayne sheet; Ontario Geological Survey, Map 2668, scale 1:250 000.
- Jolly, W.T. 1978. Metamorphic history of the Archean Abitibi Belt; In: Metamorphism in the Canadian Shield; Geological Survey of Canada, Paper 78-10, 63-78.
- Kettles, I.M. and Way Nee, V. 1998. Surficial geology, Vein Lake, Ontario; Geological Survey of Canada, Map 1921A, scale 1:50,000.
- Kraus, J. and Menard, T. 1997. A thermal gradient at constant pressure: Implications for low- to medium-pressure metamorphism in a compressional tectonic setting, Flin Flon and Kiseynew domains, Trans-Hudson Orogen, Central Canada; *The Canadian Mineralogist*, **35**: 1117-1136.
- Leliak, P. 1961. Identification and evaluation of magnetic field sources of magnetic airborne detector equipped aircraft. *IRE Transactions on Aerospace and Navigational Electronics*, **8(3)**: 95-105.
- Lin, S. 2001. Stratigraphic and Structural Setting of the Hemlo Gold Deposit, Ontario, Canada. *Economic Geology*, **96**: 477-507.
- Lin, S. and Beakhouse, G.P. 2013. Synchronous vertical and horizontal tectonism at late stages of Archean cratonization and genesis of Hemlo gold deposit, Superior craton, Ontario, Canada; *Geology*, **41**: no. 3; 359-362.
- MacLeod, I.N. 1993. 3-D Analytic Signal in the Interpretation of Total Magnetic Field Data at Low Magnetic Latitudes, *Exploration Geophysics*, **24**: 679-688.
- Menard, T. and Gordon, T.M. 1997. Metamorphic P-T paths from the Eastern Flin Flon Belt and Kiseynew Domain, Snow Lake, Manitoba; *The Canadian Mineralogist*, **35**: 1093-1115.
- Miles, W.F. 1998. An Interpretation of high resolution aeromagnetic data over the Manitouwadge greenstone belt, Ontario, Canada; MSc Thesis, Ottawa-Carleton Geoscience Centre and University of Ottawa, Ottawa, Canada.
- Miller, H.G., and Singh, V. 1994. Potential field tilt – a new concept for location of potential field sources, *Journal of Applied Geophysics*, **32**: 213-217.
- Muir, T.L. 2013. Ontario Precambrian Bedrock Magnetic Susceptibility Geodatabase for 2001 to 2012, Ontario Geological Survey, Miscellaneous Release – Data 273 – Revised.

- Muir, T.L. 2003. Structural evolution of the Hemlo greenstone belt in the vicinity of the world-class Hemlo gold deposit. *Canadian Journal of Earth Sciences*, **40**: 395-430.
- Nabighian, M.N. 1972. The analytic signal of two-dimensional magnetic bodies with polygonal cross-section: Its properties and use for automated anomaly interpretation. *Geophysics*, **37**: 507-517.
- OGS (Ontario Geological Survey), 1967. Agonzon Lake Sheet. Map 2145. Ontario Department of Mine, scale 1:31 680.
- OGS (Ontario Geological Survey), 2011b. 1:250 000 Scale Bedrock Geology of Ontario; Ontario Geological Survey, Miscellaneous Release – Data 126 Revision 1.
- Osmani, I.A. 1991. Proterozoic mafic dyke swarms in the Superior Province of Ontario. *Geology of Ontario*, Ontario Geological Survey, Special Volume 4, Part 1, 661-681.
- Pan, Y., Fleet, M.E., Williams, H.R., 1994. Granulite-facies metamorphism in the Quetico Subprovince, north of Manitouwadge, Ontario. *Canadian Journal of Earth Sciences*, **31**: 1427-1439.
- Pease, V., Percival, J., Smithies, H., Stevens, G. and Van Kranendonk, M. 2008. When did plate tectonics begin? Evidence from the orogenic record; In: Condie, K.C. and Pease, V., eds., *When Did Plate Tectonics Begin on Earth?* Geological Society of America Special Paper 440, 199-228.
- Percival, J.A. 1989. A regional perspective of the Quetico metasedimentary belt, Superior Province, Canada, *Canadian Journal of Earth Sciences*, **26**: 677-693.
- Percival, J.A. and Williams, H.R. 1989. Late Archean Quetico accretionary complex, Superior Province, Canada. *Geology*, **17**: 23-25.
- Percival, J.A., Sanborn-Barrie, M., Skulski, T., Stott, G.M., Helmstaedt, H. and White, D.J. 2006. Tectonic evolution of the western Superior Province from NATMAP and Lithoprobe studies; *Canadian Journal of Earth Sciences*, **43**: 1085-1117.
- Peterson, V.L., and Zaleski, E. 1999. Structural history of the Hornepayne greenstone belt and its volcanogenic Cu-Zn massive sulphide deposits, Wawa Subprovince, south-central Superior Province; *Canadian Journal of Earth Sciences*, **36**: 605-625.
- Phillips, J.D. 1997. Potential-field geophysical software for the PC, version 2.2, U.S. Geological Survey Open-File Report, 97-725.
- Phillips, J.D. 2000. Locating magnetic contacts: a comparison of the horizontal gradient, analytic signal, and local wavenumber methods, *Society of Exploration Geophysics, Expanded Abstracts with Biographies*, 2000 Technical Program, **1**: 402-405.
- Polat, A. 1998. Geodynamics of the Late Archean Wawa Subprovince greenstone belts, Superior Province, Canada. PhD Thesis, Department of Geological Sciences, University of Saskatchewan, Saskatoon.
- Polat, A., Kerrich, R. and Wyman, D.A. 1998. The late Archean Schreiber–Hemlo and Hornepayne–Dayohessarah greenstone belts, Superior Province: collages of oceanic plateaus, oceanic arcs, and subduction–accretion complexes; *Tectonophysics*, **289**: 295-326.
- Powell, W.G., Carmichael, D.M. and Hodgson, C.J. 1993. Thermobarometry in a subgreenschist to greenschist transition in metabasites of the Abitibi greenstone belt, Superior Province, Canada; *J. Metamorphic Geology*, **11**: 165-178.

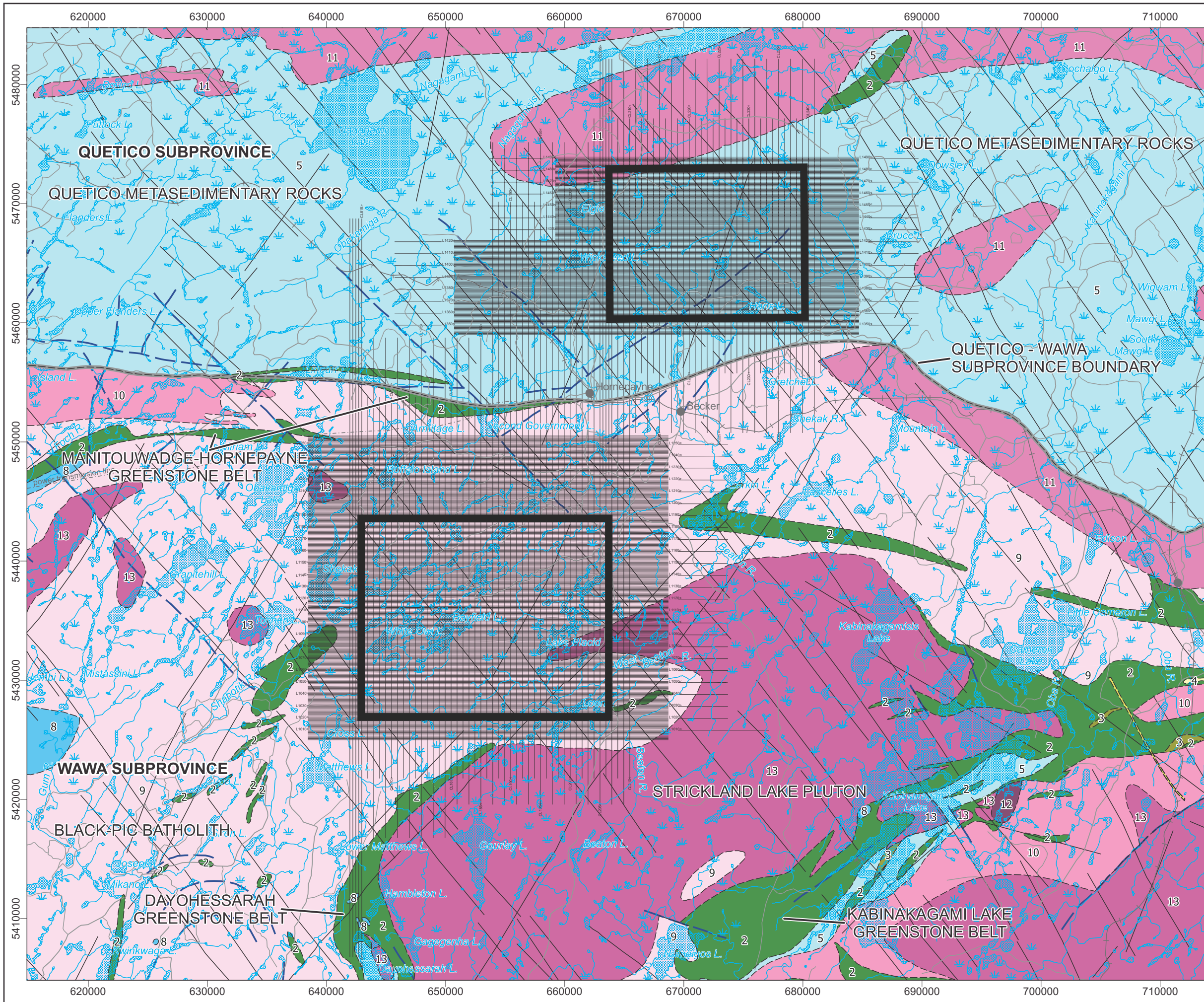
- Prest, V.K. 1970. Quaternary geology of Canada; in *Geology and Economic Minerals of Canada*, Geological Survey of Canada, Economic Geology Report no.1, Fifth Edition, 675-764.
- Roest, W., and Pilkington, M. 1993. Identifying Remanent Magnetization Effects in Magnetic Data, *Geophysics*, **58**: no. 5, 653-659.
- Salem, A., Williams, S., Fairhead, J. D., Ravat, D., and Smith, R. 2007. Tilt-depth method: A Simple depth estimation method using first-order magnetic derivatives, *The Leading Edge*, **26**: 1502-1505.
- SGL (Sander Geophysics Limited). 2017a. Phase 2 Geoscientific Preliminary Assessment, Acquisition, Processing and Interpretation of High-Resolution Airborne Geophysical Data, Township of Manitouwadge and Area, Ontario. Prepared for Nuclear Waste Management Organization (NWMO). NWMO Report Number: APM-REP-01332-0213.
- SGL (Sander Geophysics Limited). 2017b. Phase 2 Geoscientific Preliminary Assessment, Acquisition, Processing and Interpretation of High-Resolution Airborne Geophysical Data, Township of White River and Area, Ontario. Prepared for Nuclear Waste Management Organization (NWMO). NWMO Report Number: APM-REP-01332-0209.
- Siragusa, G.M. 1977. Geology of the Kabinakagami Lake area, District of Algoma; Ontario Division of Mines, Geoscience Report 159, accompanied by Map 2355, scale 1:63,360 or 1 inch to 1 mile.
- Siragusa, G.M. 1976. Kabinakagami Lake, Algoma District, Ontario Geological Survey, Map 2355, scale 1:63,360.
- SRK Consulting Inc. 2017. Phase 2 Geoscientific Preliminary Assessment Lineament Interpretation, Township of Hornepayne and Area, Ontario. Prepared for Nuclear Waste Management Organization (NWMO). NWMO Report Number: APM-REP-01332-0206
- Stott, G.M. 1999. Precambrian geology of the Dayohessarah Lake area, Hornepayne, Ontario; Ontario Geological Survey, Open File Report 5984.
- Sutcliffe, R.H. 1991. Proterozoic Geology of the Lake Superior Area. In: *Geology of Ontario*, Ontario Geological Survey, Special Volume 4, Part 1, 627-658.
- Telford, W.M., Geldart, L.P., and Sheriff, R.E. 1990. *Applied geophysics*. 2nd edition. Cambridge University Press.
- Verduzco B., Fairhead J.D., Green C.M., and MacKenzie C. 2004. New insights into magnetic derivatives for structural mapping, *The Leading Edge*, 116-119.
- Williams, H. R., Stott, G.M., Heather, K.B., Muir, T.L. and Sage, R.P. 1991. Wawa Subprovince; In: *Geology of Ontario*, Ontario Geological Survey, Special Volume 4, Part 1, 485-525.
- Williams, H.R. 1991. The Quetico Subprovince; In: *The Geology of Ontario*, Ontario Geological Survey, Special Volume 4, Part 1, 383-403.
- Williams, H.R. and Breaks, F.W. 1989. Geological studies in the Hornepayne-Hornepayne area; Ontario Geological Survey, Miscellaneous Paper 146, 79-91.
- Williams, H.R., 1989. Geological studies in the Wabigoon, Quetico and Abitibi-Wawa subprovinces, Superior Province of Ontario, with emphasis on the structural development of the Beardmore-Geraldton Belt, Ontario Geological Survey, Open File Report 5724.

- Williams, H.R., and Breaks, F.W. 1990. Geology of the Manitouwadge-Hornepayne area; Ontario Geological Survey, Open File Map 142, scale 1:50 000.
- Williams, H.R., and F.R. Breaks. 1996. Geology of the Manitouwadge-Hornepayne region, Ontario; Ontario Geological Survey, Open File Report 5953.
- Williams, H.R., Stott, G.M., Heather, K.B., Muir, T.L., and Sage, R.P. 1991. Wawa Subprovince; In: The Geology of Ontario, Ontario Geological Survey, Special Volume 4, Part 1, 485-539.
- Zaleski, E. and Peterson, V.L. 1993. Geology of the Hornepayne greenstone belt, Ontario; Geological Survey of Canada, Open File 2753, scale 1:25,000.
- Zaleski, E. and Peterson, V.L. 1995. Depositional setting and deformation of massive sulfide deposits, iron-formation, and associated alteration in the Manitouwadge greenstone belt, Superior Province, Ontario; *Economic Geology*, **90(8)**: 2244-2261.
- Zaleski, E., Peterson, V.L., and van Breemen, O., 1995. Geological and age relationships of the margins of the Hornepayne greenstone belt and the Wawa-Quetico subprovince boundary, northwestern Ontario. *Current Research 1995-C*, Geological Survey of Canada, 35-44.
- Zaleski, E., van Breemen O. and Peterson, V.L. 1999. Geological evolution of the Hornepayne greenstone belt and the Wawa-Quetico subprovince boundary, Superior Province, Ontario, constrained by U-Pb zircon dates of supracrustal and plutonic rocks. *Canadian Journal of Earth Sciences*, **36**: 945-966.

8 FIGURES

- 1.1 Survey Area
- 1.2 Flight Lines
- 3.1 Digital Elevation Model (25 m cell)
- 4.1 Bouguer Gravity (Density: $2.67\text{g}/\text{cm}^3$) (25 m cell)
- 4.2 Bouguer Gravity (Density: $2.67\text{g}/\text{cm}^3$) (250 m cell)
- 4.3 Free Air Gravity (25 m cell)
- 4.4 Free Air Gravity (250 m cell)
- 4.5 Total Magnetic Intensity (25 m cell)
- 4.6 Total Magnetic Intensity (250 m cell)
- 4.7 Reduction to the Pole of the Magnetic Field (25 m cell)
- 4.8 Reduction to the Pole of the Magnetic Field (250 m cell)
- 4.9 First Vertical Derivative of the Reduction to the Pole of the Total Magnetic Intensity (25 m cell)
- 4.10 First Vertical Derivative of the Reduction to the Pole of the Total Magnetic Intensity (250 m cell)
- 4.11 First Vertical Derivative of the Bouguer Gravity (Density: $2.67\text{g}/\text{cm}^3$) (25 m cell)
- 4.12 First Vertical Derivative of the Bouguer Gravity (Density: $2.67\text{g}/\text{cm}^3$) (250 m cell)
- 4.13 First Vertical Derivative of the Free Air Gravity (25 m cell)
- 4.14 First Vertical Derivative of the Free Air Gravity (250 m cell)
- 4.15 Second Vertical Derivative of the Reduction to the Pole of the Total Magnetic Intensity (25 m cell)
- 4.16 Second Vertical Derivative of the Reduction to the Pole of the Total Magnetic Intensity (250 m cell)
- 4.17 Total Horizontal Derivative of the Reduction to the Pole of the Total Magnetic Intensity (25 m cell)
- 4.18 Total Horizontal Derivative of the Reduction to the Pole of the Total Magnetic Intensity (250 m cell)
- 4.19 Total Horizontal Derivative of the Bouguer Gravity (Density: $2.67\text{g}/\text{cm}^3$) (25 m cell)
- 4.20 Total Horizontal Derivative of the Bouguer Gravity (Density: $2.67\text{g}/\text{cm}^3$) (250 m cell)
- 4.21 Total Horizontal Derivative of the Free Air Gravity (25 m cell)
- 4.22 Total Horizontal Derivative of the Free Air Gravity (250 m cell)
- 4.23 Analytic Signal of the Total Magnetic Intensity (25 m cell)
- 4.24 Analytic Signal of the Total Magnetic Intensity (250 m cell)

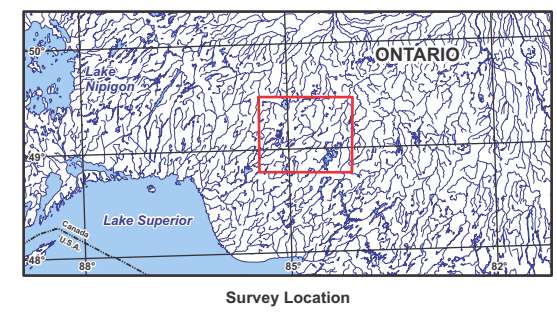
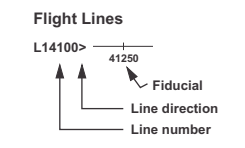
- 4.25 Tilt Angle of the Reduction to the Pole of the Total Magnetic Intensity (25 m cell)
- 4.26 Tilt Angle of the Reduction to the Pole of the Total Magnetic Intensity (250 m cell)
- 4.27 Trend Analysis Solutions of Bouguer Gravity (terrain correction density = 2.67 g/cm³)
- 4.28 Trend Analysis Solutions of Reduction to the Pole of the Total Magnetic Intensity
- 5.1 Bouguer Gravity (terrain correction density = 2.67 g/cm³) with Selected Interpretation Features
- 5.2 First Vertical Derivative of the Bouguer Gravity (terrain correction density = 2.67 g/cm³) with Selected Interpretation Features
- 5.3 Total Horizontal Derivative of the Bouguer Gravity (terrain correction density = 2.67 g/cm³) with Selected Interpreted Features
- 5.4 Reduction to the Pole of the Total Magnetic Intensity with Selected Interpretation Features
- 5.5 First Vertical Derivative of the Reduction to the Pole of the Total Magnetic Intensity with Selected Interpretation Features
- 5.6 Total Horizontal Derivative of the Reduction to the Pole of the Total Magnetic Intensity with Selected Interpretation Features
- 5.7 Location of 2.5D Model Lines shown with Bouguer Gravity (terrain correction density = 2.67 g/cm³)
- 5.8 Location of 2D Model Lines shown with Total Magnetic Intensity
- 5.9 Forward Modeling Results: Line 1, Hornepayne, Ontario
- 5.10 Forward Modeling Results: Line 1-Alternative, Hornepayne, Ontario
- 5.11 Forward Modeling Results: Line 2, Hornepayne, Ontario
- 5.12 Forward Modeling Results: Line 2-Alternative, Hornepayne, Ontario



- Legend**
- Hydrography
 - Roads
 - Railway
 - Powerline
 - Mine

- Geology**
- Fault
 - Dyke
 - Subprovince Boundary

- 2: Mafic metavolcanics
- 3: Felsic and intermediate metavolcanics
- 4: Felsic volcanics
- 5: Metasedimentary rocks
- 8: Gabbroic rocks
- 9: Gneissic tonalite suite
- 10: Foliate tonalite suite
- 11: Granite-granodiorite, muscovite/biotite bearing rocks
- 12: Diorite-monzonite-granodiorite
- 13: Granite-granodiorite



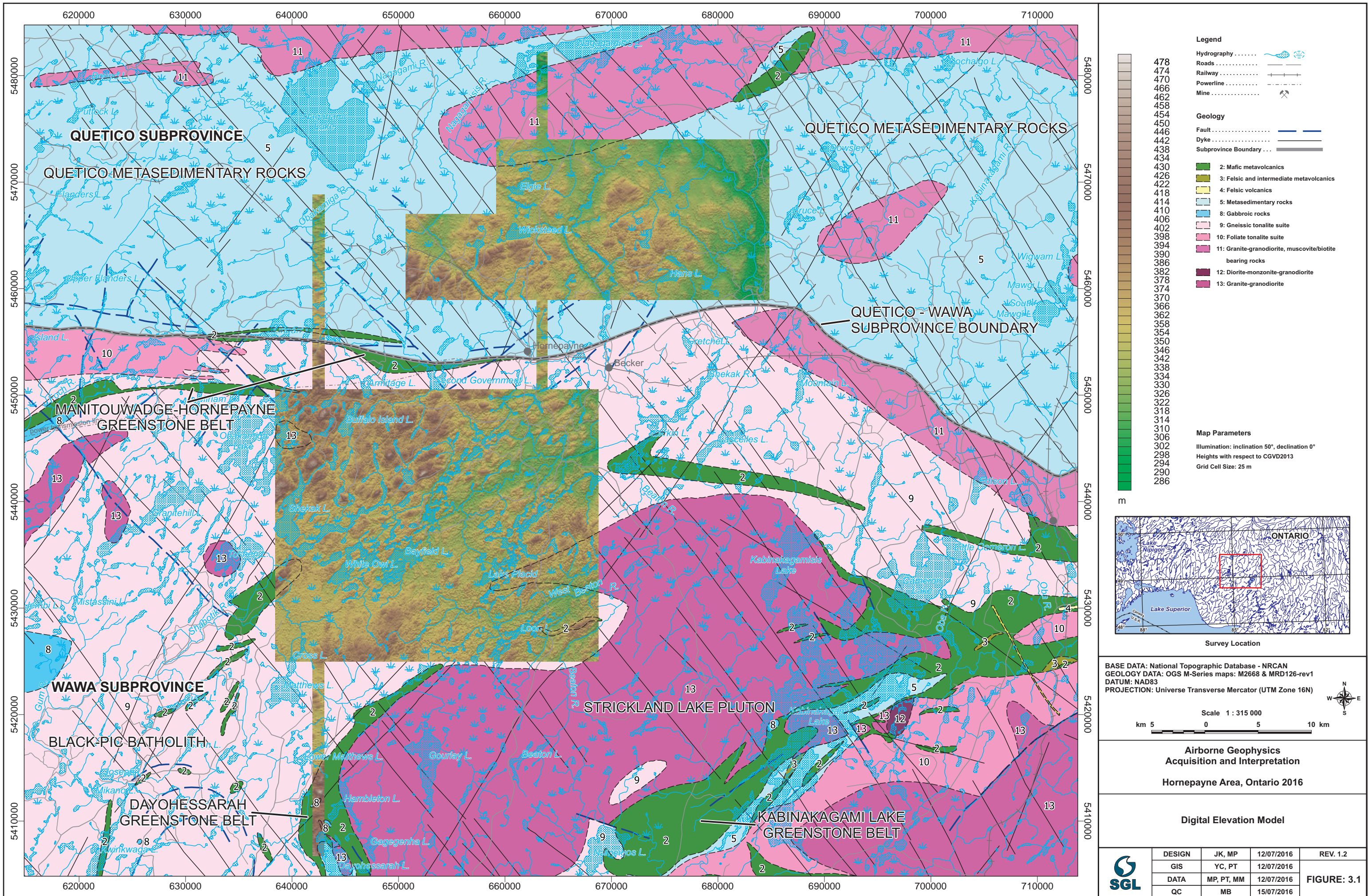
BASE DATA: National Topographic Database - NRCAN
 GEOLOGY DATA: OGS M-Series maps: M2668 & MRD126-rev1
 DATUM: NAD83
 PROJECTION: Universal Transverse Mercator (UTM Zone 16N)

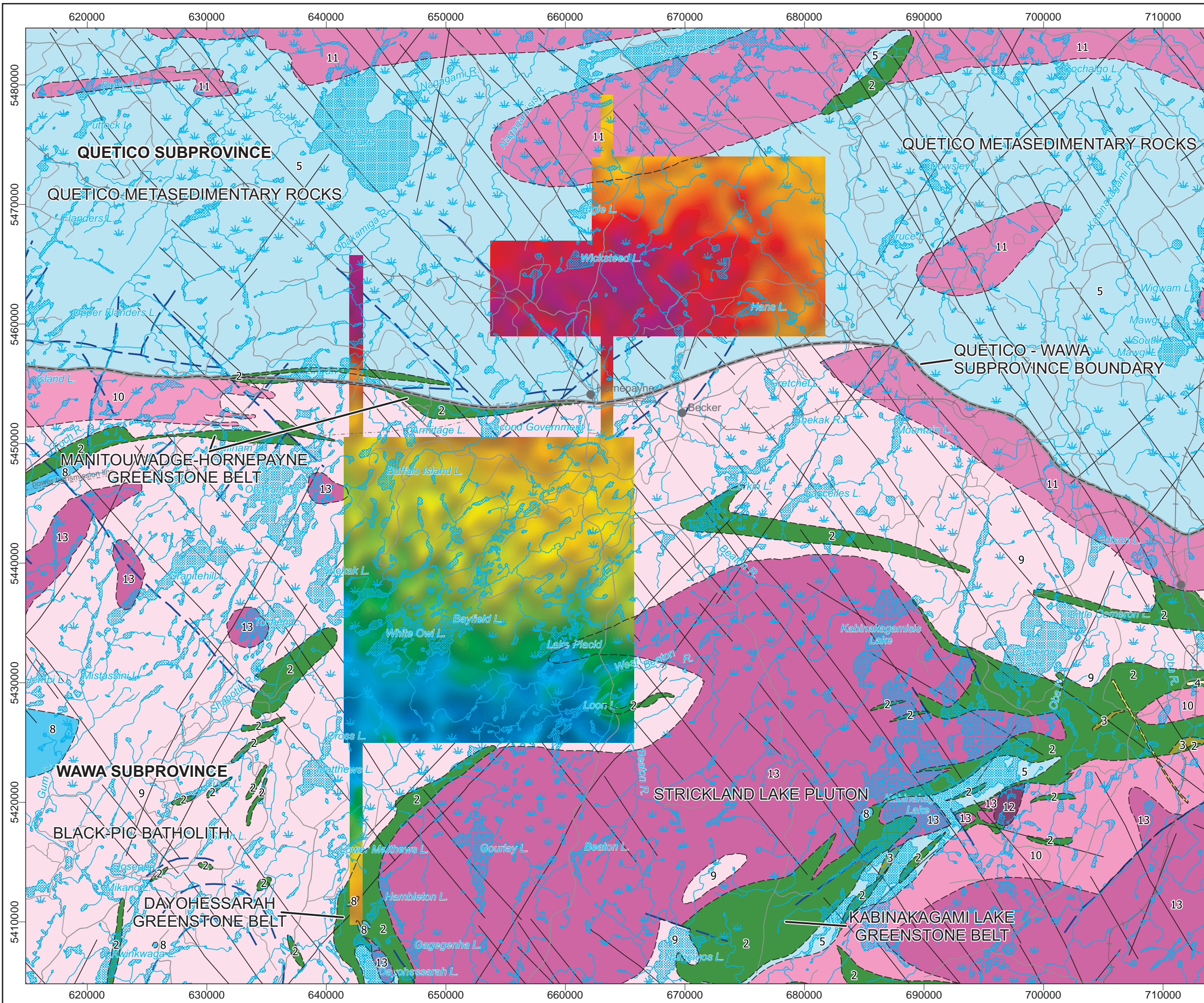


**Airborne Geophysics
 Acquisition and Interpretation**
 Hornepayne Area, Ontario 2016

Flight Lines

	DESIGN	JK, MP	12/07/2016	REV. 1.2
	GIS	YC, PT	12/07/2016	
	DATA	MP, PT, MM	12/07/2016	FIGURE: 1.2
	QC	MB	15/07/2016	





Legend

Hydrography

Roads

Railway

Powerline

Mine

Geology

Fault

Dyke

Subprovince Boundary

2: Mafic metavolcanics

3: Felsic and intermediate metavolcanics

4: Felsic volcanics

5: Metasedimentary rocks

8: Gabbroic rocks

9: Gneissic tonalite suite

10: Foliate tonalite suite

11: Granite-granodiorite, muscovite/biotite bearing rocks

12: Diorite-monzonite-granodiorite

13: Granite-granodiorite

Map Parameters

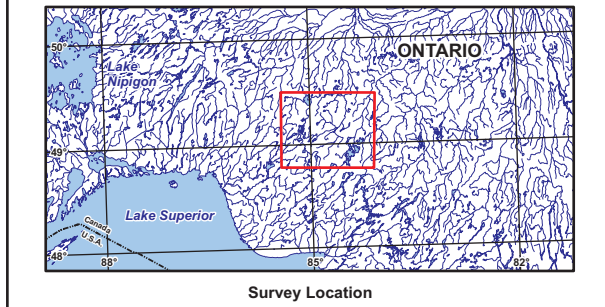
Illumination: inclination 50°, declination 0°

Spatial Filter (half-wavelength): 1000 m

Bouguer Density: 2.67 g/cm³

Grid Cell Size: 25 m

mGal



BASE DATA: National Topographic Database - NRCAN
 GEOLOGY DATA: OGS M-Series maps: M2668 & MRD126-rev1
 DATUM: NAD83
 PROJECTION: Universe Transverse Mercator (UTM Zone 16N)

Scale 1 : 315 000

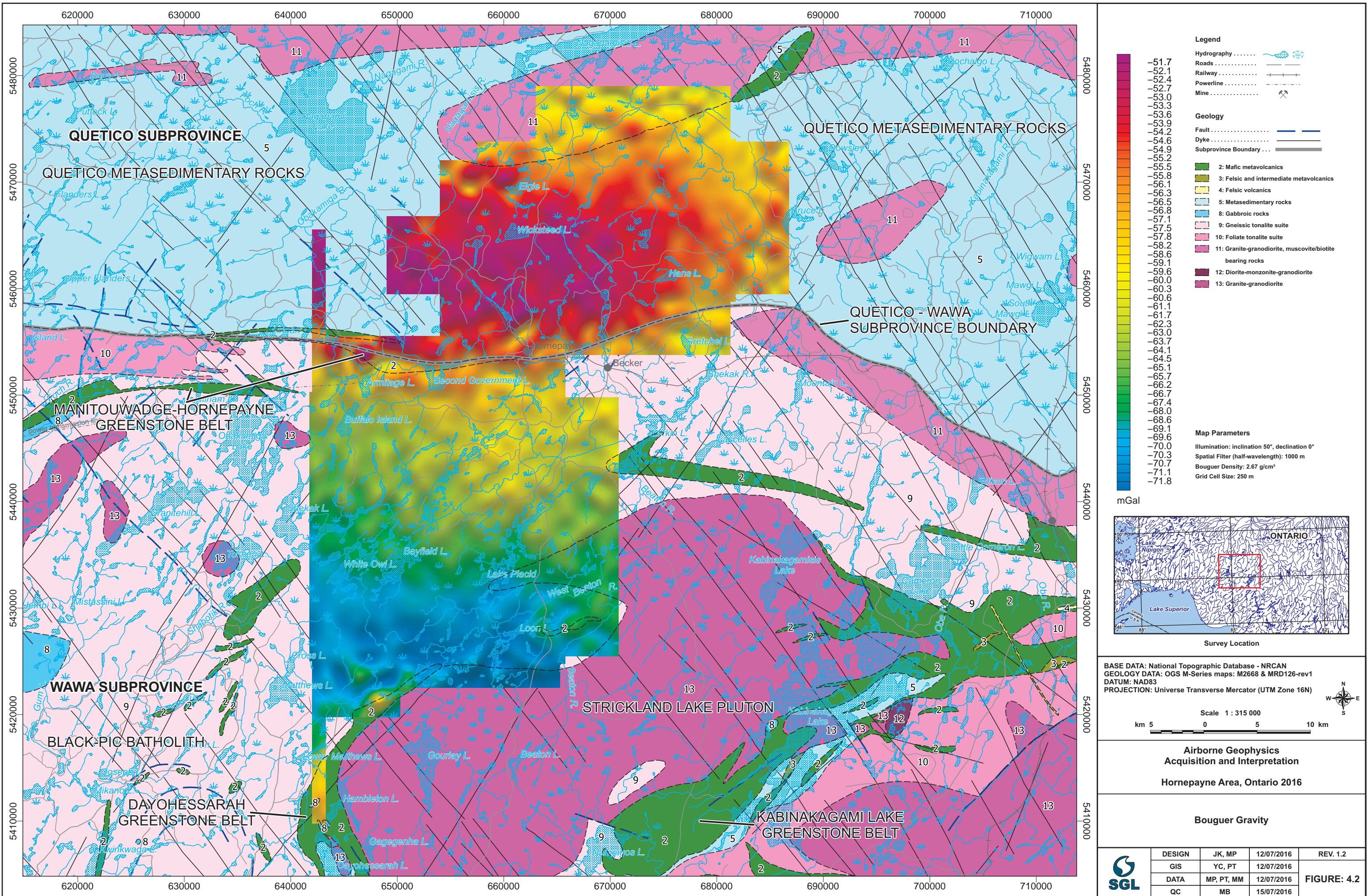
km 5 0 5 10 km

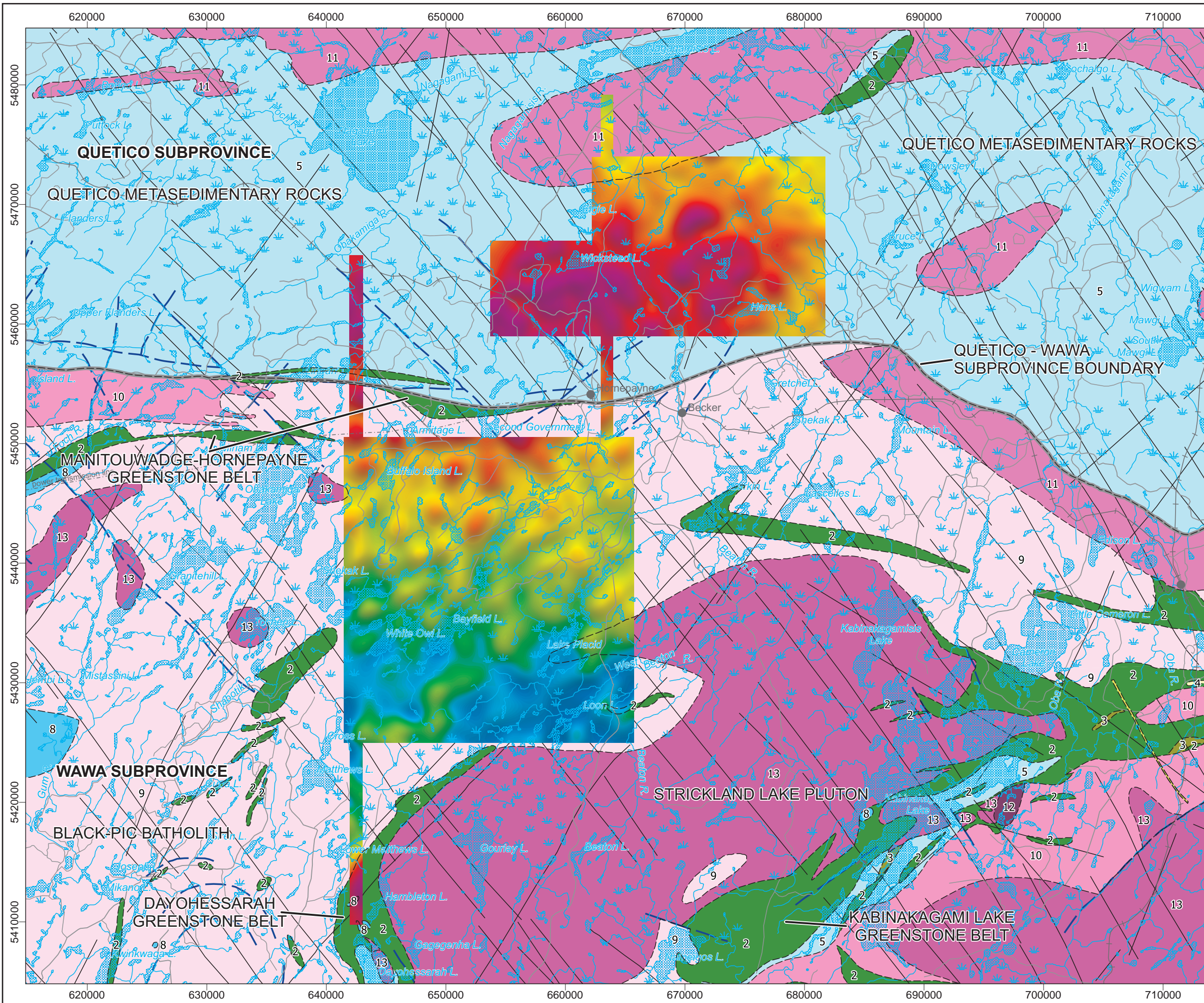
Airborne Geophysics Acquisition and Interpretation

Hornepayne Area, Ontario 2016

Bouguer Gravity

	DESIGN	JK, MP	12/07/2016	REV. 1.2
	GIS	YC, PT	12/07/2016	
	DATA	MP, PT, MM	12/07/2016	FIGURE: 4.1
	QC	MB	15/07/2016	





Legend

Hydrography

Roads

Railway

Powerline

Mine

Geology

Fault

Dyke

Subprovince Boundary

2: Mafic metavolcanics

3: Felsic and intermediate metavolcanics

4: Felsic volcanics

5: Metasedimentary rocks

8: Gabbroic rocks

9: Gneissic tonalite suite

10: Foliate tonalite suite

11: Granite-granodiorite, muscovite/biotite bearing rocks

12: Diorite-monzonite-granodiorite

13: Granite-granodiorite

Map Parameters

Illumination: inclination 50°, declination 0°

Spatial Filter (half-wavelength): 1000 m

Grid Cell Size: 25 m

mGal

Survey Location

BASE DATA: National Topographic Database - NRCAN
 GEOLOGY DATA: OGS M-Series maps: M2668 & MRD126-rev1
 DATUM: NAD83
 PROJECTION: Universe Transverse Mercator (UTM Zone 16N)

Scale 1 : 315 000

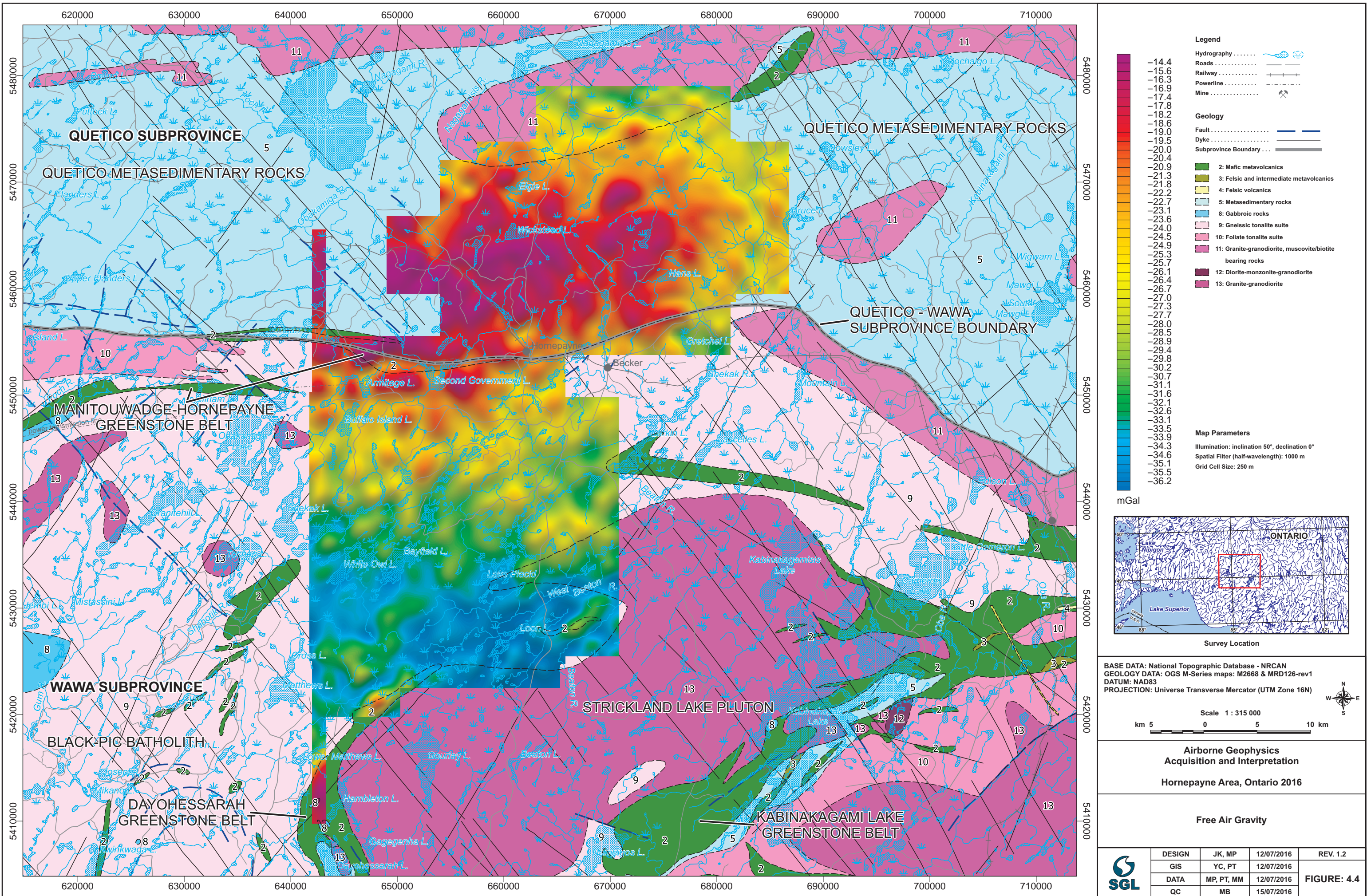
km 5 0 5 10 km

**Airborne Geophysics
 Acquisition and Interpretation**

Hornepayne Area, Ontario 2016

Free Air Gravity

	DESIGN	JK, MP	12/07/2016	REV. 1.2
	GIS	YC, PT	12/07/2016	
	DATA	MP, PT, MM	12/07/2016	FIGURE: 4.3
	QC	MB	15/07/2016	

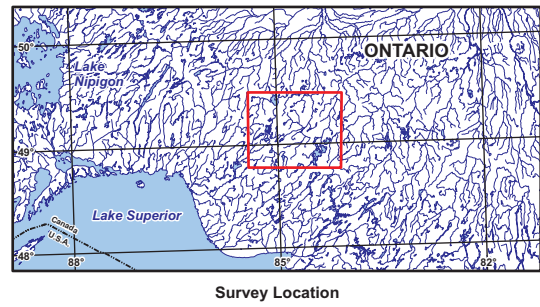


- Legend**
- Hydrography
 - Roads
 - Railway
 - Powerline
 - Mine
- Geology**
- Fault
 - Dyke
 - Subprovince Boundary

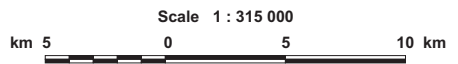
- 2: Mafic metavolcanics
- 3: Felsic and intermediate metavolcanics
- 4: Felsic volcanics
- 5: Metasedimentary rocks
- 8: Gabbroic rocks
- 9: Gneissic tonalite suite
- 10: Foliate tonalite suite
- 11: Granite-granodiorite, muscovite/biotite bearing rocks
- 12: Diorite-monzonite-granodiorite
- 13: Granite-granodiorite

Map Parameters

Illumination: inclination 50°, declination 0°
 Spatial Filter (half-wavelength): 1000 m
 Grid Cell Size: 250 m



BASE DATA: National Topographic Database - NRCAN
 GEOLOGY DATA: OGS M-Series maps: M2668 & MRD126-rev1
 DATUM: NAD83
 PROJECTION: Universe Transverse Mercator (UTM Zone 16N)

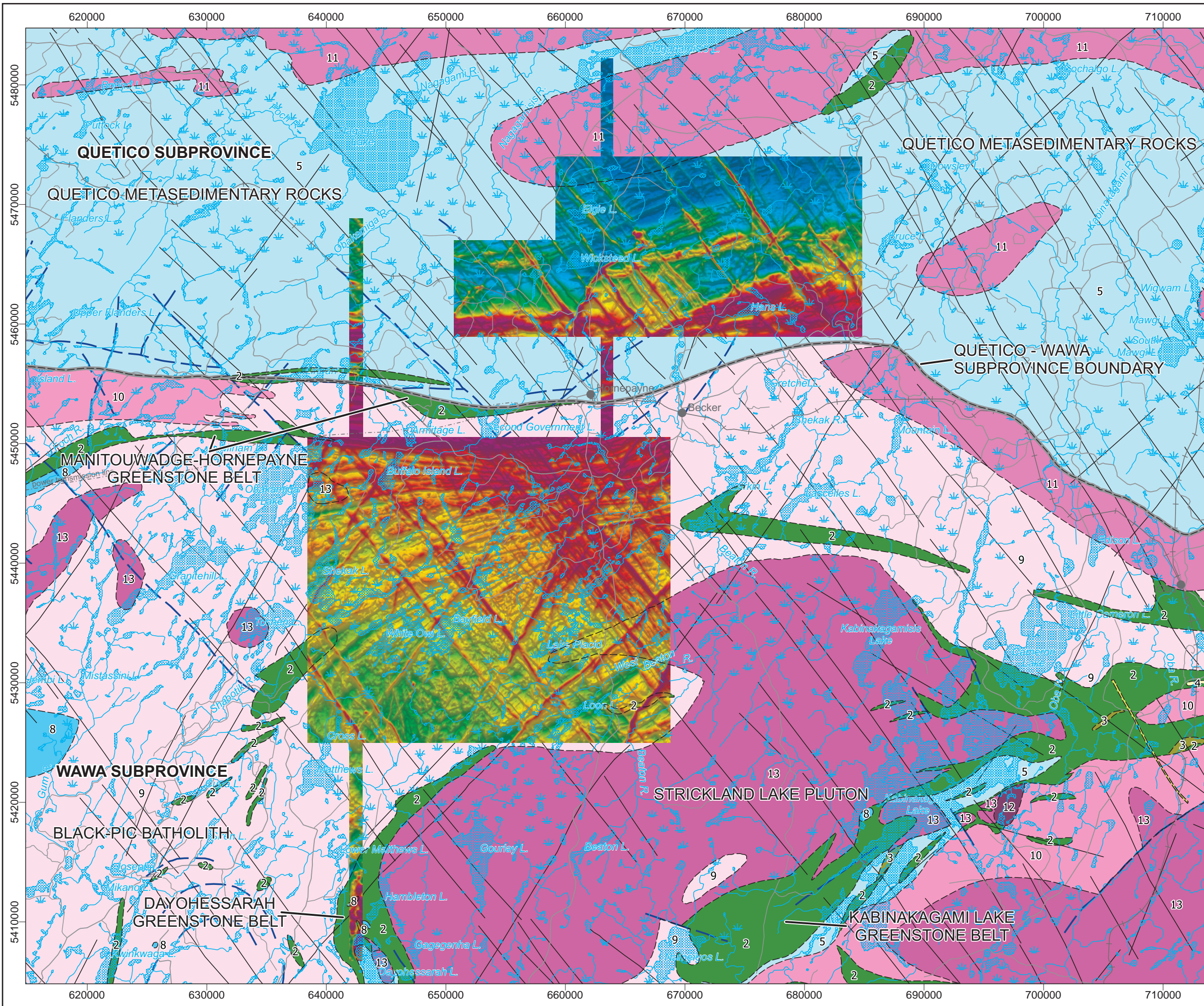


**Airborne Geophysics
 Acquisition and Interpretation**

Hornepayne Area, Ontario 2016

Free Air Gravity

	DESIGN	JK, MP	12/07/2016	REV. 1.2
	GIS	YC, PT	12/07/2016	
	DATA	MP, PT, MM	12/07/2016	FIGURE: 4.4
	QC	MB	15/07/2016	



Legend

Hydrography

Roads

Railway

Powerline

Mine

Geology

Fault

Dyke

Subprovince Boundary

2: Mafic metavolcanics

3: Felsic and intermediate metavolcanics

4: Felsic volcanics

5: Metasedimentary rocks

8: Gabbroic rocks

9: Gneissic tonalite suite

10: Foliate tonalite suite

11: Granite-granodiorite, muscovite/biotite bearing rocks

12: Diorite-monzonite-granodiorite

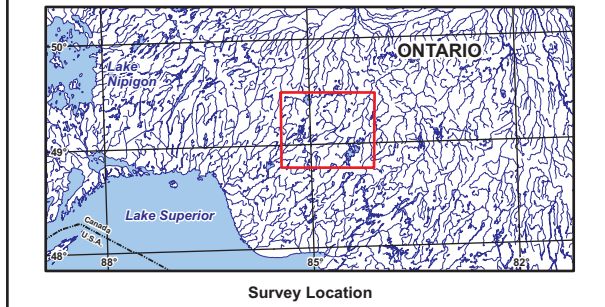
13: Granite-granodiorite

Map Parameters

Illumination: inclination 50°, declination 0°

Grid Cell Size: 25 m

nT



BASE DATA: National Topographic Database - NRCAN
 GEOLOGY DATA: OGS M-Series maps: M2668 & MRD126-rev1
 DATUM: NAD83
 PROJECTION: Universal Transverse Mercator (UTM Zone 16N)

Scale 1 : 315 000

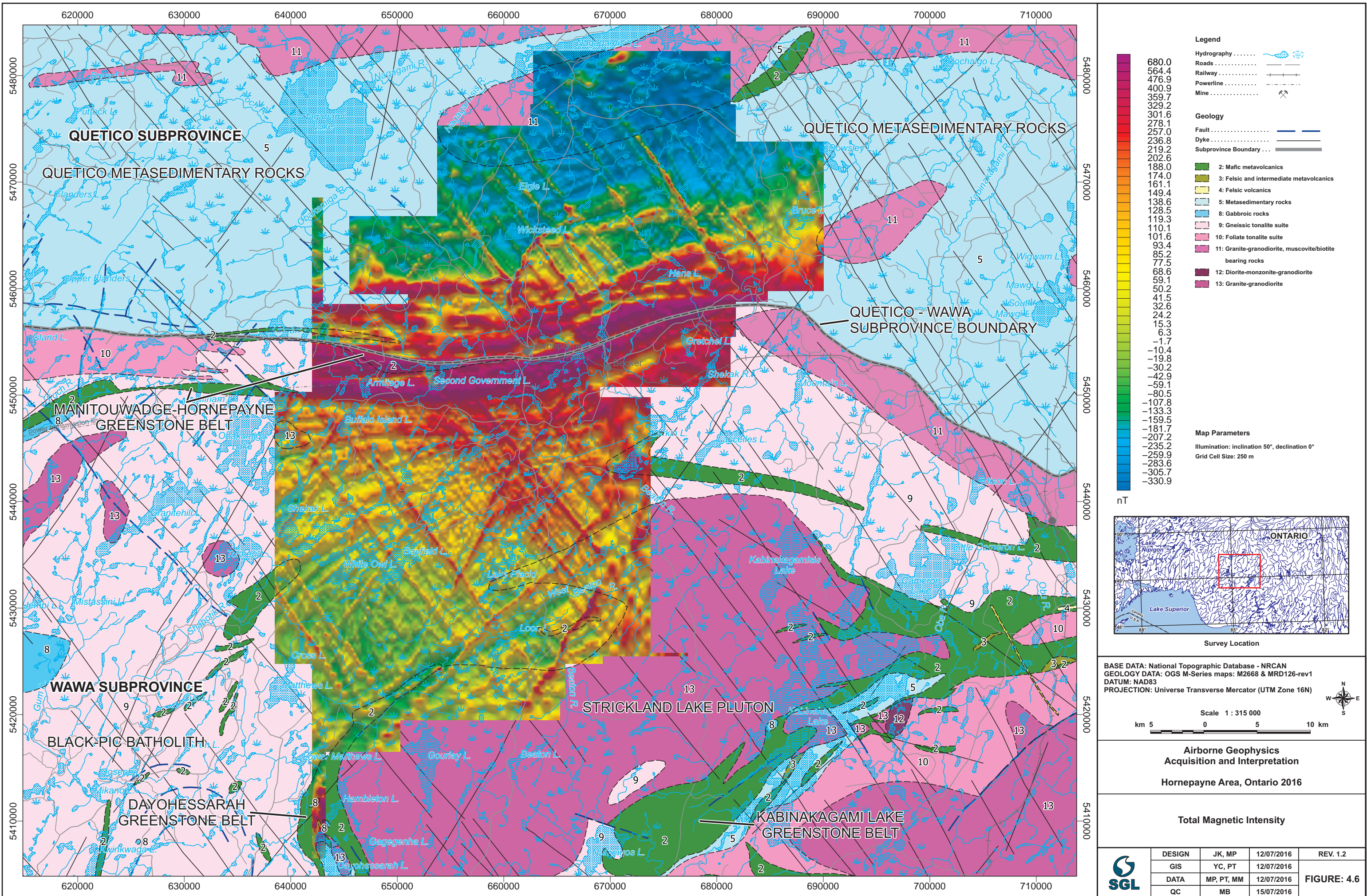
km 5 0 5 10 km

Airborne Geophysics Acquisition and Interpretation

Hornepayne Area, Ontario 2016

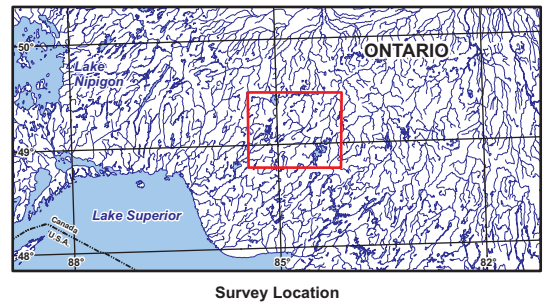
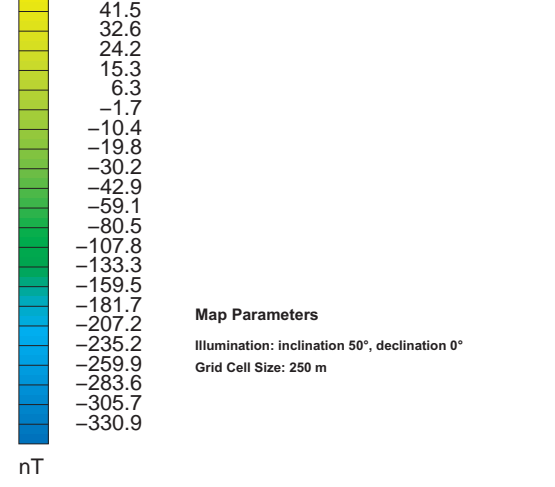
Total Magnetic Intensity

	DESIGN	JK, MP	12/07/2016	REV. 1.2
	GIS	YC, PT	12/07/2016	
	DATA	MP, PT, MM	12/07/2016	FIGURE: 4.5
	QC	MB	15/07/2016	



- Legend**
- Hydrography
 - Roads
 - Railway
 - Powerline
 - Mine
- Geology**
- Fault
 - Dyke
 - Subprovince Boundary

- 2: Mafic metavolcanics
- 3: Felsic and intermediate metavolcanics
- 4: Felsic volcanics
- 5: Metasedimentary rocks
- 8: Gabbroic rocks
- 9: Gneissic tonalite suite
- 10: Foliate tonalite suite
- 11: Granite-granodiorite, muscovite/biotite bearing rocks
- 12: Diorite-monzonite-granodiorite
- 13: Granite-granodiorite



BASE DATA: National Topographic Database - NRCAN
 GEOLOGY DATA: OGS M-Series maps: M2668 & MRD126-rev1
 DATUM: NAD83
 PROJECTION: Universe Transverse Mercator (UTM Zone 16N)

Scale 1 : 315 000

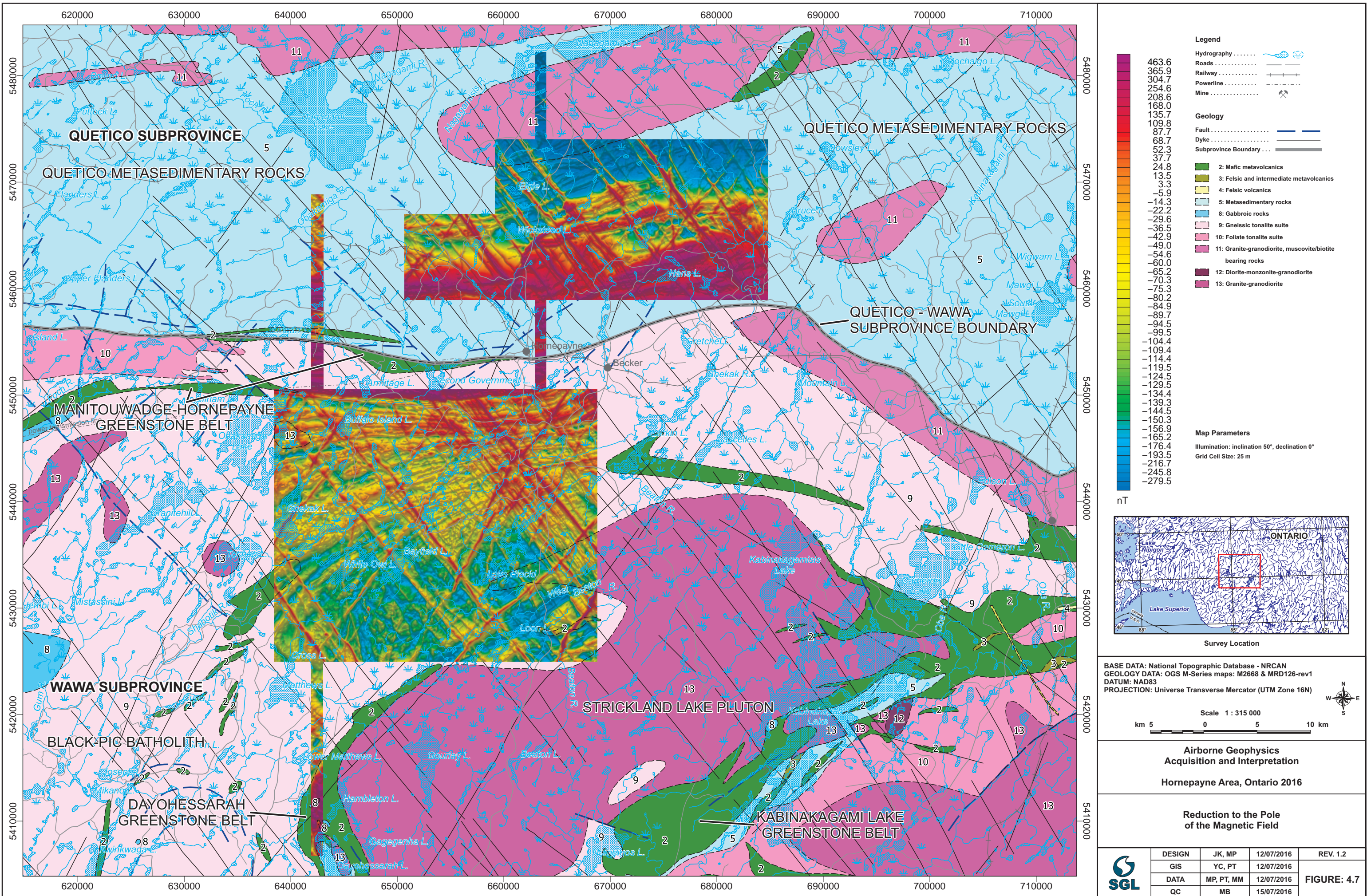
km 5 0 5 10 km

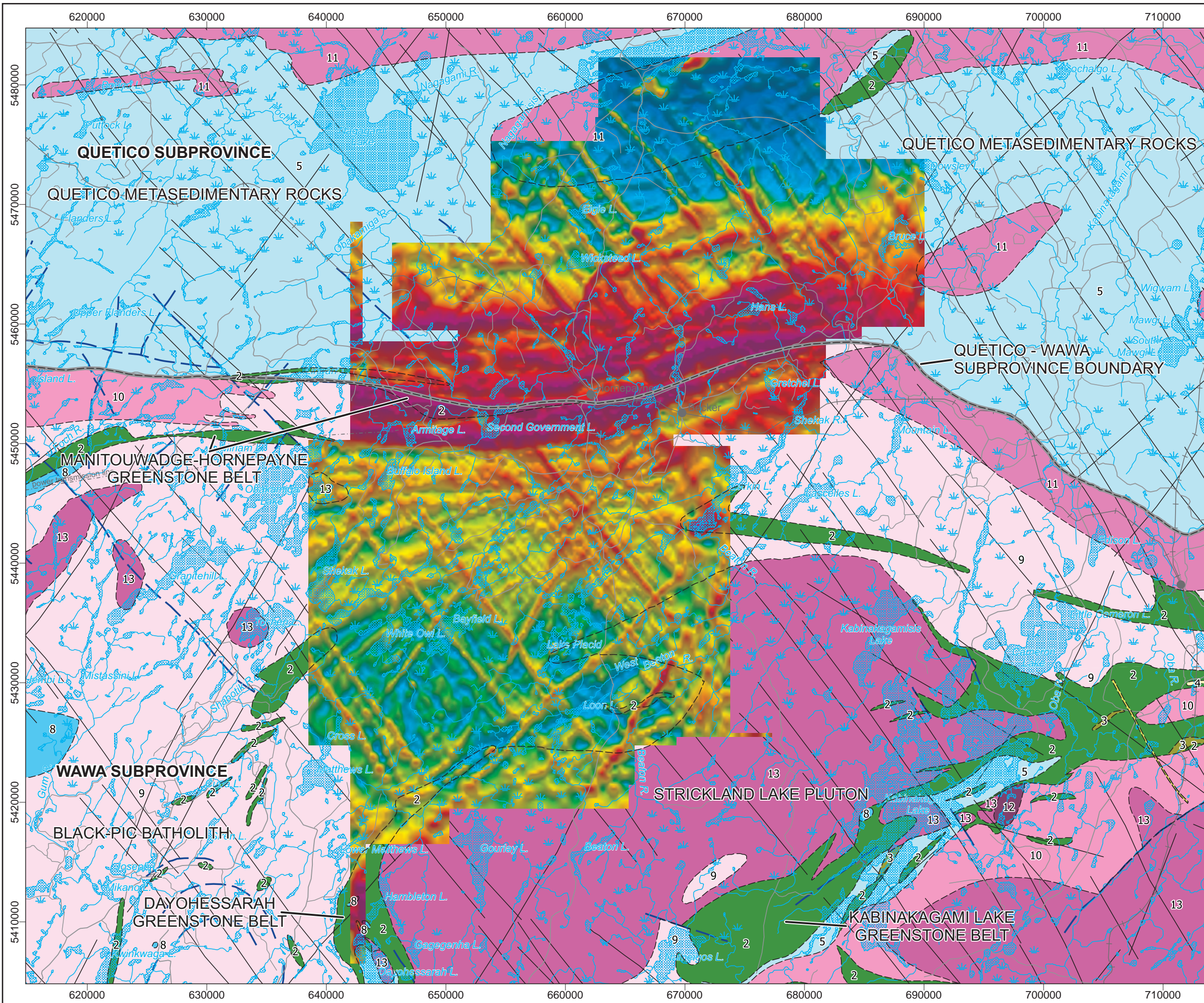
Airborne Geophysics Acquisition and Interpretation

Hornepayne Area, Ontario 2016

Total Magnetic Intensity

	DESIGN	JK, MP	12/07/2016	REV. 1.2
	GIS	YC, PT	12/07/2016	
	DATA	MP, PT, MM	12/07/2016	FIGURE: 4.6
	QC	MB	15/07/2016	





Legend

Hydrography

Roads

Railway

Powerline

Mine

Geology

Fault

Dyke

Subprovince Boundary

2: Mafic metavolcanics

3: Felsic and intermediate metavolcanics

4: Felsic volcanics

5: Metasedimentary rocks

8: Gabbroic rocks

9: Gneissic tonalite suite

10: Foliate tonalite suite

11: Granite-granodiorite, muscovite/biotite bearing rocks

12: Diorite-monzonite-granodiorite

13: Granite-granodiorite

Map Parameters

Illumination: inclination 50°, declination 0°

Grid Cell Size: 250 m

nT

574.4

480.0

410.0

356.9

311.6

273.6

237.5

206.9

179.2

154.5

132.3

111.5

91.2

70.4

52.4

35.1

20.6

7.5

-4.9

-15.4

-24.9

-33.8

-42.3

-50.1

-57.5

-64.4

-71.1

-77.1

-83.2

-89.2

-95.1

-100.7

-106.6

-112.9

-119.5

-126.4

-133.8

-141.1

-148.2

-154.9

-161.8

-169.4

-177.6

-188.4

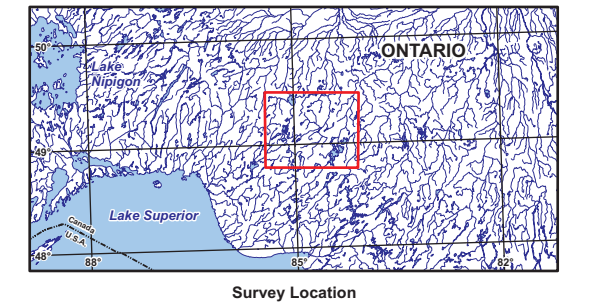
-203.4

-227.8

-257.3

-296.5

-339.1



BASE DATA: National Topographic Database - NRCAN
 GEOLOGY DATA: OGS M-Series maps: M2668 & MRD126-rev1
 DATUM: NAD83
 PROJECTION: Universe Transverse Mercator (UTM Zone 16N)

Scale 1 : 315 000

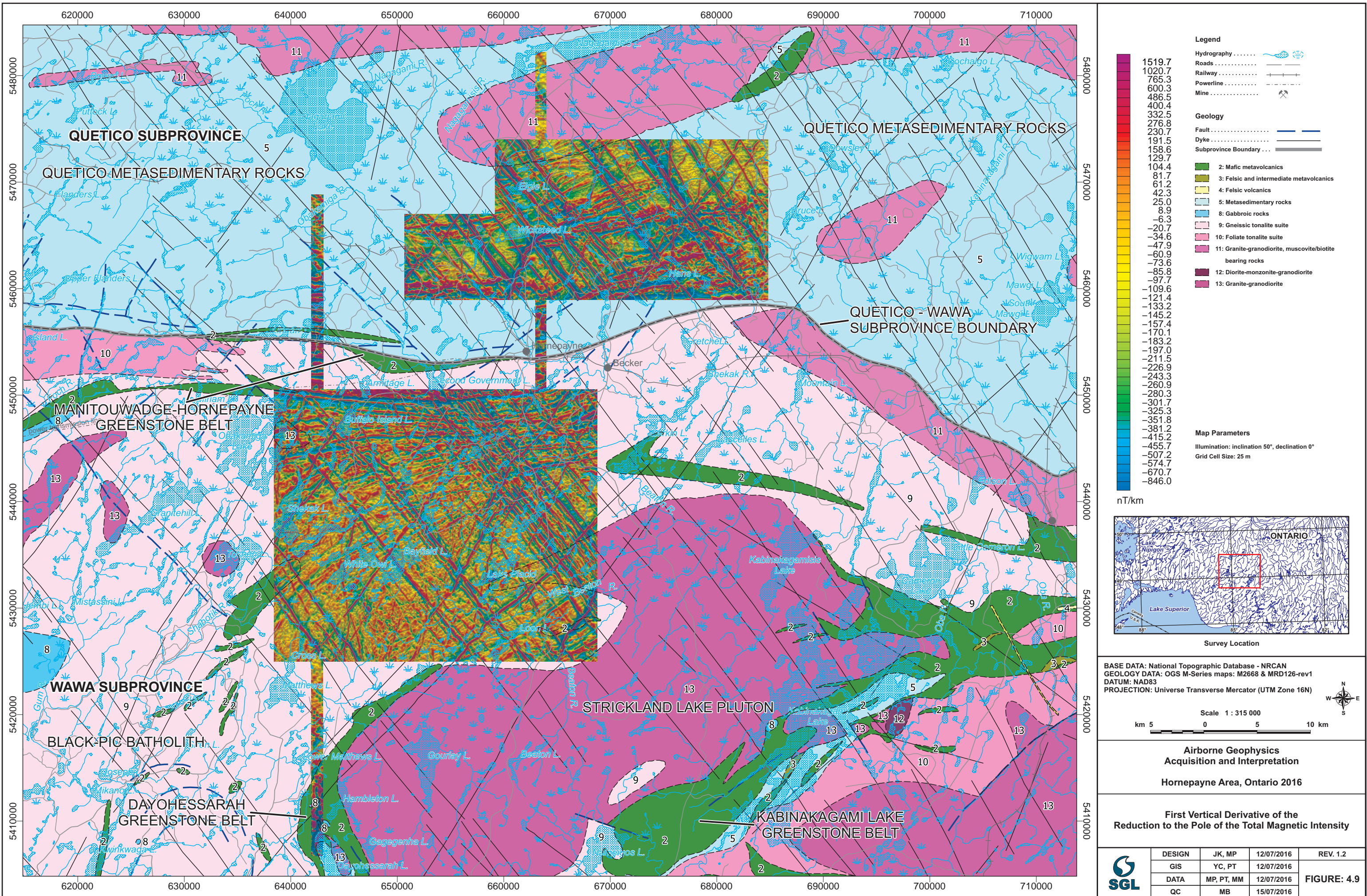
km 5 0 5 10 km

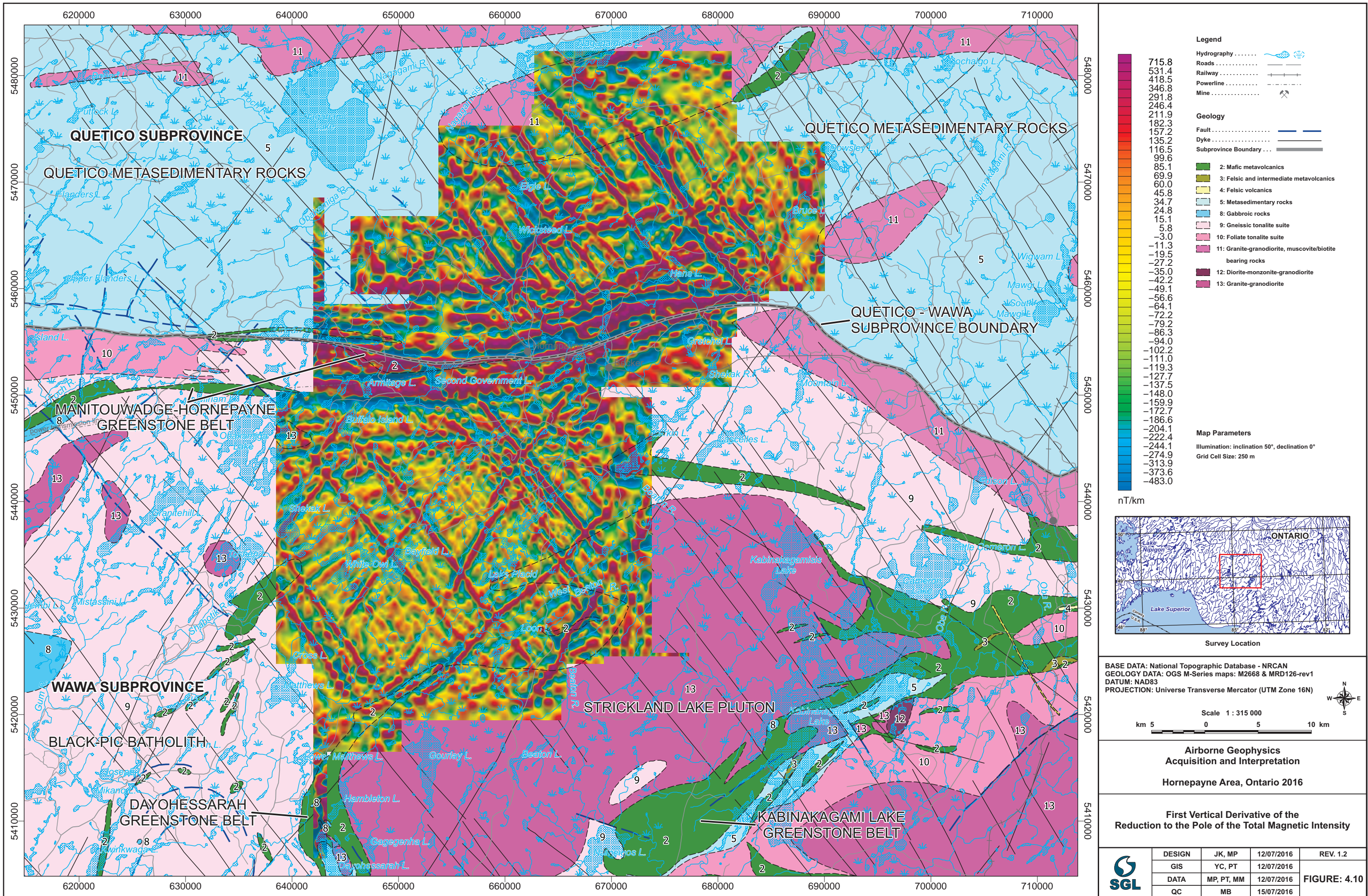
**Airborne Geophysics
 Acquisition and Interpretation**

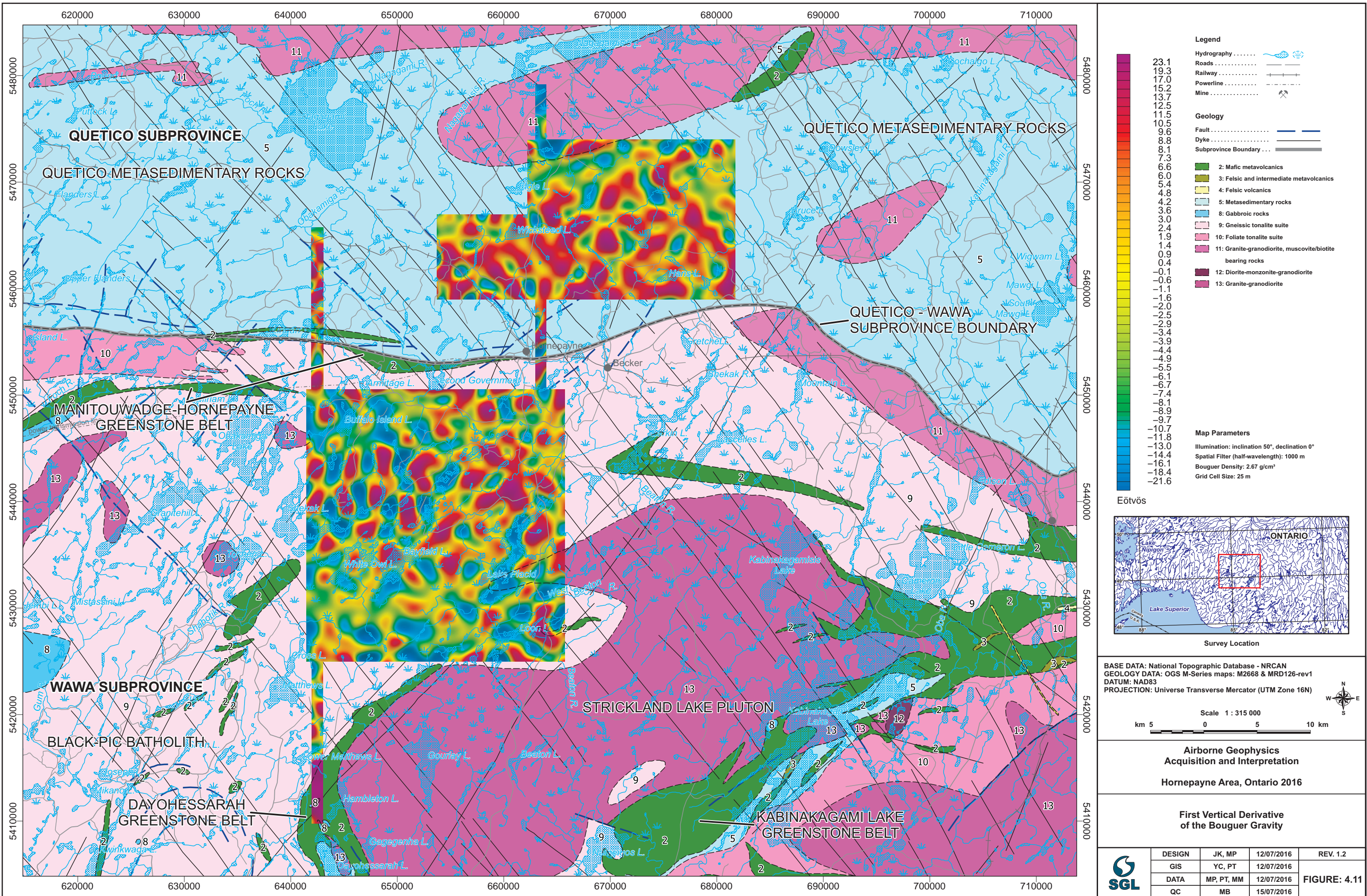
Hornepayne Area, Ontario 2016

**Reduction to the Pole
 of the Magnetic Field**

	DESIGN	JK, MP	12/07/2016	REV. 1.2
	GIS	YC, PT	12/07/2016	
	DATA	MP, PT, MM	12/07/2016	FIGURE: 4.8
	QC	MB	15/07/2016	

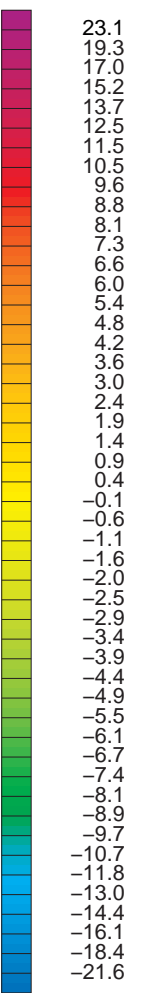






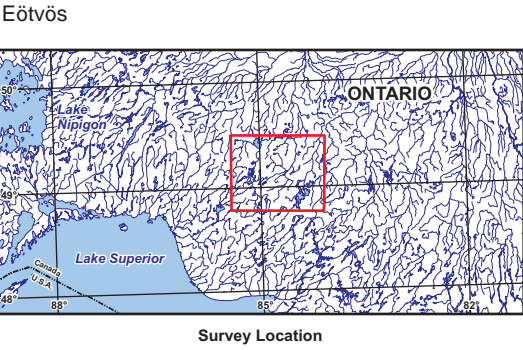
- Legend**
- Hydrography
 - Roads
 - Railway
 - Powerline
 - Mine

- Geology**
- Fault
 - Dyke
 - Subprovince Boundary
- 2: Mafic metavolcanics
 - 3: Felsic and intermediate metavolcanics
 - 4: Felsic volcanics
 - 5: Metasedimentary rocks
 - 8: Gabbroic rocks
 - 9: Gneissic tonalite suite
 - 10: Foliate tonalite suite
 - 11: Granite-granodiorite, muscovite/biotite bearing rocks
 - 12: Diorite-monzonite-granodiorite
 - 13: Granite-granodiorite

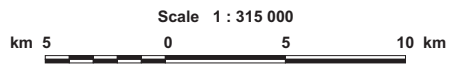


Map Parameters

Illumination: inclination 50°, declination 0°
 Spatial Filter (half-wavelength): 1000 m
 Bouguer Density: 2.67 g/cm³
 Grid Cell Size: 25 m



BASE DATA: National Topographic Database - NRCAN
 GEOLOGY DATA: OGS M-Series maps: M2668 & MRD126-rev1
 DATUM: NAD83
 PROJECTION: Universe Transverse Mercator (UTM Zone 16N)

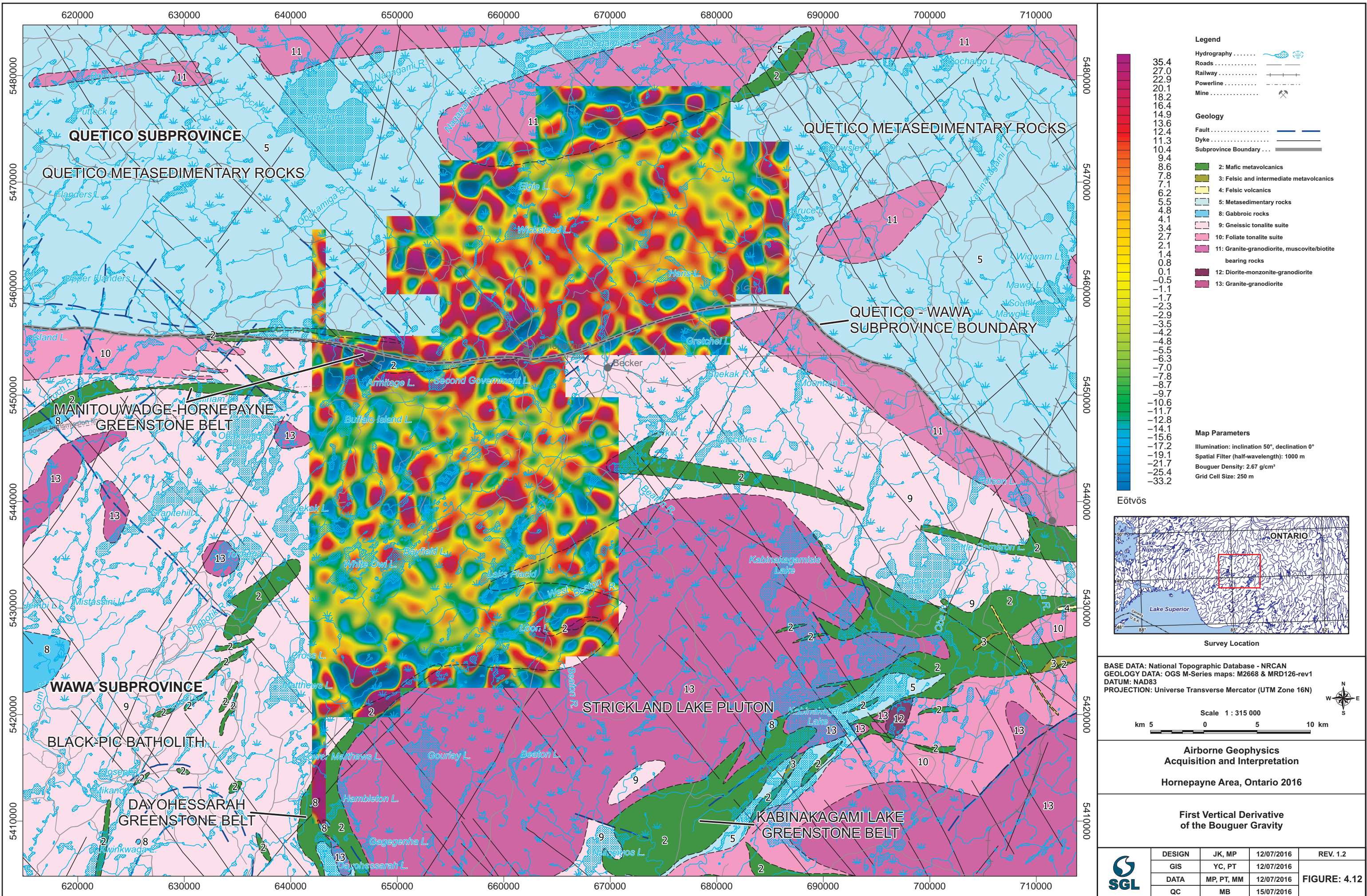


**Airborne Geophysics
 Acquisition and Interpretation**

Hornepayne Area, Ontario 2016

First Vertical Derivative
 of the Bouguer Gravity

	DESIGN	JK, MP	12/07/2016	REV. 1.2
	GIS	YC, PT	12/07/2016	
	DATA	MP, PT, MM	12/07/2016	FIGURE: 4.11
	QC	MB	15/07/2016	



Legend

Hydrography

Roads

Railway

Powerline

Mine

Geology

Fault

Dyke

Subprovince Boundary

2: Mafic metavolcanics

3: Felsic and intermediate metavolcanics

4: Felsic volcanics

5: Metasedimentary rocks

8: Gabbroic rocks

9: Gneissic tonalite suite

10: Foliate tonalite suite

11: Granite-granodiorite, muscovite/biotite bearing rocks

12: Diorite-monzonite-granodiorite

13: Granite-granodiorite

Map Parameters

Illumination: inclination 50°, declination 0°

Spatial Filter (half-wavelength): 1000 m

Bouguer Density: 2.67 g/cm³

Grid Cell Size: 250 m

Eötvös

Survey Location

BASE DATA: National Topographic Database - NRCAN
 GEOLOGY DATA: OGS M-Series maps: M2668 & MRD126-rev1
 DATUM: NAD83
 PROJECTION: Universe Transverse Mercator (UTM Zone 16N)

Scale 1 : 315 000

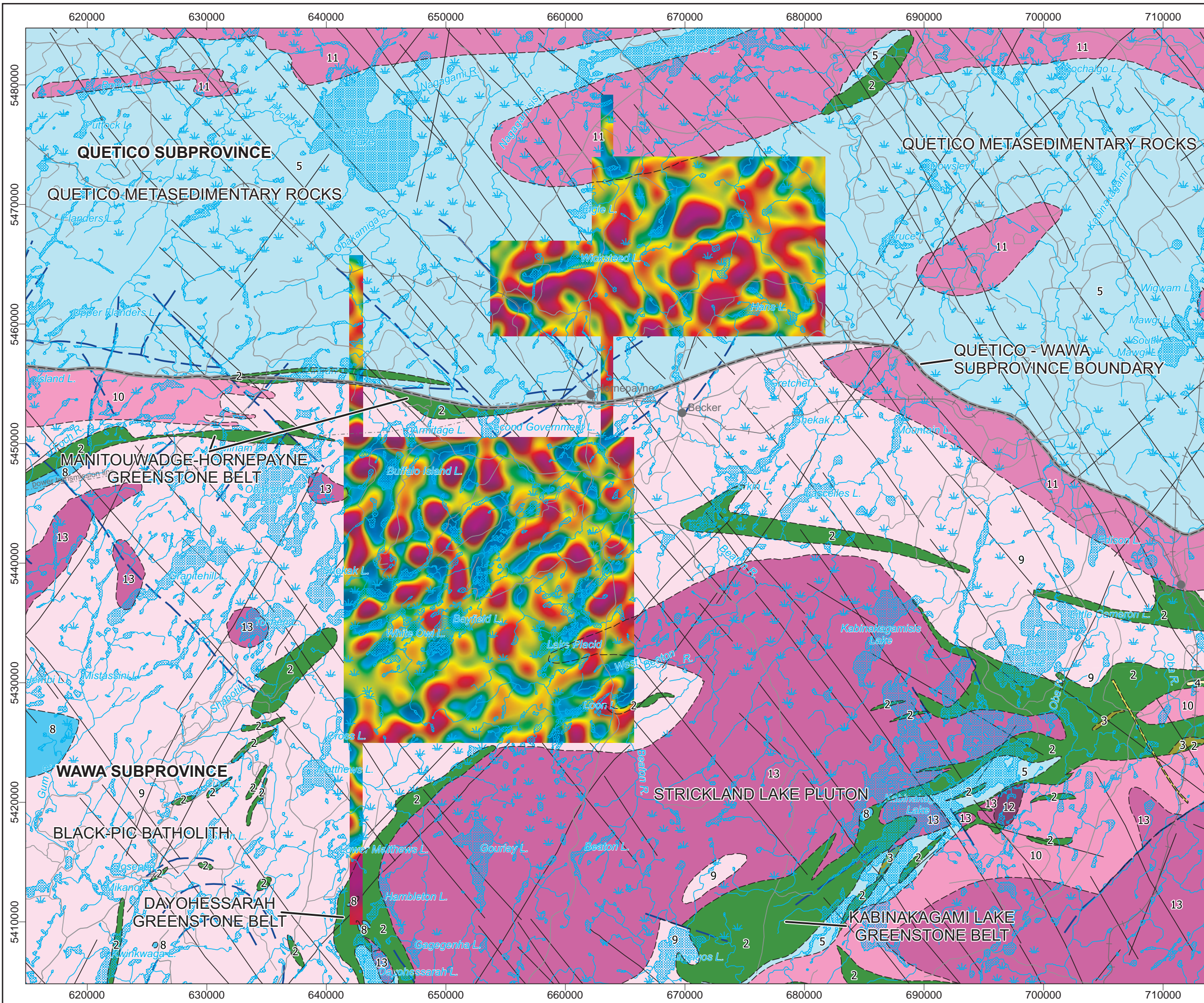
km 5 0 5 10 km

**Airborne Geophysics
 Acquisition and Interpretation**

Hornepayne Area, Ontario 2016

**First Vertical Derivative
 of the Bouguer Gravity**

	DESIGN	JK, MP	12/07/2016	REV. 1.2
	GIS	YC, PT	12/07/2016	
	DATA	MP, PT, MM	12/07/2016	FIGURE: 4.12
	QC	MB	15/07/2016	



Legend

Hydrography

Roads

Railway

Powerline

Mine

Geology

Fault

Dyke

Subprovince Boundary

2: Mafic metavolcanics

3: Felsic and intermediate metavolcanics

4: Felsic volcanics

5: Metasedimentary rocks

8: Gabbroic rocks

9: Gneissic tonalite suite

10: Foliate tonalite suite

11: Granite-granodiorite, muscovite/biotite bearing rocks

12: Diorite-monzonite-granodiorite

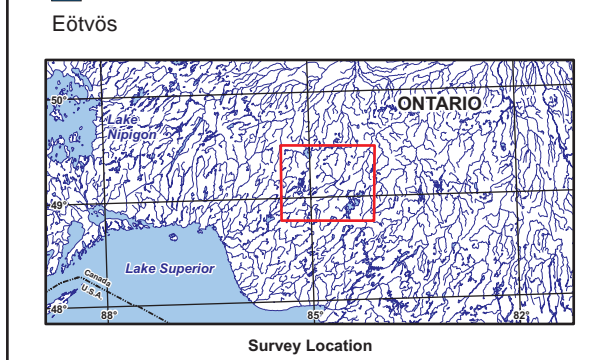
13: Granite-granodiorite

Map Parameters

Illumination: inclination 50°, declination 0°

Spatial Filter (half-wavelength): 1000 m

Grid Cell Size: 25 m



BASE DATA: National Topographic Database - NRCAN
 GEOLOGY DATA: OGS M-Series maps: M2668 & MRD126-rev1
 DATUM: NAD83
 PROJECTION: Universe Transverse Mercator (UTM Zone 16N)

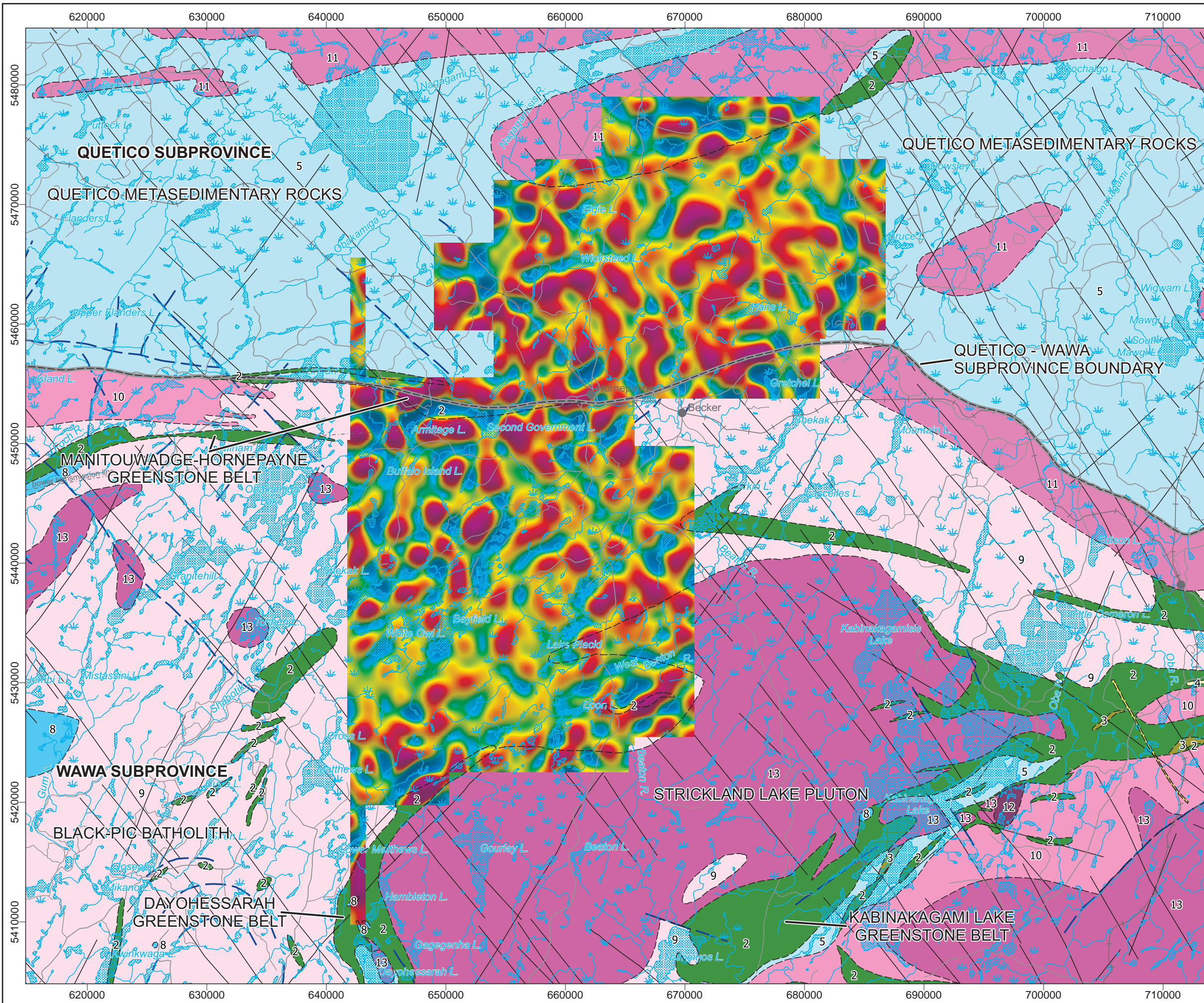
Scale 1 : 315 000

**Airborne Geophysics
 Acquisition and Interpretation**

Hornepayne Area, Ontario 2016

First Vertical Derivative of the Free Air Gravity

	DESIGN	JK, MP	12/07/2016	REV. 1.2
	GIS	YC, PT	12/07/2016	
	DATA	MP, PT, MM	12/07/2016	FIGURE: 4.13
	QC	MB	15/07/2016	



Legend

Hydrography

Roads

Railway

Powerline

Mine

Geology

Fault

Dyke

Subprovince Boundary

- 2: Mafic metavolcanics
- 3: Felsic and intermediate metavolcanics
- 4: Felsic volcanics
- 5: Metasedimentary rocks
- 8: Gabbroic rocks
- 9: Gneissic tonalite suite
- 10: Foliate tonalite suite
- 11: Granite-granodiorite, muscovite/biotite bearing rocks
- 12: Diorite-monzonite-granodiorite
- 13: Granite-granodiorite

Map Parameters

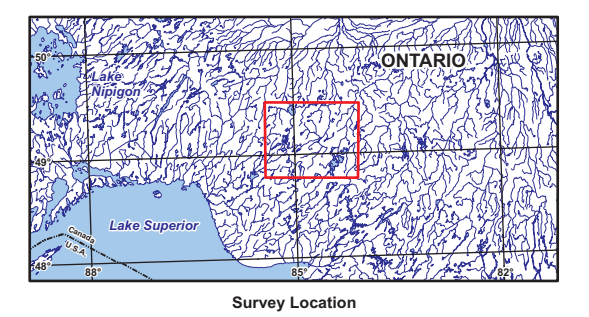
Illumination: inclination 50°, declination 0°

Spatial Filter (half-wavelength): 1000 m

Grid Cell Size: 250 m

Eötvös

57.8
46.2
39.6
34.9
31.2
28.2
25.6
23.2
21.1
19.1
17.3
15.5
13.9
12.3
10.9
9.5
8.2
6.9
5.6
4.4
3.3
2.2
1.1
0.0
-1.1
-2.2
-3.2
-4.2
-5.1
-6.1
-7.2
-8.2
-9.2
-10.3
-11.4
-12.5
-13.7
-15.0
-16.3
-17.7
-19.1
-20.6
-22.2
-24.0
-26.2
-28.7
-32.0
-36.7
-45.1



BASE DATA: National Topographic Database - NRCAN
 GEOLOGY DATA: OGS M-Series maps: M2668 & MRD126-rev1
 DATUM: NAD83
 PROJECTION: Universe Transverse Mercator (UTM Zone 16N)

Scale 1 : 315 000

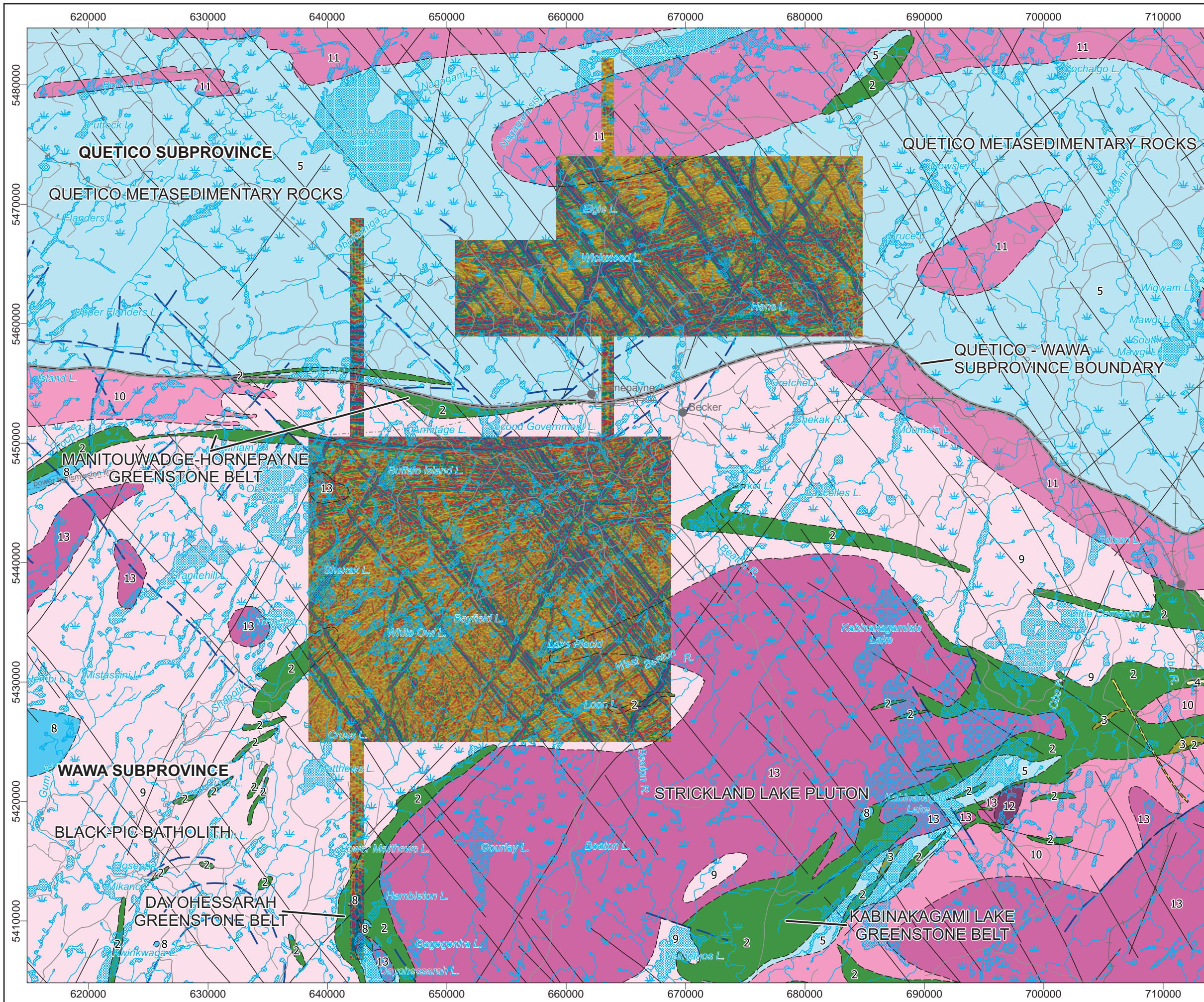
km 5 0 5 10 km

**Airborne Geophysics
 Acquisition and Interpretation**

Hornepayne Area, Ontario 2016

First Vertical Derivative of the Free Air Gravity

	DESIGN	JK, MP	12/07/2016	REV. 1.2
	GIS	YC, PT	12/07/2016	
	DATA	MP, PT, MM	12/07/2016	FIGURE: 4.14
	QC	MB	15/07/2016	



Legend

Hydrography

Roads

Railway

Powerline

Mine

Geology

Fault

Dyke

Subprovince Boundary

2: Mafic metavolcanics

3: Felsic and intermediate metavolcanics

4: Felsic volcanics

5: Metasedimentary rocks

8: Gabbroic rocks

9: Gneissic tonalite suite

10: Foliate tonalite suite

11: Granite-granodiorite, muscovite/biotite bearing rocks

12: Diorite-monzonite-granodiorite

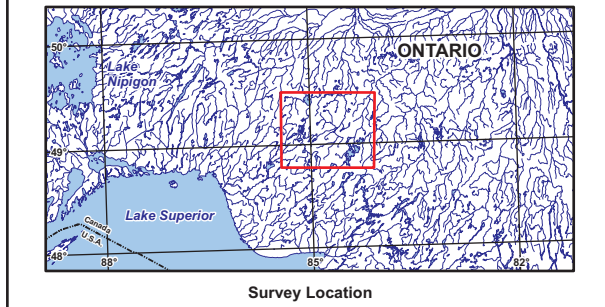
13: Granite-granodiorite

Map Parameters

Illumination: inclination 50°, declination 0°

Grid Cell Size: 25 m

nT/km²



BASE DATA: National Topographic Database - NRCAN
 GEOLOGY DATA: OGS M-Series maps: M2668 & MRD126-rev1
 DATUM: NAD83
 PROJECTION: Universe Transverse Mercator (UTM Zone 16N)

Scale 1 : 315 000

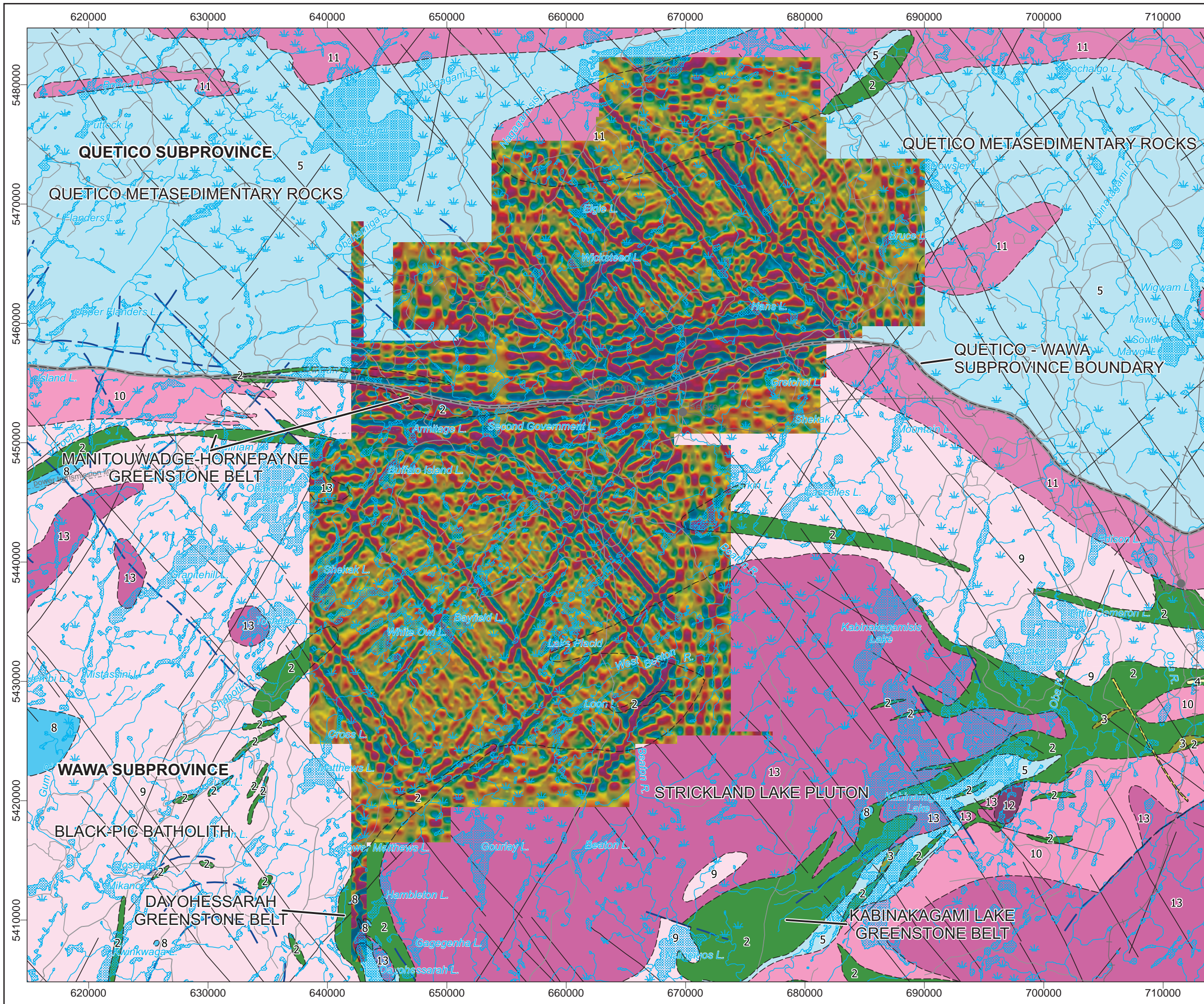
km 5 0 5 10 km

Airborne Geophysics Acquisition and Interpretation

Hornepayne Area, Ontario 2016

Second Vertical Derivative of the Reduction to the Pole of the Total Magnetic Intensity

	DESIGN	JK, MP	12/07/2016	REV. 1.2
	GIS	YC, PT	12/07/2016	
	DATA	MP, PT, MM	12/07/2016	FIGURE: 4.15
	QC	MB	15/07/2016	



Legend

Hydrography

Roads

Railway

Powerline

Mine

Geology

Fault

Dyke

Subprovince Boundary

2: Mafic metavolcanics

3: Felsic and intermediate metavolcanics

4: Felsic volcanics

5: Metasedimentary rocks

8: Gabbroic rocks

9: Gneissic tonalite suite

10: Foliate tonalite suite

11: Granite-granodiorite, muscovite/biotite bearing rocks

12: Diorite-monzonite-granodiorite

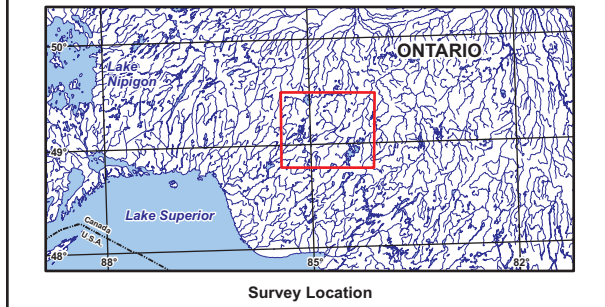
13: Granite-granodiorite

Map Parameters

Illumination: inclination 50°, declination 0°

Grid Cell Size: 250 m

nT/km²



BASE DATA: National Topographic Database - NRCAN
 GEOLOGY DATA: OGS M-Series maps: M2668 & MRD126-rev1
 DATUM: NAD83
 PROJECTION: Universal Transverse Mercator (UTM Zone 16N)

Scale 1 : 315 000

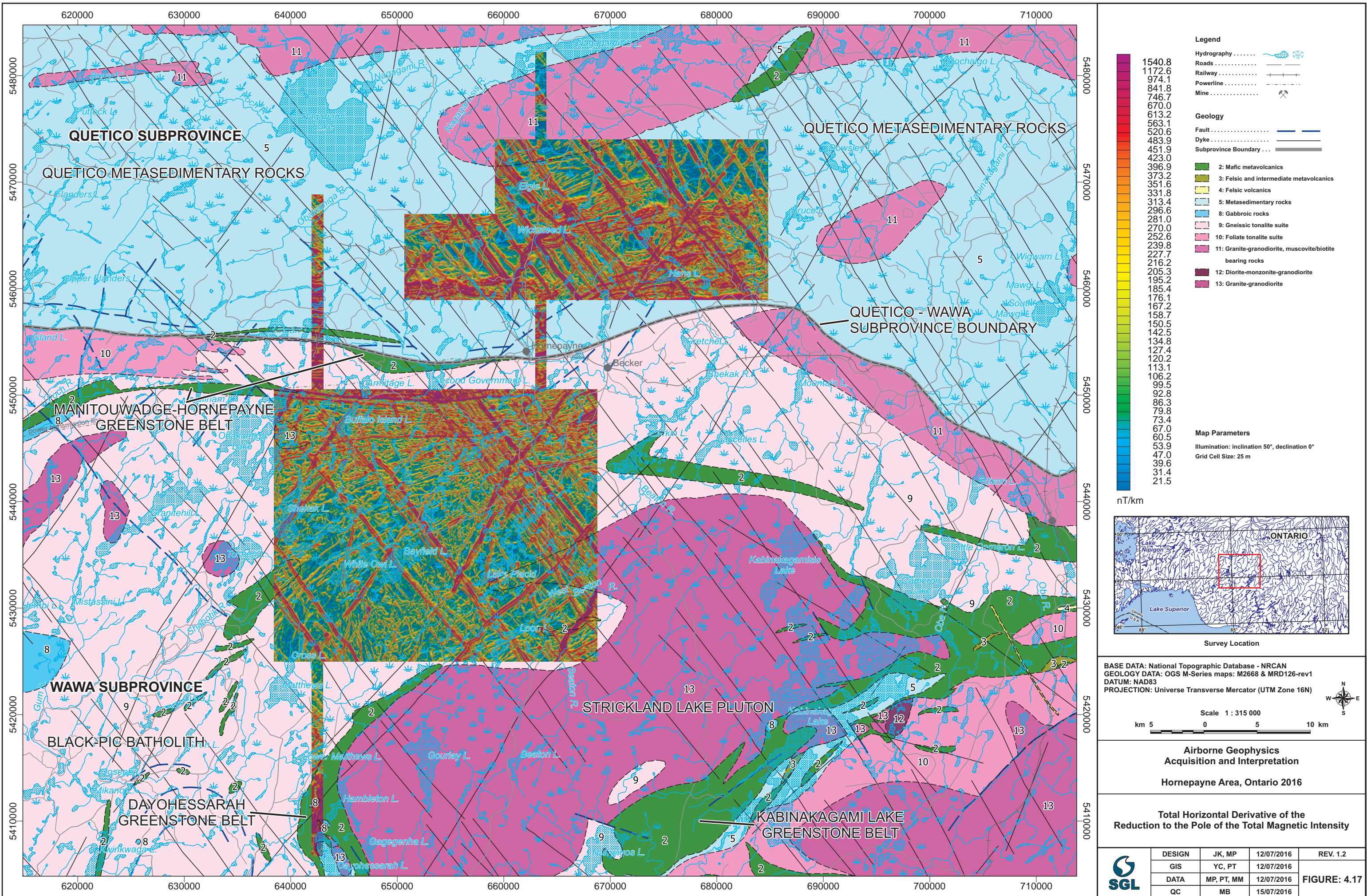
km 5 0 5 10 km

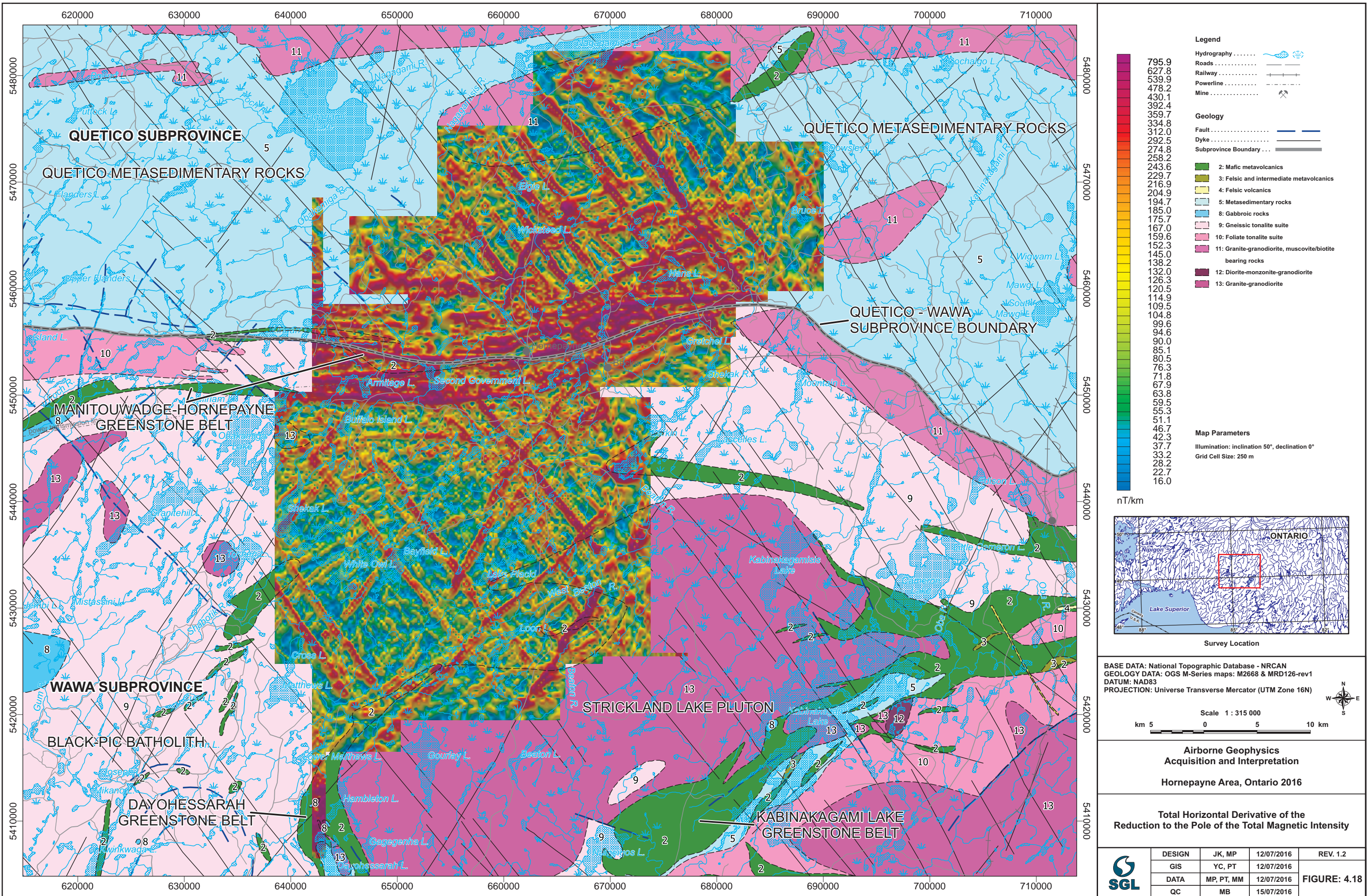
Airborne Geophysics Acquisition and Interpretation

Hornepayne Area, Ontario 2016

Second Vertical Derivative of the Reduction to the Pole of the Total Magnetic Intensity

	DESIGN	JK, MP	12/07/2016	REV. 1.2
	GIS	YC, PT	12/07/2016	
	DATA	MP, PT, MM	12/07/2016	FIGURE: 4.16
	QC	MB	15/07/2016	





Legend

Hydrography

Roads

Railway

Powerline

Mine

Geology

Fault

Dyke

Subprovince Boundary

2: Mafic metavolcanics

3: Felsic and intermediate metavolcanics

4: Felsic volcanics

5: Metasedimentary rocks

8: Gabbroic rocks

9: Gneissic tonalite suite

10: Foliate tonalite suite

11: Granite-granodiorite, muscovite/biotite bearing rocks

12: Diorite-monzonite-granodiorite

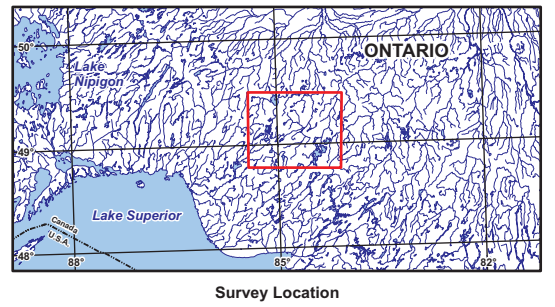
13: Granite-granodiorite

Map Parameters

Illumination: inclination 50°, declination 0°

Grid Cell Size: 250 m

nT/km



BASE DATA: National Topographic Database - NRCAN
 GEOLOGY DATA: OGS M-Series maps: M2668 & MRD126-rev1
 DATUM: NAD83
 PROJECTION: Universe Transverse Mercator (UTM Zone 16N)

Scale 1 : 315 000

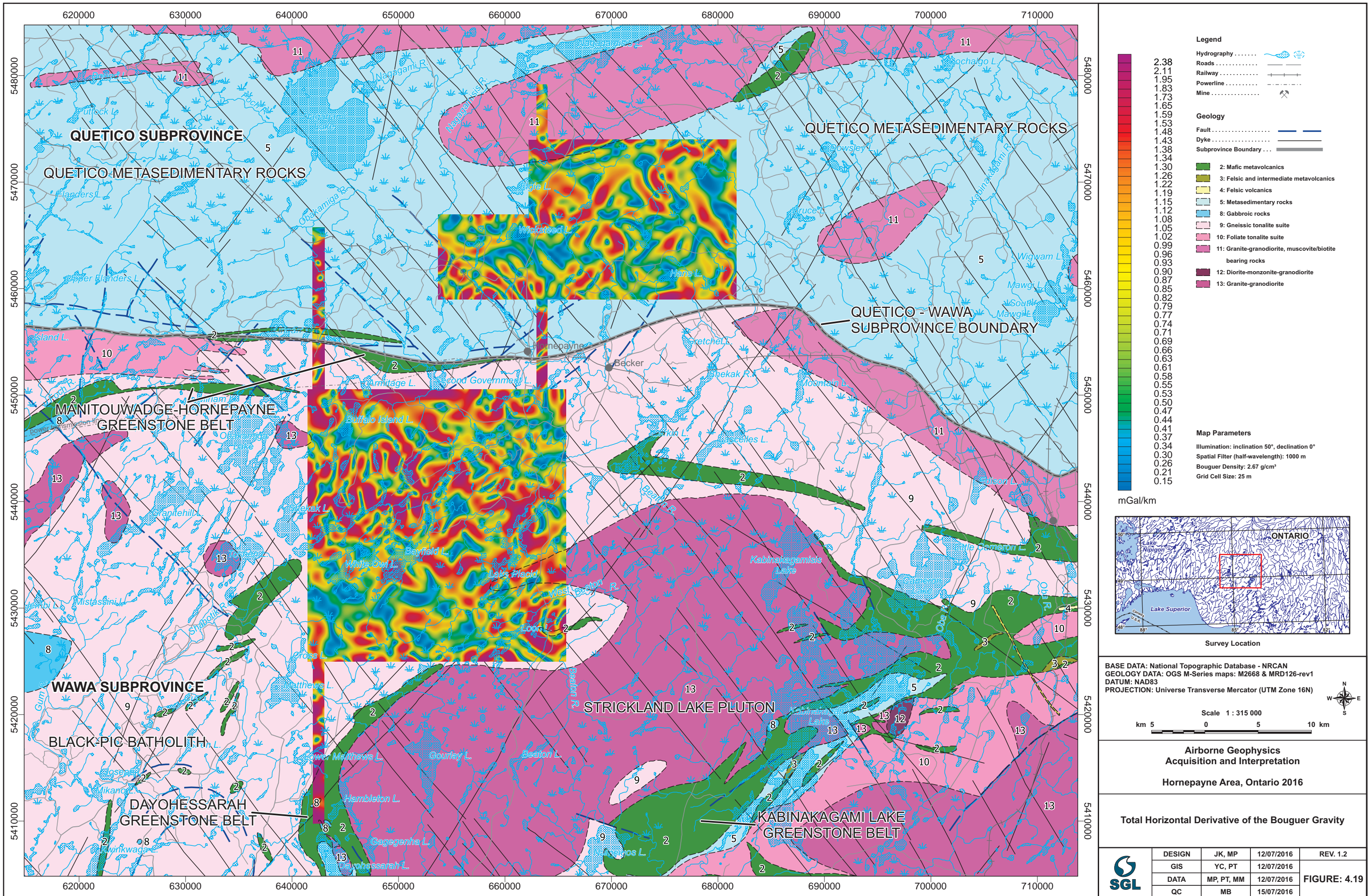
km 5 0 5 10 km

Airborne Geophysics Acquisition and Interpretation

Hornepayne Area, Ontario 2016

Total Horizontal Derivative of the Reduction to the Pole of the Total Magnetic Intensity

	DESIGN	JK, MP	12/07/2016	REV. 1.2
	GIS	YC, PT	12/07/2016	
	DATA	MP, PT, MM	12/07/2016	FIGURE: 4.18
	QC	MB	15/07/2016	

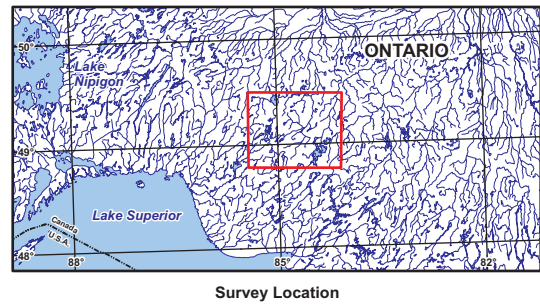


- Legend**
- Hydrography
 - Roads
 - Railway
 - Powerline
 - Mine
- Geology**
- Fault
 - Dyke
 - Subprovince Boundary

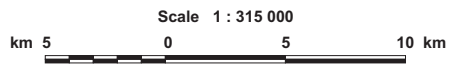
- 2: Mafic metavolcanics
- 3: Felsic and intermediate metavolcanics
- 4: Felsic volcanics
- 5: Metasedimentary rocks
- 8: Gabbroic rocks
- 9: Gneissic tonalite suite
- 10: Foliate tonalite suite
- 11: Granite-granodiorite, muscovite/biotite bearing rocks
- 12: Diorite-monzonite-granodiorite
- 13: Granite-granodiorite

Map Parameters

Illumination: inclination 50°, declination 0°
 Spatial Filter (half-wavelength): 1000 m
 Bouguer Density: 2.67 g/cm³
 Grid Cell Size: 25 m



BASE DATA: National Topographic Database - NRCAN
 GEOLOGY DATA: OGS M-Series maps: M2668 & MRD126-rev1
 DATUM: NAD83
 PROJECTION: Universe Transverse Mercator (UTM Zone 16N)



**Airborne Geophysics
 Acquisition and Interpretation**
 Hornepayne Area, Ontario 2016

Total Horizontal Derivative of the Bouguer Gravity

	DESIGN	JK, MP	12/07/2016	REV. 1.2
	GIS	YC, PT	12/07/2016	
	DATA	MP, PT, MM	12/07/2016	FIGURE: 4.19
	QC	MB	15/07/2016	



Legend

Hydrography

Roads

Railway

Powerline

Mine

Geology

Fault

Dyke

Subprovince Boundary

2: Mafic metavolcanics

3: Felsic and intermediate metavolcanics

4: Felsic volcanics

5: Metasedimentary rocks

8: Gabbroic rocks

9: Gneissic tonalite suite

10: Foliate tonalite suite

11: Granite-granodiorite, muscovite/biotite bearing rocks

12: Diorite-monzonite-granodiorite

13: Granite-granodiorite

Map Parameters

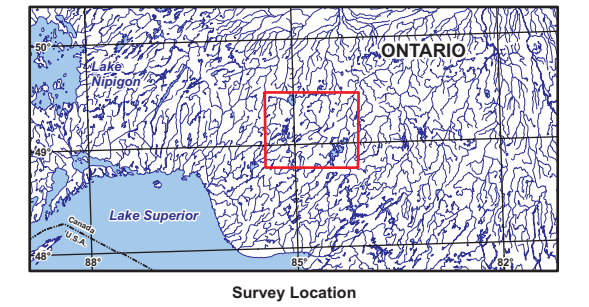
Illumination: inclination 50°, declination 0°

Spatial Filter (half-wavelength): 1000 m

Bouguer Density: 2.67 g/cm³

Grid Cell Size: 250 m

mGal/km



BASE DATA: National Topographic Database - NRCAN
 GEOLOGY DATA: OGS M-Series maps: M2668 & MRD126-rev1
 DATUM: NAD83
 PROJECTION: Universe Transverse Mercator (UTM Zone 16N)

Scale 1 : 315 000

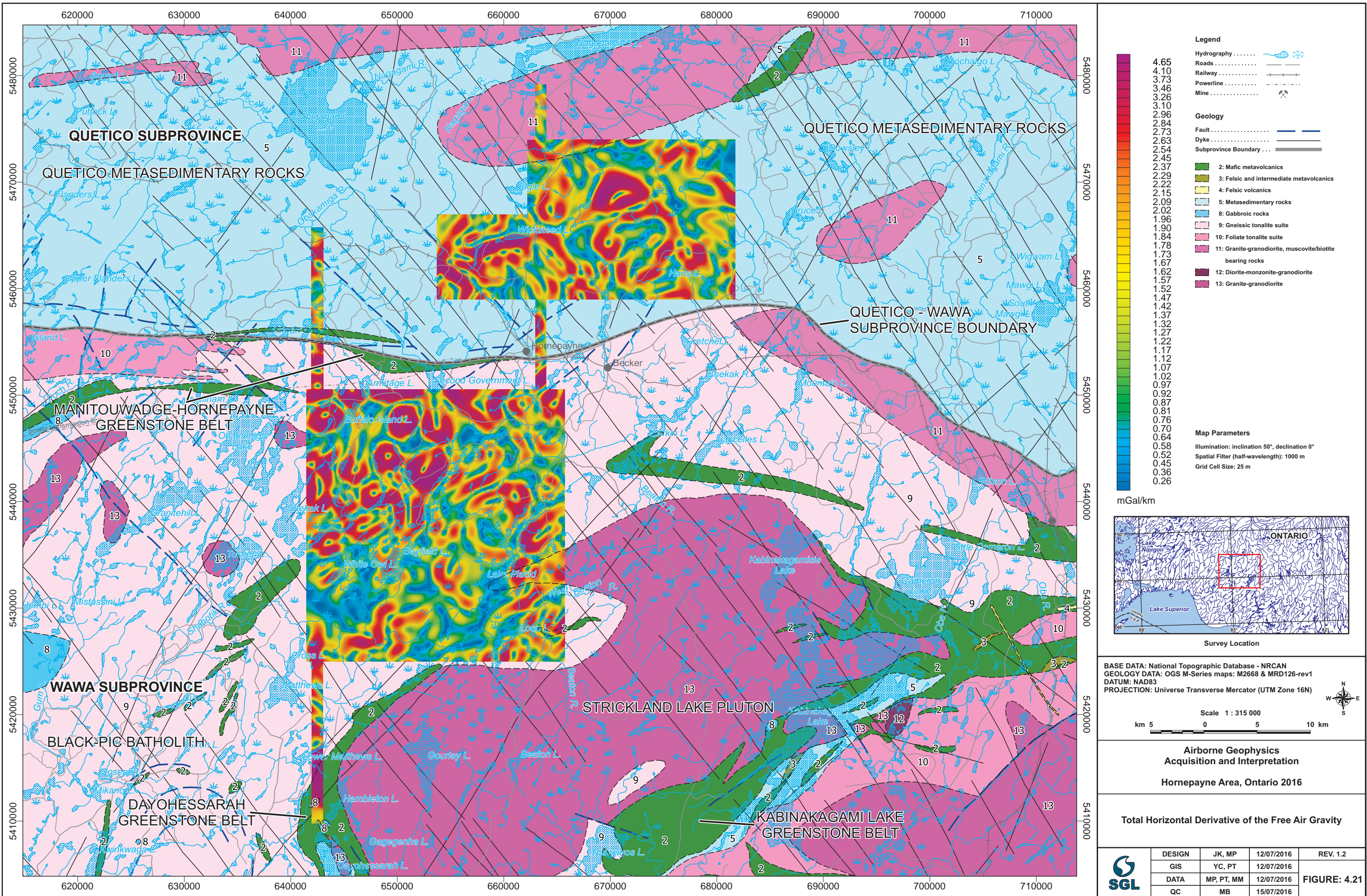
km 5 0 5 10 km

**Airborne Geophysics
 Acquisition and Interpretation**

Hornepayne Area, Ontario 2016

Total Horizontal Derivative of the Bouguer Gravity

	DESIGN	JK, MP	12/07/2016	REV. 1.2
	GIS	YC, PT	12/07/2016	
	DATA	MP, PT, MM	12/07/2016	FIGURE: 4.20
	QC	MB	15/07/2016	

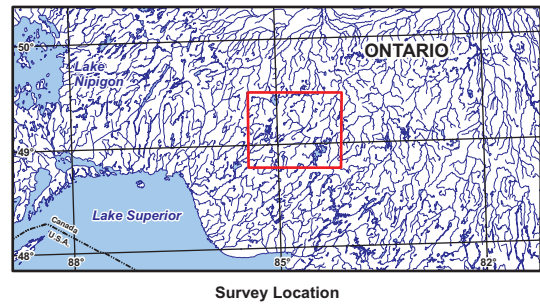


- Legend**
- Hydrography
 - Roads
 - Railway
 - Powerline
 - Mine
- Geology**
- Fault
 - Dyke
 - Subprovince Boundary

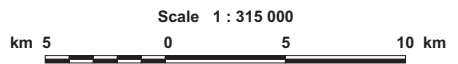
- 2: Mafic metavolcanics
- 3: Felsic and intermediate metavolcanics
- 4: Felsic volcanics
- 5: Metasedimentary rocks
- 8: Gabbroic rocks
- 9: Gneissic tonalite suite
- 10: Foliate tonalite suite
- 11: Granite-granodiorite, muscovite/biotite bearing rocks
- 12: Diorite-monzonite-granodiorite
- 13: Granite-granodiorite

Map Parameters

Illumination: inclination 50°, declination 0°
 Spatial Filter (half-wavelength): 1000 m
 Grid Cell Size: 25 m



BASE DATA: National Topographic Database - NRCAN
 GEOLOGY DATA: OGS M-Series maps: M2668 & MRD126-rev1
 DATUM: NAD83
 PROJECTION: Universe Transverse Mercator (UTM Zone 16N)

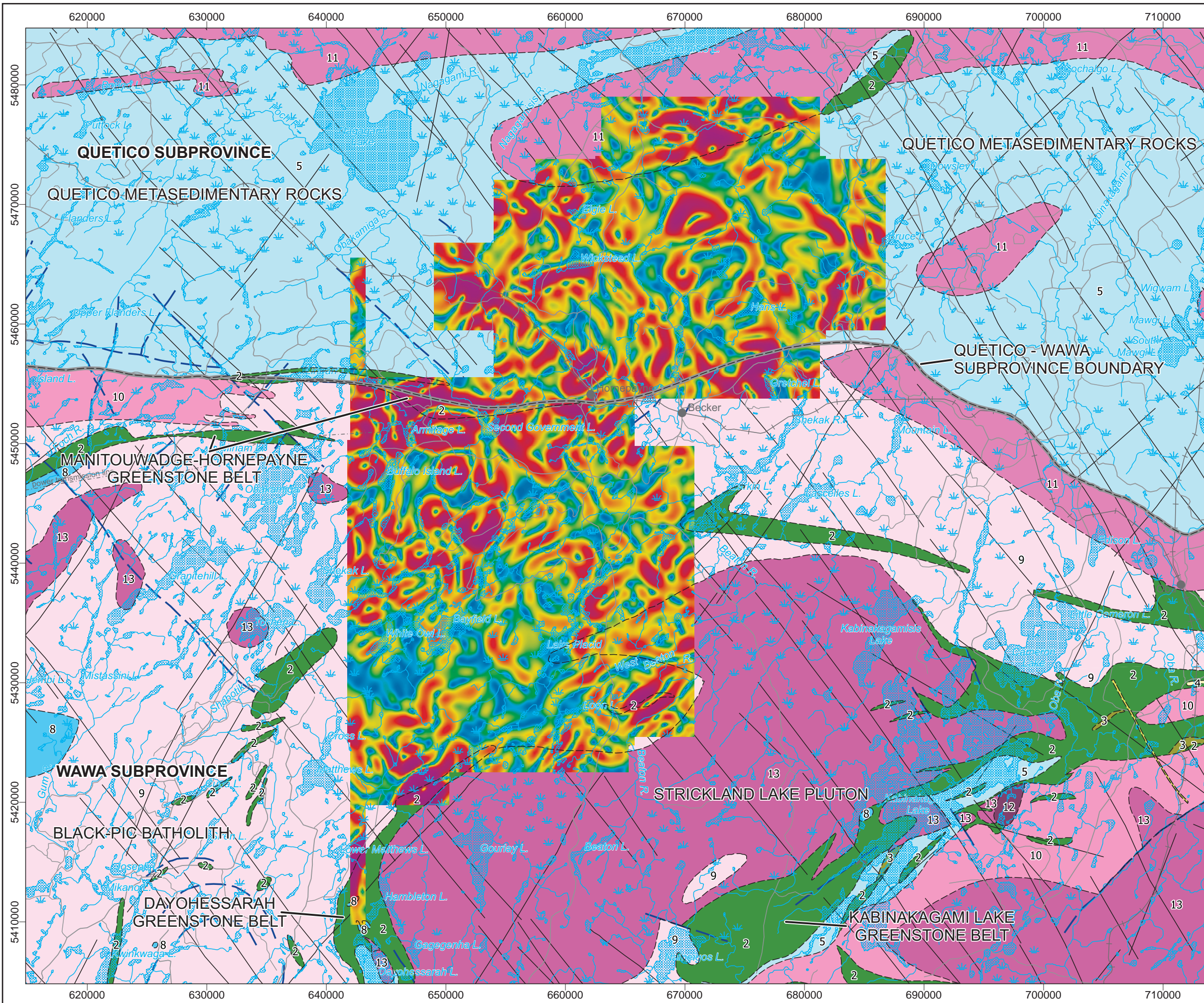


**Airborne Geophysics
 Acquisition and Interpretation**

Hornepayne Area, Ontario 2016

Total Horizontal Derivative of the Free Air Gravity

	DESIGN	JK, MP	12/07/2016	REV. 1.2
	GIS	YC, PT	12/07/2016	
	DATA	MP, PT, MM	12/07/2016	FIGURE: 4.21
	QC	MB	15/07/2016	



Legend

Hydrography

Roads

Railway

Powerline

Mine

Geology

Fault

Dyke

Subprovince Boundary

2: Mafic metavolcanics

3: Felsic and intermediate metavolcanics

4: Felsic volcanics

5: Metasedimentary rocks

8: Gabbroic rocks

9: Gneissic tonalite suite

10: Foliate tonalite suite

11: Granite-granodiorite, muscovite/biotite bearing rocks

12: Diorite-monzonite-granodiorite

13: Granite-granodiorite

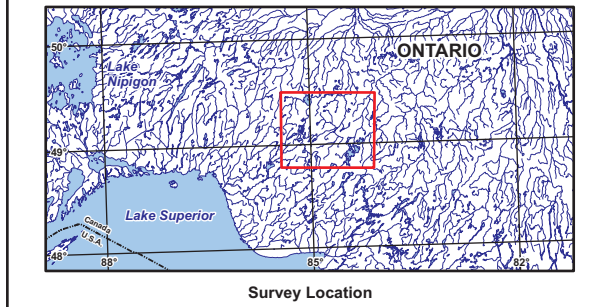
Map Parameters

Illumination: inclination 50°, declination 0°

Spatial Filter (half-wavelength): 1000 m

Grid Cell Size: 250 m

mGal/km



BASE DATA: National Topographic Database - NRCAN
 GEOLOGY DATA: OGS M-Series maps: M2668 & MRD126-rev1
 DATUM: NAD83
 PROJECTION: Universe Transverse Mercator (UTM Zone 16N)

Scale 1 : 315 000

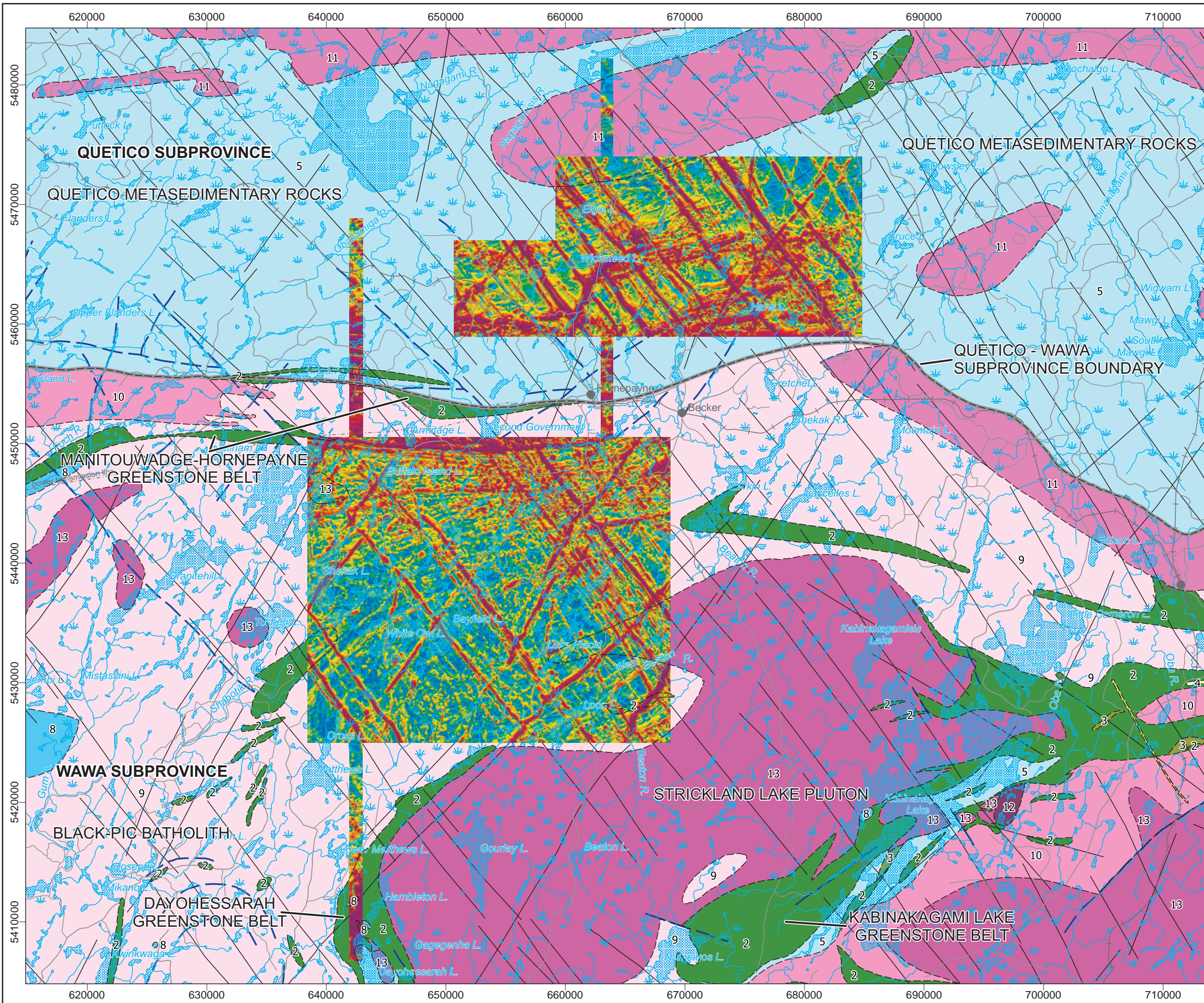
km 5 0 5 10 km

**Airborne Geophysics
 Acquisition and Interpretation**

Hornepayne Area, Ontario 2016

Total Horizontal Derivative of the Free Air Gravity

	DESIGN	JK, MP	12/07/2016	REV. 1.2
	GIS	YC, PT	12/07/2016	
	DATA	MP, PT, MM	12/07/2016	FIGURE: 4.22
	QC	MB	15/07/2016	



Legend

Hydrography

Roads

Railway

Powerline

Mine

Geology

Fault

Dyke

Subprovince Boundary

2: Mafic metavolcanics

3: Felsic and intermediate metavolcanics

4: Felsic volcanics

5: Metasedimentary rocks

8: Gabbroic rocks

9: Gneissic tonalite suite

10: Foliate tonalite suite

11: Granite-granodiorite, muscovite/biotite bearing rocks

12: Diorite-monzonite-granodiorite

13: Granite-granodiorite

Map Parameters

Illumination: inclination 50°, declination 0°

Grid Cell Size: 25 m

nT/km

Survey Location

BASE DATA: National Topographic Database - NRCAN
 GEOLOGY DATA: OGS M-Series maps: M2668 & MRD126-rev1
 DATUM: NAD83
 PROJECTION: Universe Transverse Mercator (UTM Zone 16N)

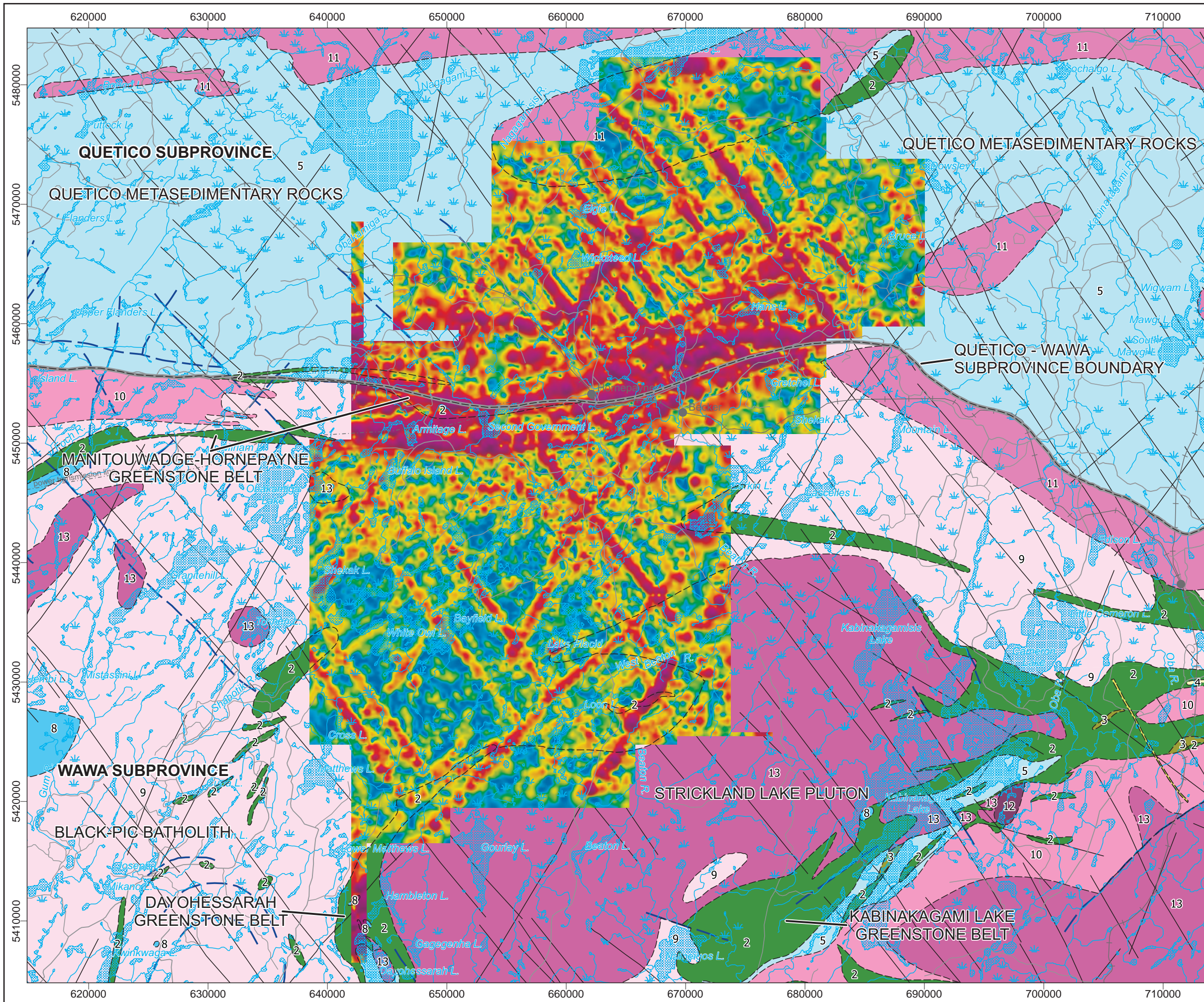
Scale 1 : 315 000

Airborne Geophysics Acquisition and Interpretation

Hornepayne Area, Ontario 2016

Total Gradient Amplitude of the Total Magnetic Intensity

	DESIGN	JK, MP	12/07/2016	REV. 1.2
	GIS	YC, PT	12/07/2016	
	DATA	MP, PT, MM	12/07/2016	FIGURE: 4.23
	QC	MB	15/07/2016	



Legend

Hydrography

Roads

Railway

Powerline

Mine

Geology

Fault

Dyke

Subprovince Boundary

2: Mafic metavolcanics

3: Felsic and intermediate metavolcanics

4: Felsic volcanics

5: Metasedimentary rocks

8: Gabbroic rocks

9: Gneissic tonalite suite

10: Foliate tonalite suite

11: Granite-granodiorite, muscovite/biotite bearing rocks

12: Diorite-monzonite-granodiorite

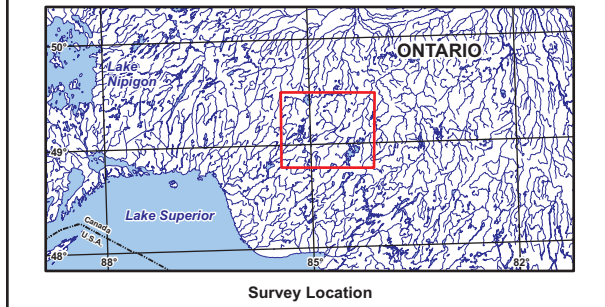
13: Granite-granodiorite

Map Parameters

Illumination: inclination 50°, declination 0°

Grid Cell Size: 250 m

nT/km



BASE DATA: National Topographic Database - NRCAN
 GEOLOGY DATA: OGS M-Series maps: M2668 & MRD126-rev1
 DATUM: NAD83
 PROJECTION: Universe Transverse Mercator (UTM Zone 16N)

Scale 1 : 315 000

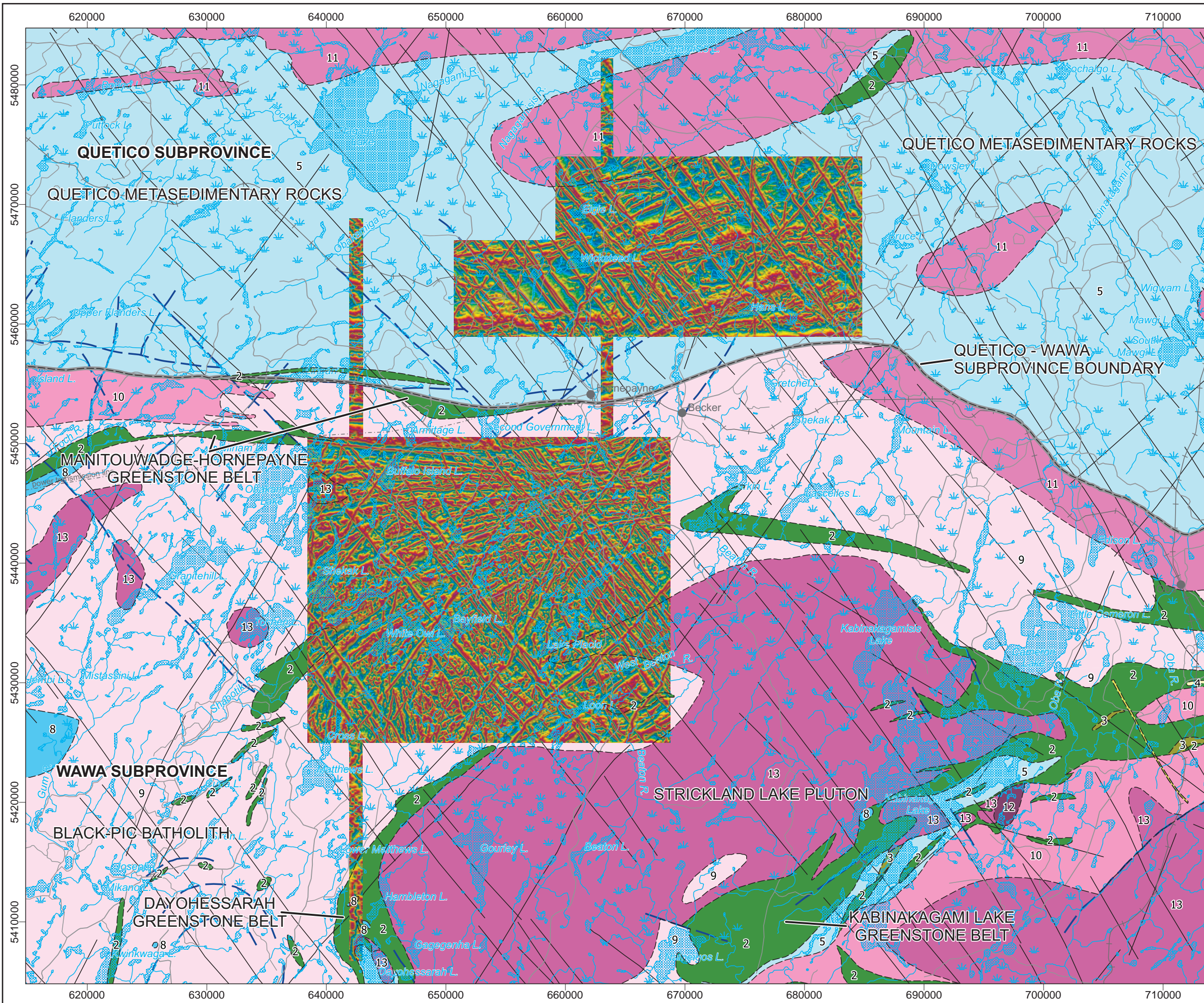
km 5 0 5 10 km

**Airborne Geophysics
 Acquisition and Interpretation**

Hornepayne Area, Ontario 2016

**Total Gradient Amplitude
 of the Total Magnetic Intensity**

	DESIGN	JK, MP	12/07/2016	REV. 1.2
	GIS	YC, PT	12/07/2016	
	DATA	MP, PT, MM	12/07/2016	FIGURE: 4.24
	QC	MB	15/07/2016	



Legend

Hydrography

Roads

Railway

Powerline

Mine

Geology

Fault

Dyke

Subprovince Boundary

2: Mafic metavolcanics

3: Felsic and intermediate metavolcanics

4: Felsic volcanics

5: Metasedimentary rocks

8: Gabbroic rocks

9: Gneissic tonalite suite

10: Foliate tonalite suite

11: Granite-granodiorite, muscovite/biotite bearing rocks

12: Diorite-monzonite-granodiorite

13: Granite-granodiorite

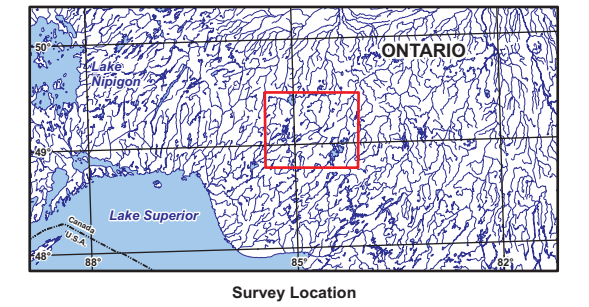
Map Parameters

Illumination: inclination 50°, declination 0°

Tilt Angle Grid: -45° to +45°

Grid Cell Size: 25 m

degrees



BASE DATA: National Topographic Database - NRCAN
 GEOLOGY DATA: OGS M-Series maps: M2668 & MRD126-rev1
 DATUM: NAD83
 PROJECTION: Universe Transverse Mercator (UTM Zone 16N)

Scale 1 : 315 000

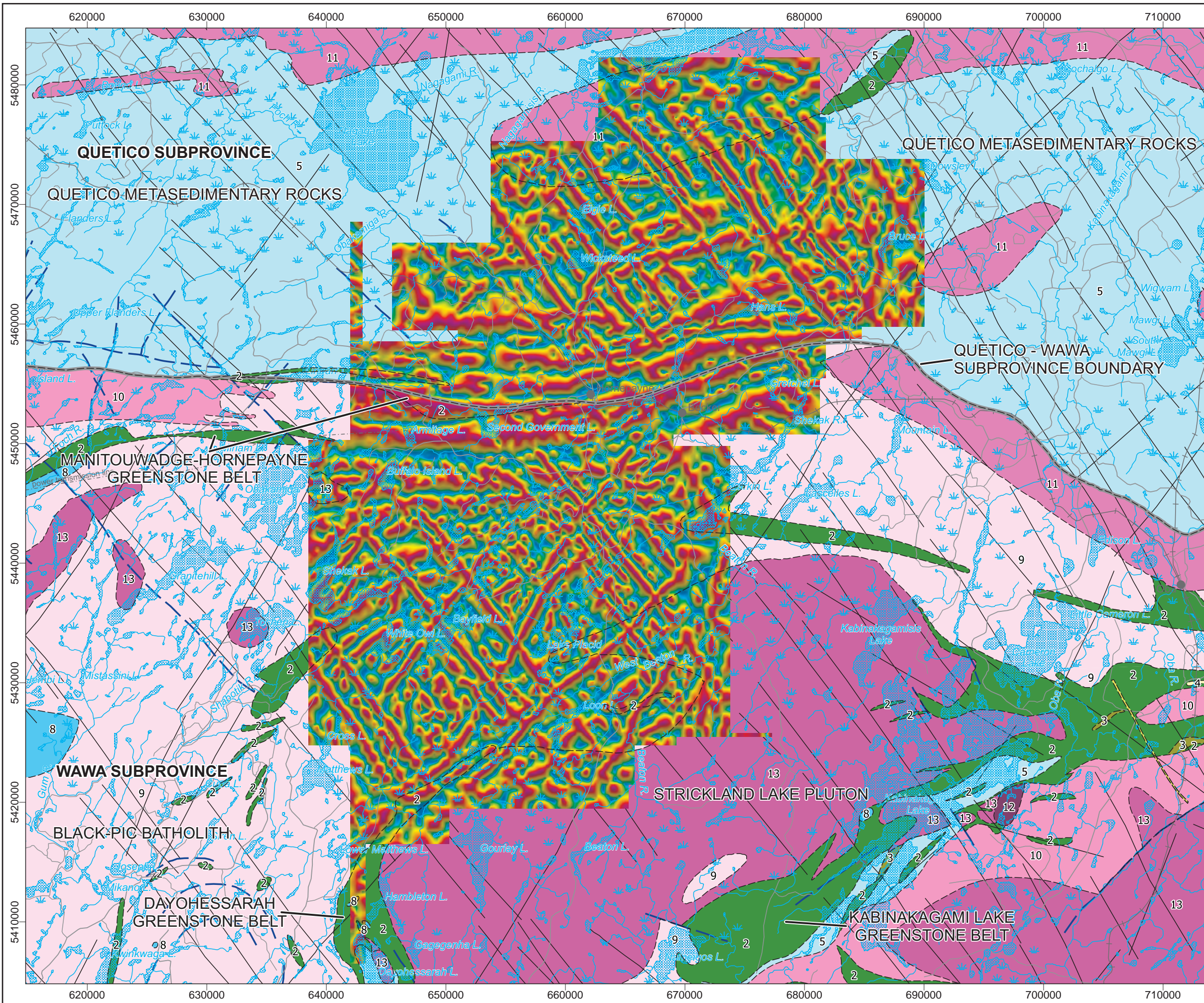
km 5 0 5 10 km

**Airborne Geophysics
 Acquisition and Interpretation**

Hornepayne Area, Ontario 2016

Tilt Angle of the Reduction to the Pole
 of the Total Magnetic Intensity

	DESIGN	JK, MP	12/07/2016	REV. 1.2
	GIS	YC, PT	12/07/2016	
	DATA	MP, PT, MM	12/07/2016	FIGURE: 4.25
	QC	MB	15/07/2016	



Legend

Hydrography

Roads

Railway

Powerline

Mine

Geology

Fault

Dyke

Subprovince Boundary

2: Mafic metavolcanics

3: Felsic and intermediate metavolcanics

4: Felsic volcanics

5: Metasedimentary rocks

8: Gabbroic rocks

9: Gneissic tonalite suite

10: Foliate tonalite suite

11: Granite-granodiorite, muscovite/biotite bearing rocks

12: Diorite-monzonite-granodiorite

13: Granite-granodiorite

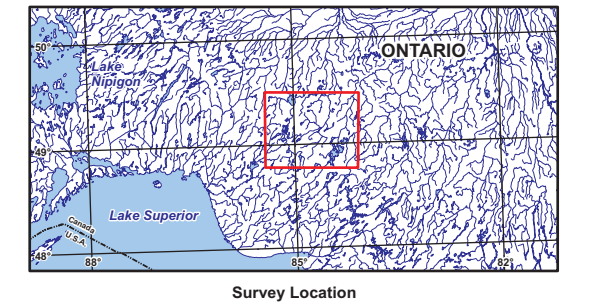
Map Parameters

Illumination: inclination 50°, declination 0°

Tilt Angle Grid: -45° to +45°

Grid Cell Size: 250 m

degrees



BASE DATA: National Topographic Database - NRCAN
 GEOLOGY DATA: OGS M-Series maps: M2668 & MRD126-rev1
 DATUM: NAD83
 PROJECTION: Universe Transverse Mercator (UTM Zone 16N)

Scale 1 : 315 000

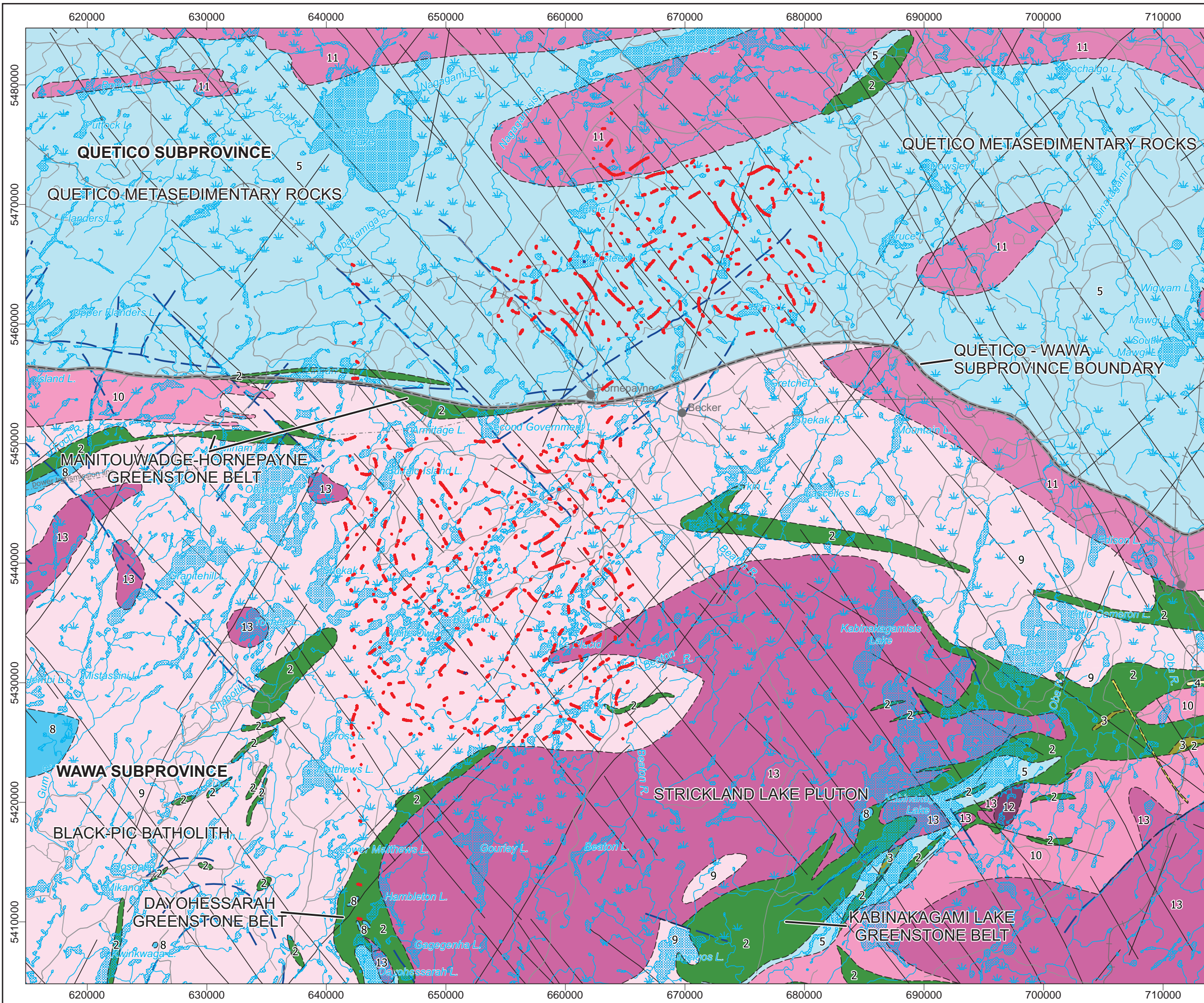
km 5 0 5 10 km

**Airborne Geophysics
 Acquisition and Interpretation**

Hornepayne Area, Ontario 2016

Tilt Angle of the Reduction to the Pole
 of the Total Magnetic Intensity

	DESIGN	JK, MP	12/07/2016	REV. 1.2
	GIS	YC, PT	12/07/2016	
	DATA	MP, PT, MM	12/07/2016	FIGURE: 4.26
	QC	MB	15/07/2016	



Legend

Hydrography

Roads

Railway

Powerline

Mine

Geology

Fault

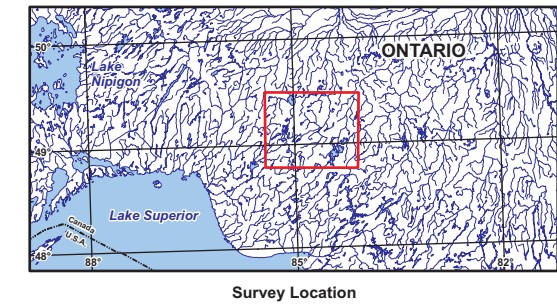
Dyke

Subprovince Boundary

Trend Analysis Solutions

Depth below surface

- 0 - 100 m
- 101 - 200 m
- > 200 m



BASE DATA: National Topographic Database - NRCAN
 GEOLOGY DATA: OGS M-Series maps: M2668 & MRD126-rev1
 DATUM: NAD83
 PROJECTION: Universe Transverse Mercator (UTM Zone 16N)

Scale 1 : 315 000

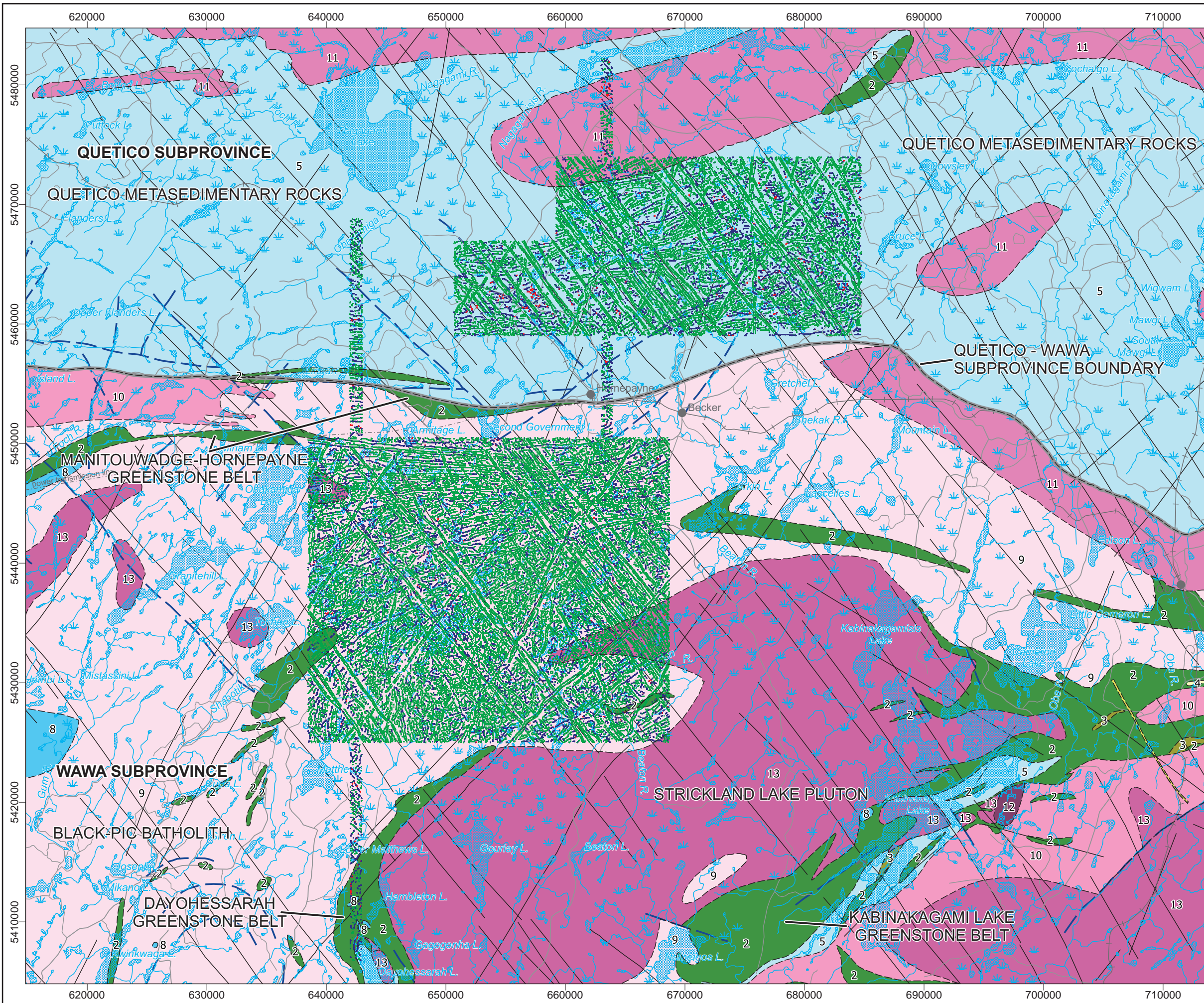
km 5 0 5 10 km

**Airborne Geophysics
 Acquisition and Interpretation**

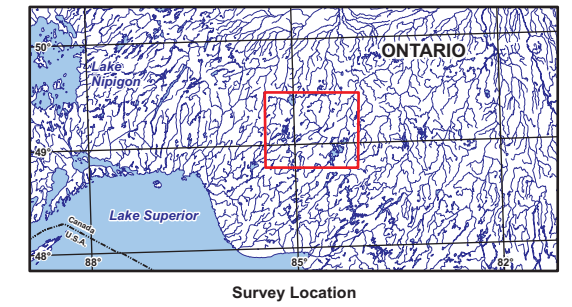
Hornepayne Area, Ontario 2016

Trend Analysis Solutions of Bouguer Gravity

	DESIGN	JK, MP	12/07/2016	REV. 1.2
	GIS	YC, PT	12/07/2016	
	DATA	MP, PT, MM	12/07/2016	FIGURE: 4.27
	QC	MB	15/07/2016	



- Legend**
- Hydrography
 - Roads
 - Railway
 - Powerline
 - Mine
- Geology**
- Fault
 - Dyke
 - Subprovince Boundary
- Trend Analysis Solutions**
- Depth from sensor
- 0 - 100 m
 - 101 - 200 m
 - > 200 m
- Geology Legend:**
- 2: Mafic metavolcanics
 - 3: Felsic and intermediate metavolcanics
 - 4: Felsic volcanics
 - 5: Metasedimentary rocks
 - 8: Gabbroic rocks
 - 9: Gneissic tonalite suite
 - 10: Foliate tonalite suite
 - 11: Granite-granodiorite, muscovite/biotite bearing rocks
 - 12: Diorite-monzonite-granodiorite
 - 13: Granite-granodiorite



BASE DATA: National Topographic Database - NRCAN
 GEOLOGY DATA: OGS M-Series maps: M2668 & MRD126-rev1
 DATUM: NAD83
 PROJECTION: Universe Transverse Mercator (UTM Zone 16N)

Scale 1 : 315 000

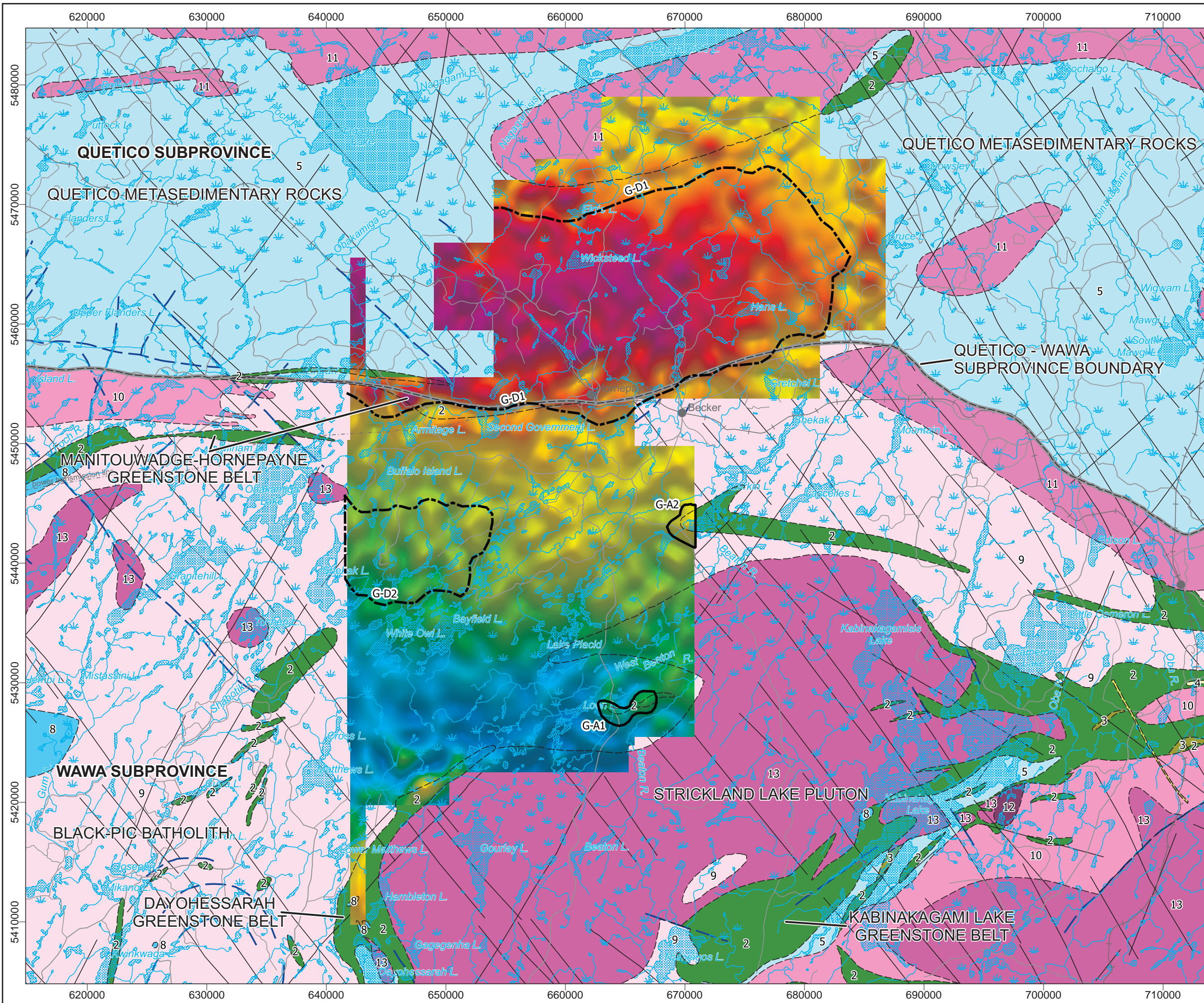
km 5 0 5 10 km

**Airborne Geophysics
 Acquisition and Interpretation**

Hornepayne Area, Ontario 2016

**Trend Analysis Solutions of Reduction to the Pole
 of the Total Magnetic Intensity**

SGL	DESIGN	JK, MP	12/07/2016	REV. 1.2
	GIS	YC, PT	12/07/2016	
	DATA	MP, PT, MM	12/07/2016	FIGURE: 4.28
	QC	MB	15/07/2016	



Legend

Hydrography

Roads

Railway

Powerline

Mine

Geology

Fault

Dyke

Subprovince Boundary

2: Mafic metavolcanics

3: Felsic and intermediate metavolcanics

4: Felsic volcanics

5: Metasedimentary rocks

8: Gabbroic rocks

9: Gneissic tonalite suite

10: Foliate tonalite suite

11: Granite-granodiorite, muscovite/biotite bearing rocks

12: Diorite-monzonite-granodiorite

13: Granite-granodiorite

Gravity Anomaly

Gravity Domain Boundary

Map Parameters

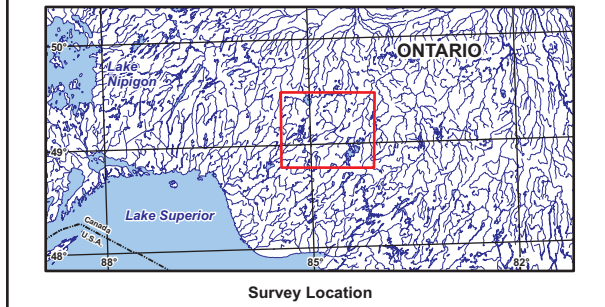
Illumination: inclination 50°, declination 0°

Spatial Filter (half-wavelength): 1000 m

Bouguer Density: 2.67 g/cm³

Grid Cell Size: 250 m

mGal



BASE DATA: National Topographic Database - NRCAN
 GEOLOGY DATA: OGS M-Series maps: M2668 & MRD126-rev1
 DATUM: NAD83
 PROJECTION: Universe Transverse Mercator (UTM Zone 16N)

Scale 1 : 315 000

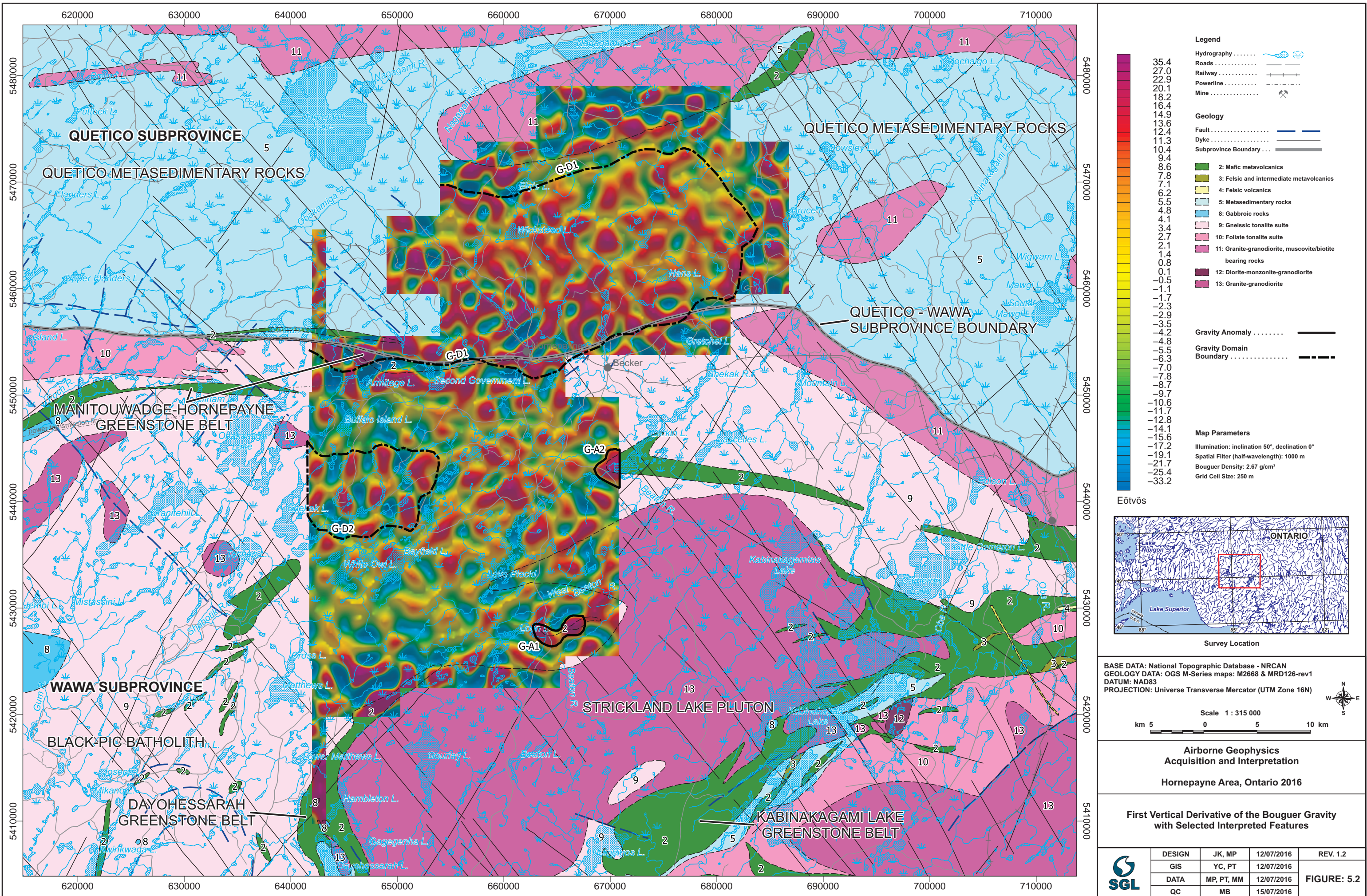
km 5 0 5 10 km

**Airborne Geophysics
 Acquisition and Interpretation**

Hornepayne Area, Ontario 2016

Bouguer Gravity with Selected Interpreted Features

	DESIGN	JK, MP	12/07/2016	REV. 1.2
	GIS	YC, PT	12/07/2016	
	DATA	MP, PT, MM	12/07/2016	FIGURE: 5.1
	QC	MB	15/07/2016	



QUETICO SUBPROVINCE

QUETICO METASEDIMENTARY ROCKS

QUETICO METASEDIMENTARY ROCKS

QUETICO - WAWA
SUBPROVINCE BOUNDARY

MANITOUWADGE-HORNEPAYNE
GREENSTONE BELT

STRICKLAND LAKE PLUTON

WAWA SUBPROVINCE

BLACK-PIC BATHOLITH

DAYOHESSARAH
GREENSTONE BELT

KABINAKAGAMI LAKE
GREENSTONE BELT

Becker

G-D1

G-D2

G-A1

G-A2

11

11

11

5

11

5

11

11

5

10

2

2

11

13

13

13

11

13

13

13

8

2

2

2

2

2

2

2

2

2

2

2

2

2

2

2

2

2

2

2

2

2

2

2

2

2

2

2

2

2

2

2

2

2

2

2

2

2

2

2

8

9

2

2

2

2

2

2

2

2

2

2

2

2

2

2

2

2

2

2

2

2

2

2

2

2

2

2

2

2

2

2

2

2

2

2

2

2

2

2

2

2

2

2

2

9

2

2

2

2

2

2

2

2

2

2

2

2

2

2

2

2

2

2

2

2

2

2

2

2

2

2

2

2

2

2

2

2

2

2

2

2

2

2

2

2

2

2

2

2

8

2

2

2

2

2

2

2

2

2

2

2

2

2

2

2

2

2

2

2

2

2

2

2

2

2

2

2

2

2

2

2

2

2

2

2

2

2

2

2

2

2

2

2

2

8

2

2

2

2

2

2

2

2

2

2

2

2

2

2

2

2

2

2

2

2

2

2

2

2

2

2

2

2

2

2

2

2

2

2

2

2

2

2

2

2

2

2

2

2

8

2

2

2

2

2

2

2

2

2

2

2

2

2

2

2

2

2

2

2

2

2

2

2

2

2

2

2

2

2

2

2

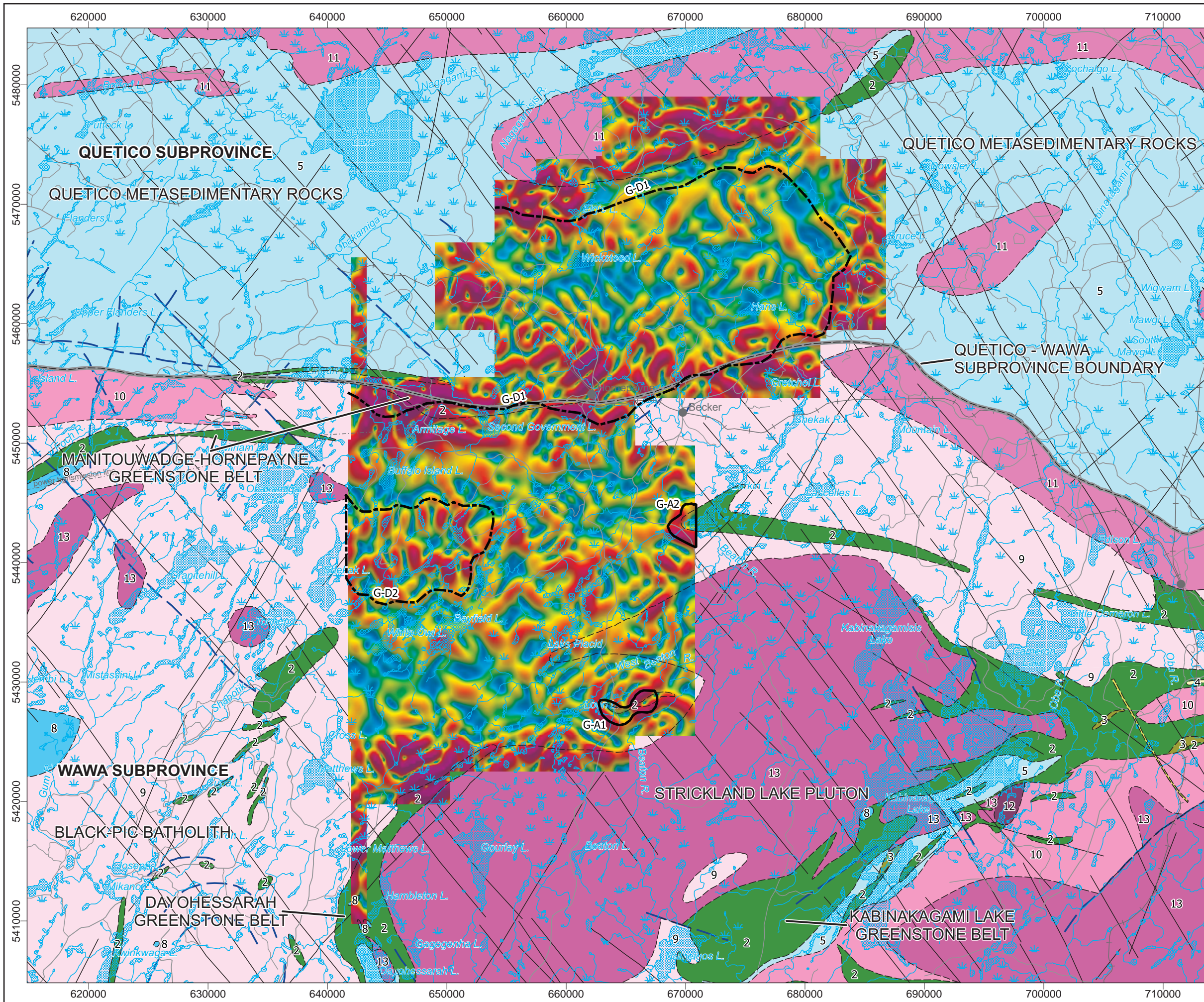
2

2

2

2

2



Legend

Hydrography

Roads

Railway

Powerline

Mine

Geology

Fault

Dyke

Subprovince Boundary

2: Mafic metavolcanics

3: Felsic and intermediate metavolcanics

4: Felsic volcanics

5: Metasedimentary rocks

8: Gabbroic rocks

9: Gneissic tonalite suite

10: Foliate tonalite suite

11: Granite-granodiorite, muscovite/biotite bearing rocks

12: Diorite-monzonite-granodiorite

13: Granite-granodiorite

Gravity Anomaly

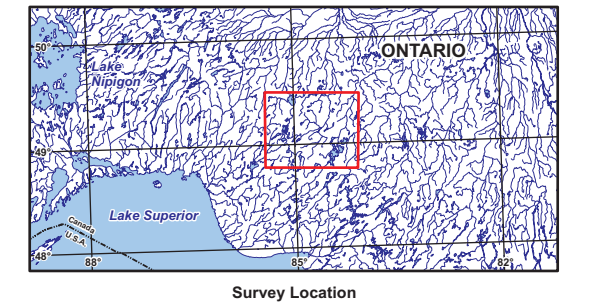
Gravity Domain Boundary

Map Parameters

Illumination: inclination 50°, declination 0°

Grid Cell Size: 250 m

mGal/km



BASE DATA: National Topographic Database - NRCAN
 GEOLOGY DATA: OGS M-Series maps: M2668 & MRD126-rev1
 DATUM: NAD83
 PROJECTION: Universe Transverse Mercator (UTM Zone 16N)

Scale 1 : 315 000

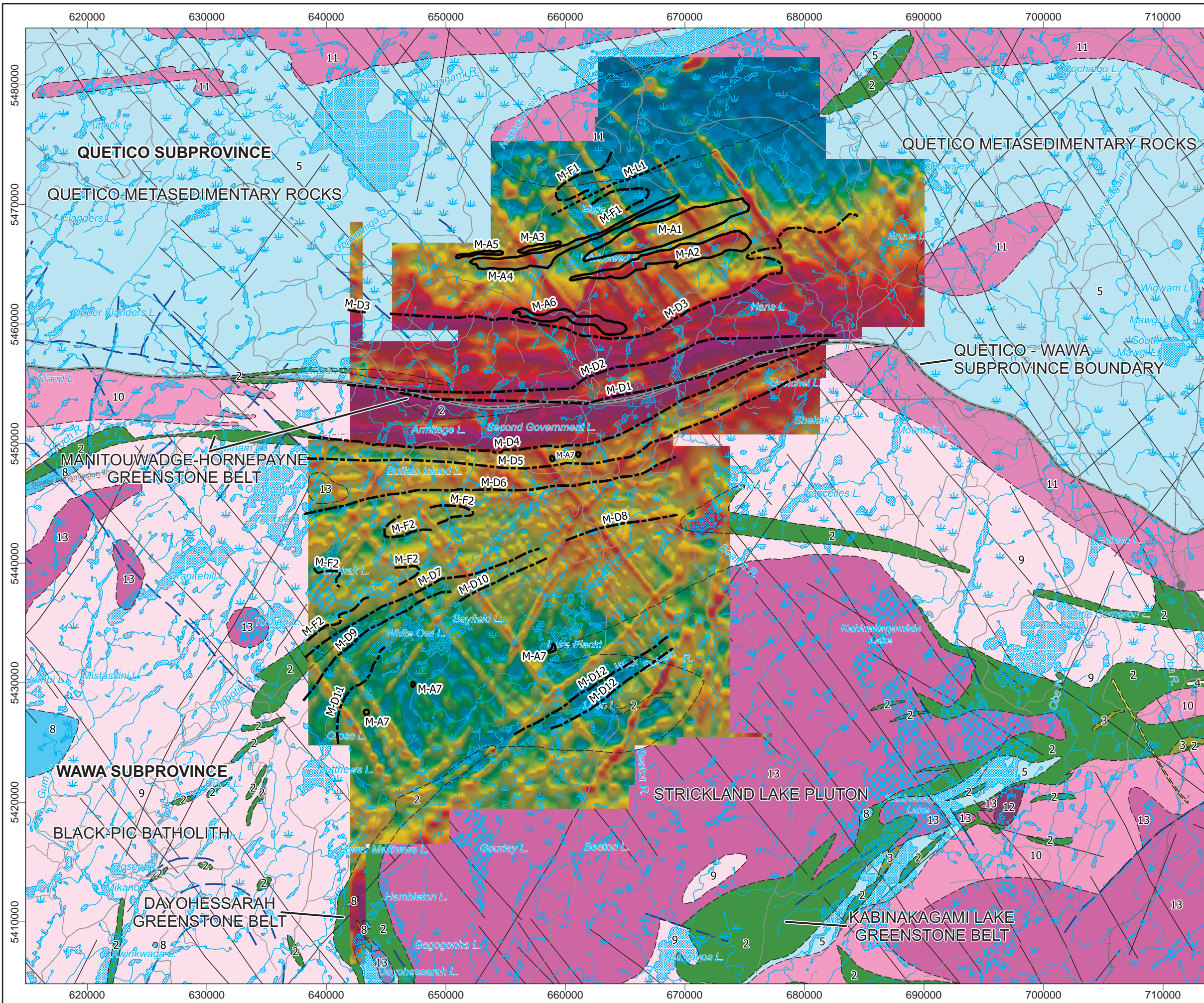
km 5 0 5 10 km

**Airborne Geophysics
 Acquisition and Interpretation**

Hornepayne Area, Ontario 2016

**Total Horizontal Derivative of the Bouguer Gravity
 with Selected Interpreted Features**

	DESIGN	JK, MP	12/07/2016	REV. 1.2
	GIS	YC, PT	12/07/2016	FIGURE: 5.3
	DATA	MP, PT, MM	12/07/2016	
	QC	MB	15/07/2016	



Legend

Hydrography

Roads

Railway

Powerline

Mine

Geology

Fault

Dyke

Subprovince Boundary

2: Mafic metavolcanics

3: Felsic and intermediate metavolcanics

4: Felsic volcanics

5: Metasedimentary rocks

8: Gabbroic rocks

9: Gneissic tonalite suite

10: Foliate tonalite suite

11: Granite-granodiorite, muscovite/biotite bearing rocks

12: Diorite-monzonite-granodiorite

13: Granite-granodiorite

Magnetic Anomaly

Magnetic Domain Boundary

Magnetic Lineament

Magnetic Defined Fold

Map Parameters

Illumination: inclination 50°, declination 0°

Grid Cell Size: 250 m

nT

575.1

480.2

410.0

356.8

311.6

273.7

237.5

206.9

179.3

154.5

132.3

111.4

91.2

70.4

52.4

35.0

20.6

7.5

-4.9

-15.4

-24.9

-33.8

-42.3

-50.1

-57.5

-64.4

-71.1

-77.1

-83.2

-89.2

-95.1

-100.7

-106.6

-112.9

-119.5

-126.4

-133.8

-141.1

-148.2

-154.9

-161.8

-169.4

-177.6

-188.4

-203.4

-227.8

-257.3

-296.5

-339.2

Survey Location

BASE DATA: National Topographic Database - NRCAN
 GEOLOGY DATA: OGS M-Series maps: M2668 & MRD126-rev1
 DATUM: NAD83
 PROJECTION: Universe Transverse Mercator (UTM Zone 16N)

Scale 1 : 315 000

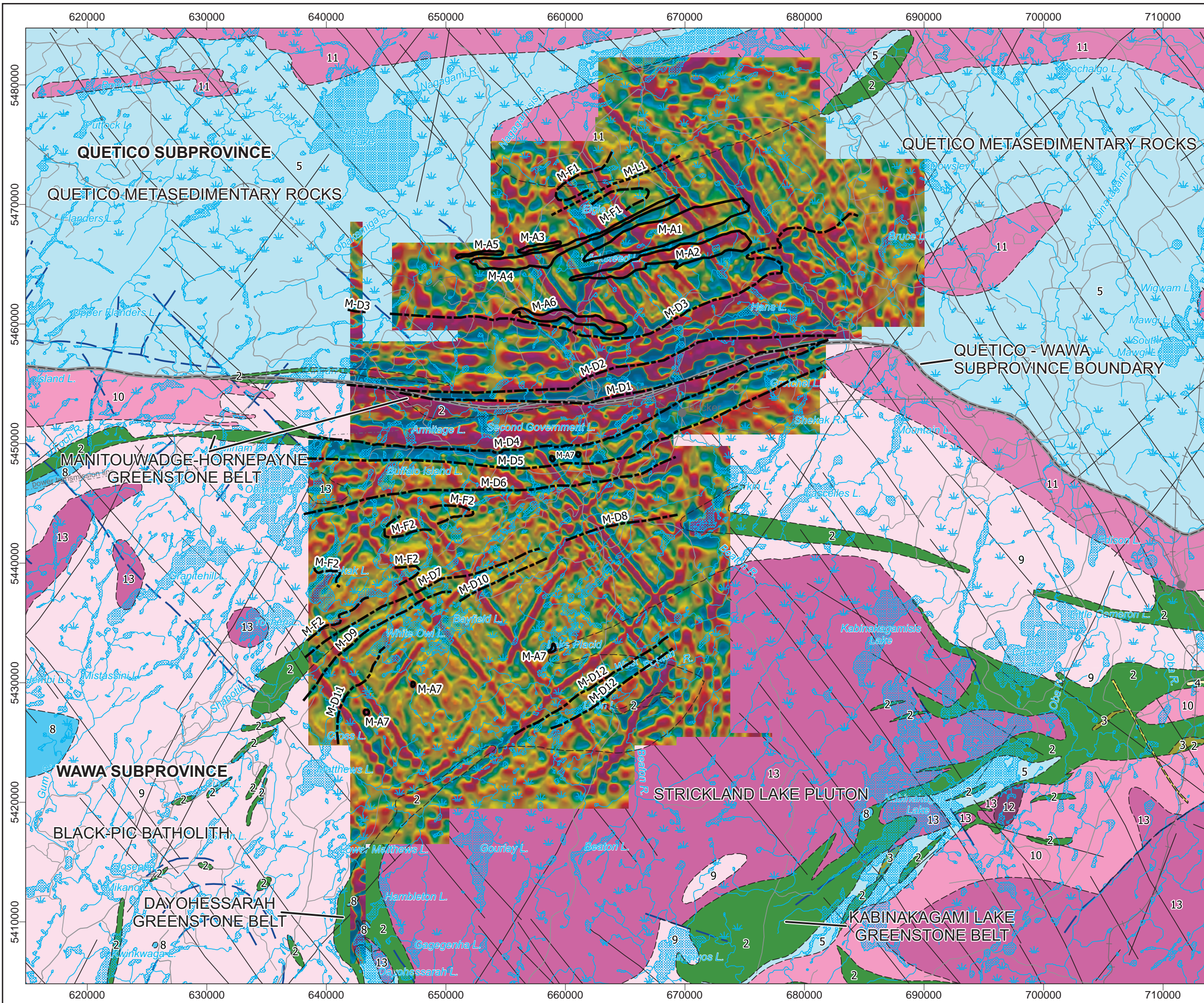
km 5 0 5 10 km

**Airborne Geophysics
 Acquisition and Interpretation**

Hornepayne Area, Ontario 2016

Reduction to the Pole of the Total Magnetic Intensity
 with Selected Interpreted Features

	DESIGN	JK, MP	12/07/2016	REV. 1.2
	GIS	YC, PT	12/07/2016	
	DATA	MP, PT, MM	12/07/2016	FIGURE: 5.4
	QC	MB	15/07/2016	



Legend

Hydrography

Roads

Railway

Powerline

Mine

Geology

Fault

Dyke

Subprovince Boundary

2: Mafic metavolcanics

3: Felsic and intermediate metavolcanics

4: Felsic volcanics

5: Metasedimentary rocks

8: Gabbroic rocks

9: Gneissic tonalite suite

10: Foliate tonalite suite

11: Granite-granodiorite, muscovite/biotite bearing rocks

12: Diorite-monzonite-granodiorite

13: Granite-granodiorite

Magnetic Anomaly

Magnetic Domain Boundary

Magnetic Lineament

Magnetic Defined Fold

Map Parameters

Illumination: inclination 50°, declination 0°

Grid Cell Size: 250 m

nT/km

716.8

531.5

418.6

346.8

291.8

246.5

211.9

182.3

157.0

135.2

116.5

99.6

85.2

70.1

57.2

45.9

34.8

24.9

15.1

5.8

-3.0

-11.4

-19.6

-27.2

-35.1

-42.2

-49.2

-56.6

-64.2

-72.2

-79.2

-86.3

-94.0

-102.2

-111.0

-119.4

-127.7

-137.5

-148.0

-159.9

-172.7

-186.6

-204.1

-222.5

-244.2

-275.0

-313.9

-373.9

-483.0

Survey Location

BASE DATA: National Topographic Database - NRCAN
 GEOLOGY DATA: OGS M-Series maps: M2668 & MRD126-rev1
 DATUM: NAD83
 PROJECTION: Universe Transverse Mercator (UTM Zone 16N)

Scale 1 : 315 000

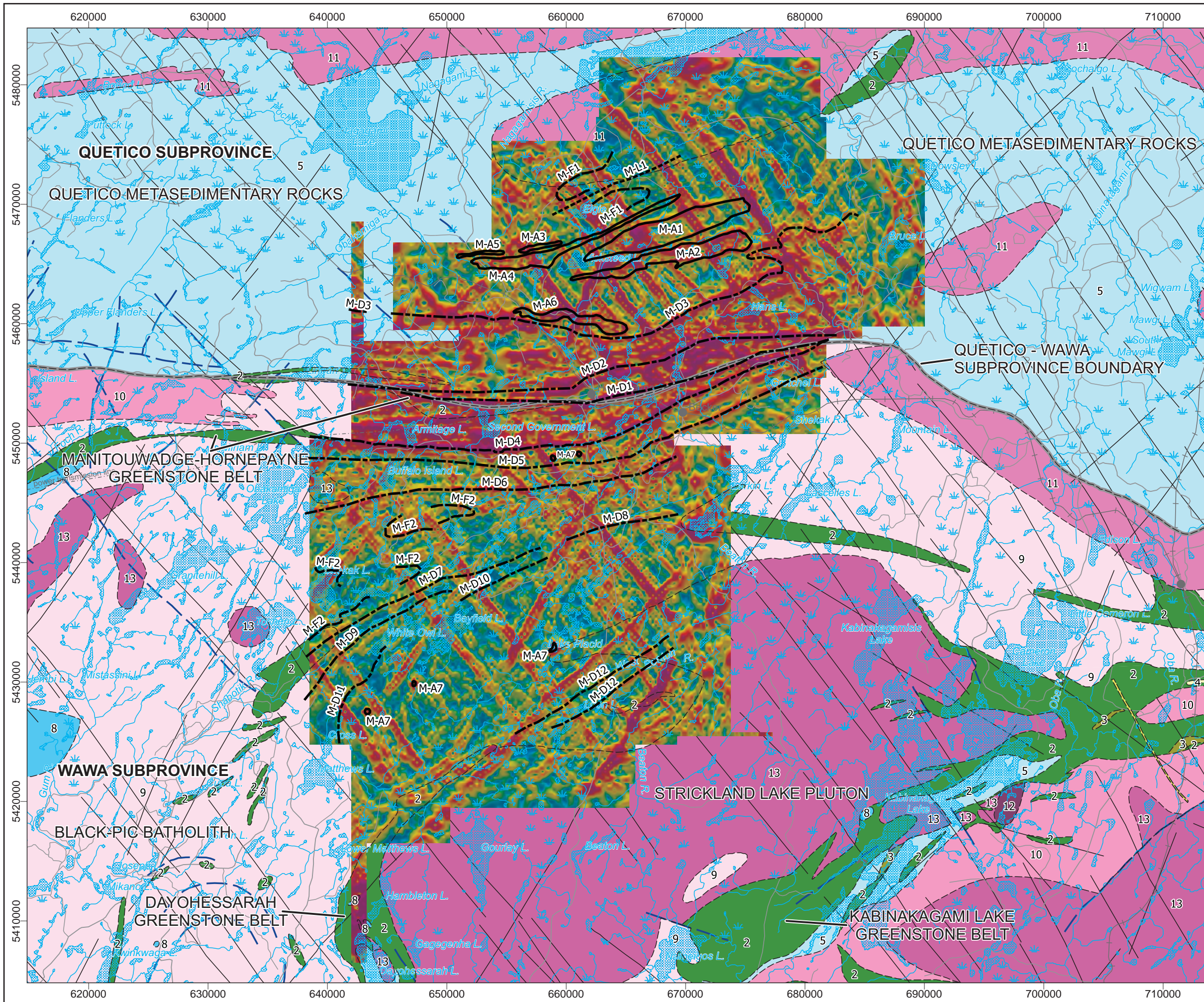
km 5 0 5 10 km

**Airborne Geophysics
 Acquisition and Interpretation**

Hornepayne Area, Ontario 2016

**First Vertical Derivative of the
 Reduction to the Pole of the Total Magnetic Intensity
 with Selected Interpreted Features**

	DESIGN	JK, MP	12/07/2016	REV. 1.2
	GIS	YC, PT	12/07/2016	
	DATA	MP, PT, MM	12/07/2016	FIGURE: 5.5
	QC	MB	15/07/2016	



Legend

Hydrography

Roads

Railway

Powerline

Mine

Geology

Fault

Dyke

Subprovince Boundary

2: Mafic metavolcanics

3: Felsic and intermediate metavolcanics

4: Felsic volcanics

5: Metasedimentary rocks

8: Gabbroic rocks

9: Gneissic tonalite suite

10: Foliate tonalite suite

11: Granite-granodiorite, muscovite/biotite bearing rocks

12: Diorite-monzonite-granodiorite

13: Granite-granodiorite

Magnetic Anomaly

Magnetic Domain Boundary

Magnetic Lineament

Magnetic Defined Fold

Map Parameters

Illumination: inclination 50°, declination 0°

Grid Cell Size: 250 m

nT/km

797.3
627.8
539.9
478.3
430.8
392.7
360.1
335.0
312.2
293.0
275.0
258.5
243.9
229.9
217.1
205.0
194.9
185.1
175.9
167.1
159.6
152.4
145.1
138.2
132.0
126.4
120.5
114.9
109.6
104.8
99.7
94.6
90.0
85.1
80.5
76.3
71.8
67.9
63.8
59.5
55.3
51.1
46.7
42.3
37.7
33.2
28.2
22.7
16.0

Survey Location

BASE DATA: National Topographic Database - NRCAN
 GEOLOGY DATA: OGS M-Series maps: M2668 & MRD126-rev1
 DATUM: NAD83
 PROJECTION: Universe Transverse Mercator (UTM Zone 16N)

Scale 1 : 315 000

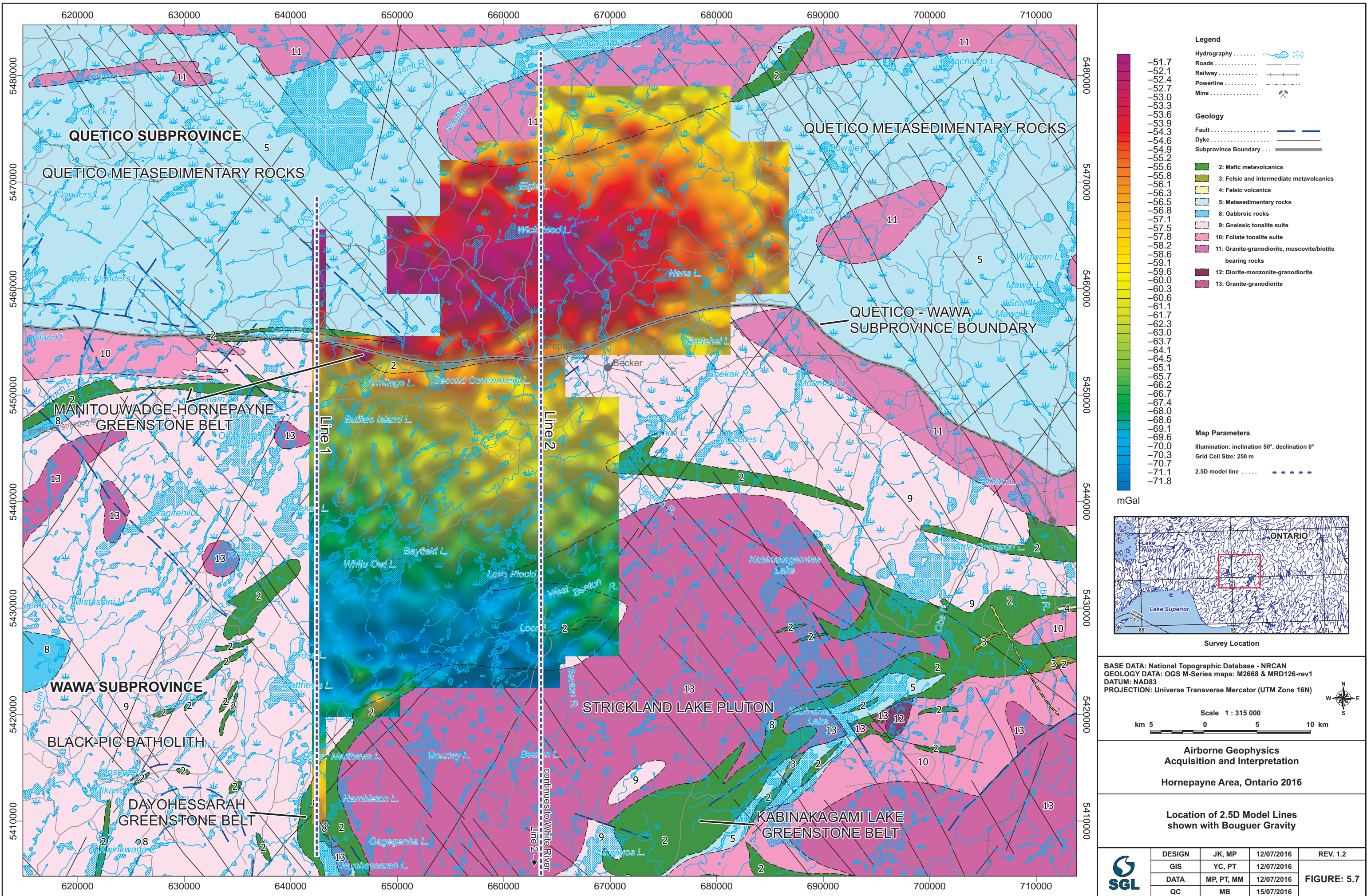
km 5 0 5 10 km

**Airborne Geophysics
 Acquisition and Interpretation**

Hornepayne Area, Ontario 2016

**Total Horizontal Derivative of the
 Reduction to the Pole of the Total Magnetic Intensity
 with Selected Interpreted Features**

	DESIGN	JK, MP	12/07/2016	REV. 1.2
	GIS	YC, PT	12/07/2016	
	DATA	MP, PT, MM	12/07/2016	FIGURE: 5.6
	QC	MB	15/07/2016	



Legend

Hydrography

Roads

Railway

Powerline

Mine

Geology

Fault

Dyke

Subprovince Boundary

2: Mafic metavolcanics

3: Felsic and intermediate metavolcanics

4: Felsic volcanics

5: Metasedimentary rocks

8: Gabbroic rocks

9: Gneissic tonalite suite

10: Foliate tonalite suite

11: Granite-granodiorite, muscovite/biotite bearing rocks

12: Diorite-monzonite-granodiorite

13: Granite-granodiorite

Map Parameters

Illumination: inclination 50°, declination 0°

Grid Cell Size: 250 m

2.5D model line

mGal

Survey Location

BASE DATA: National Topographic Database - NRCAN
 GEOLOGY DATA: OGS M-Series maps: M2668 & MRD126-rev1
 DATUM: NAD83
 PROJECTION: Universe Transverse Mercator (UTM Zone 16N)

Scale 1 : 315 000

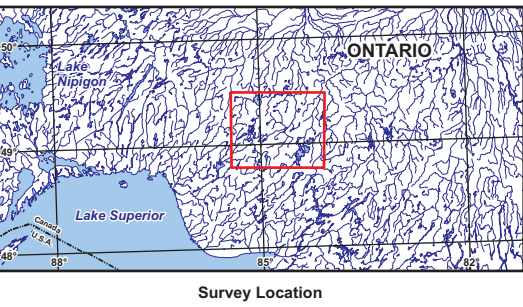
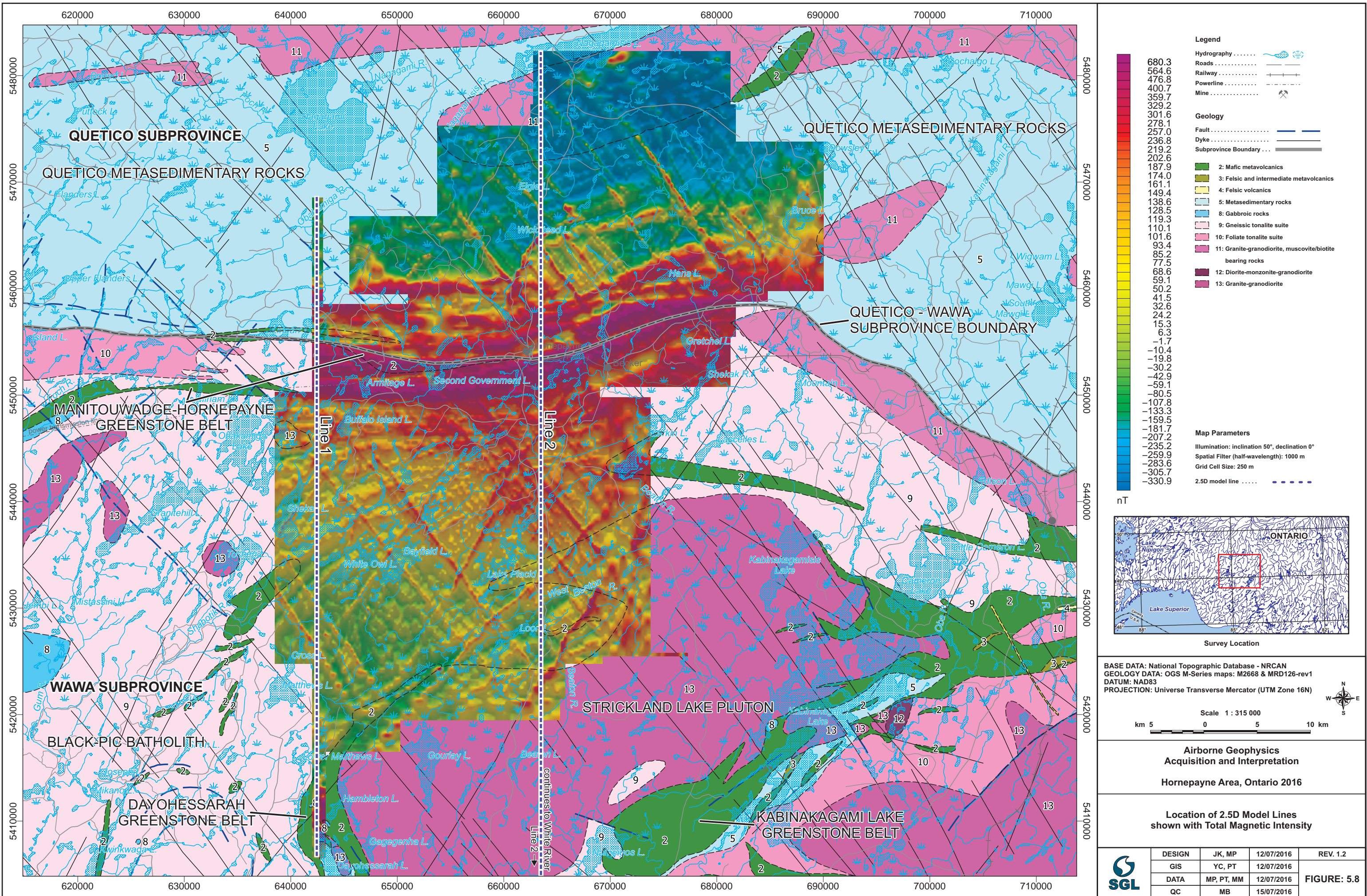
km 5 0 5 10 km

Airborne Geophysics Acquisition and Interpretation

Hornepayne Area, Ontario 2016

Location of 2.5D Model Lines shown with Bouguer Gravity

	DESIGN	JK, MP	12/07/2016	REV. 1.2
	GIS	YC, PT	12/07/2016	
	DATA	MP, PT, MM	12/07/2016	FIGURE: 5.7
	QC	MB	15/07/2016	



BASE DATA: National Topographic Database - NRCAN
 GEOLOGY DATA: OGS M-Series maps: M2668 & MRD126-rev1
 DATUM: NAD83
 PROJECTION: Universe Transverse Mercator (UTM Zone 16N)



continues to White River
 Line 2

Figure 5.9 - Forward Modeling Results: Line 1, Hornepayne, Ontario

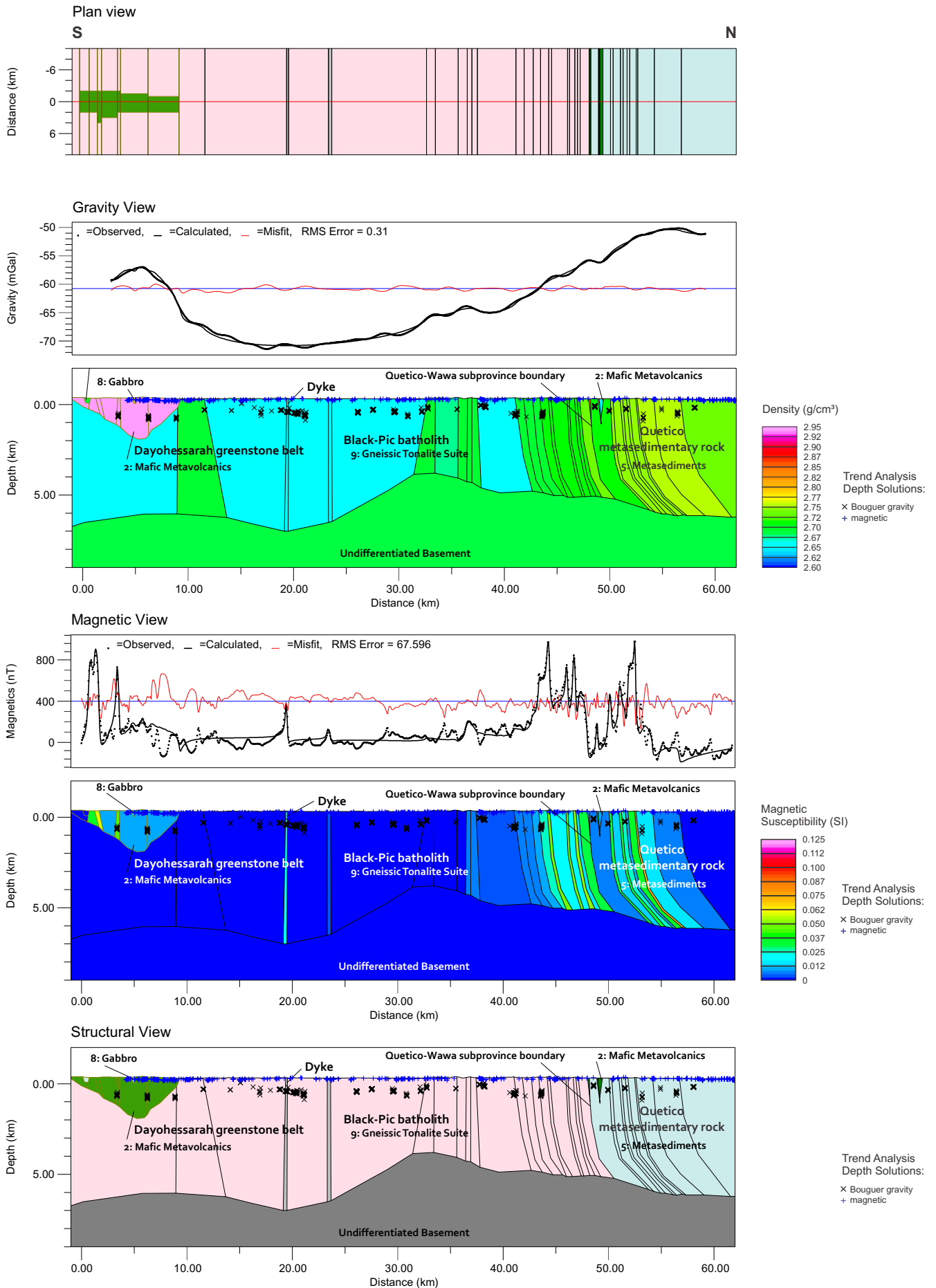


Figure 5.10 - Forward Modeling Results: Line 1-Alternative, Hornepayne, Ontario

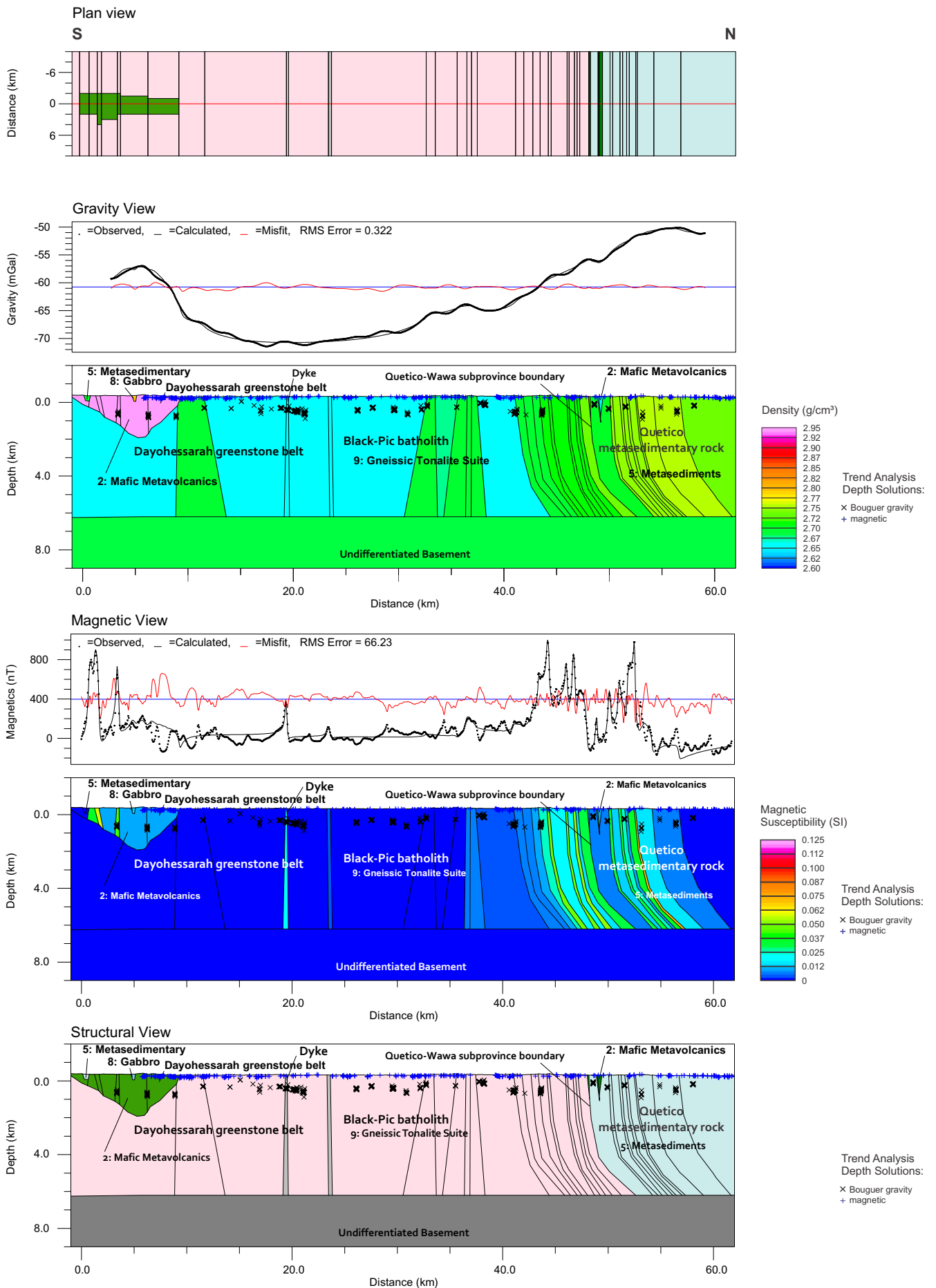


Figure 5.11 - Forward Modeling Results: Line 2, Hornepayne, Ontario

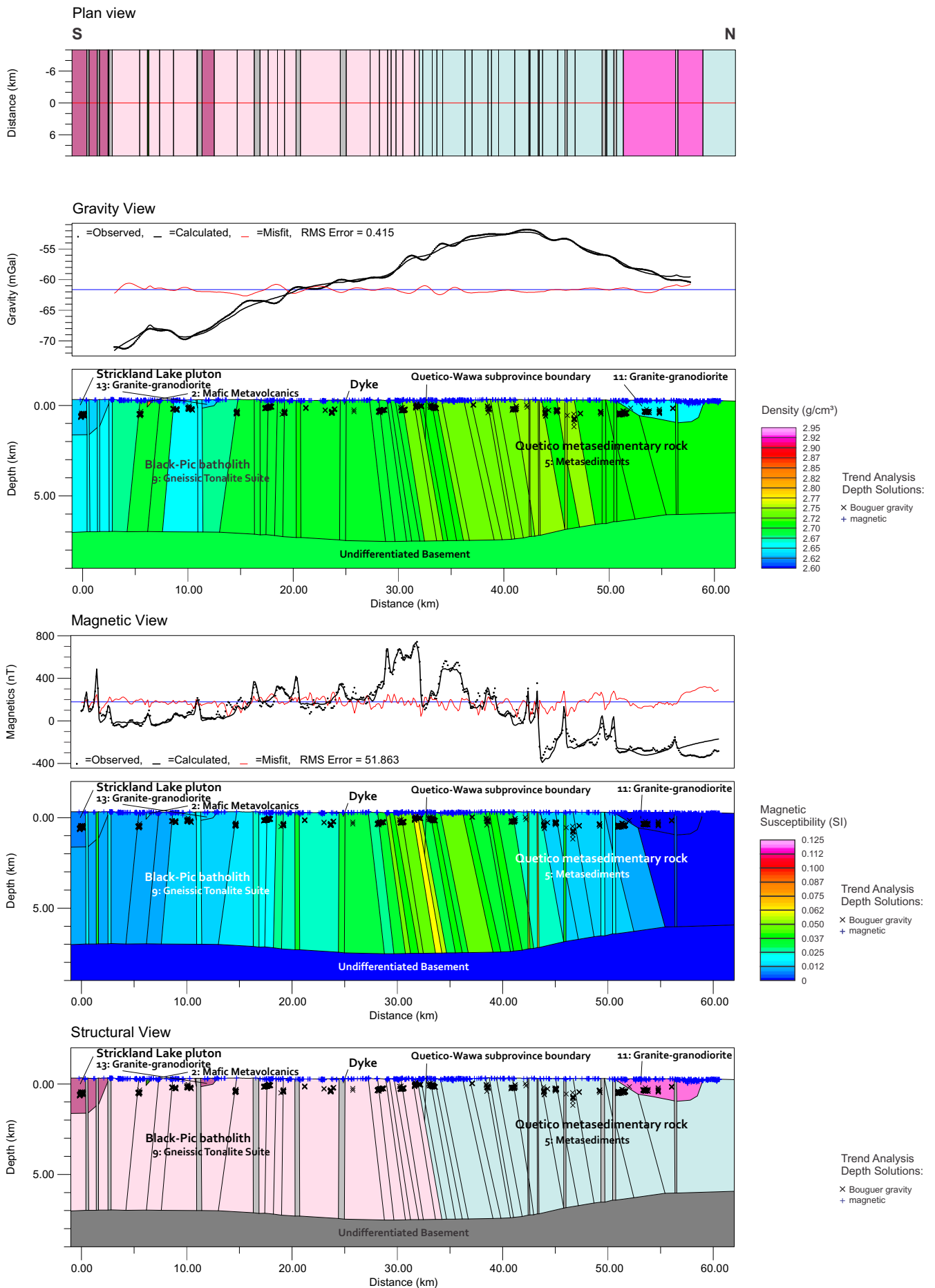


Figure 5.12 - Forward Modeling Results: Line 2-Alternative, Hornepayne, Ontario

